The viability of coral populations

in the Anthropocene

Andreas Dietzel

July 2020

Submitted in fulfilment of the requirements for the degree of
Doctor of Philosophy

ARC Centre of Excellence for Coral Reef Studies
James Cook University

Keywords

Coral demography, population viability, coral population sizes, extinction risk, reef disturbances, spatial patterns, colony size structure, reef recovery, reproduction

Abstract

Reef disturbance regimes are changing and accelerating in the Anthropocene, compromising the capacity of corals to recover between disturbance events. These changes raise concerns about the long-term viability of coral populations, and even entire species. Our understanding of coral population viability is largely based on changes in total coral cover. More nuanced ecological data, measuring trends in the abundance of individual species and on the composition and reproductive capacity of coral populations, are scarce. They are even more scarce at large spatial and temporal scales, where populations disappear, and species go extinct. This thesis examines demographic trends in corals beyond coral cover, at spatial and temporal scales relevant to the persistence of metapopulations and species. Such large-scale assessments of demographic trends in corals are urgently needed due to the unprecedented spatial scale, and pace, at which reef disturbances like mass bleaching events caused by global warming deplete coral populations in the Anthropocene.

Assessments of species extinction risk are predominantly based on the size and change in population abundance. These data are unavailable for corals at relevant biogeographic scales, and risk assessments have therefore been based on regional trends in total coral cover, and on expert elicitation. My first objective was therefore to estimate the total number of coral colonies and the population sizes of more than 300 coral species on shallow-water reefs in the Pacific, to provide a new perspective on their risk of extinction. My estimates show that the 65 most common species have population sizes greater than one billion colonies, one fifth of which are currently considered at elevated risk of extinction. Two thirds of the 318 examined species have population sizes exceeding 100 million and even the most range-restricted and locally rare species have population sizes greater than one million individual colonies. These estimates call into question earlier inferences that one third of all reef-building coral species, and one quarter of the species examined in this thesis, face an elevated risk of global extinction within the next few decades.

Changes in the colony size structure of coral populations can reveal important insights into the demographic processes underlying population decline. However, data limitations mean that long-term regional trends in size structure are rarely studied. My second objective was

therefore to measure and examine shifts in the colony size structure of coral populations along Australia's Great Barrier Reef, relative to historical baselines, following decades of declines in cover, and widespread mass coral bleaching events in 2016 and 2017. For this analysis, I used line intercept transect data, routinely collected to measure the percent benthic cover of corals, as proxy for colony size. The abundance of coral colonies declined sharply across all colony size classes in all taxa, habitats and sectors, with the exception of reefs in the far south which escaped mass mortality events in recent history. While the relative abundance of large colonies changed comparatively little, their absolute abundance declined by more than 50% in 8 out of 12 taxa on the crest and in 5 out of 12 taxa on the slope. The disproportionate loss of small colonies, particularly in slow-growing, long-lived taxa, indicates that this depletion of large fecund colonies has resulted in suppressed recruitment rates and in the erosion of population resilience.

Demographic inference beyond changes in cover, and beyond the relative abundance of small and large colonies, requires knowledge of the distribution of projected colony areas. These are not readily approximated from distributions of intercept length (i.e. lengths of transect segments that intersect particular colonies), which often intersect colonies only partially, or at odd angles. I present a method to reconstruct the distribution of projected colony areas that is most likely have produced a given distribution of measured intercept lengths. The method exhibits low, non-systematic biases and performs significantly better than two standard alternatives: using the intercept as the colony radius or diameter. I demonstrate the potential of the method for demographic inference by examining long-term trends in the reproductive output of coral populations on the Great Barrier Reef. In many taxa, fecundity declined more steeply than percent cover, signalling the depletion of brood stocks and illustrating the need for more detailed demographic data to assess the viability of coral populations.

In demographically open populations like corals, the capacity for recovery following disturbance depends on the proximity to undisturbed populations within the distance of larval dispersal, and thus on the spatial footprint and patchiness of reef disturbances. I examined differences in the spatial patterns of mass coral bleaching events and cyclones on Australia's Great Barrier Reef and their implications for population connectivity and recovery. In particular the bleaching events in 2016 and 2017 had markedly larger spatial footprints and were less patchy than a severe category 5 tropical cyclone (Yasi in 2011). Severely bleached reefs in 2016 and 2017 were isolated from the nearest lightly affected reefs by up to 146 and

200 km respectively, whereas reefs severely damaged by Cyclone Yasi were isolated from the nearest reefs with minor damage by a maximum of 77 km. I present a model of coral reef disturbance and recovery dynamics to illustrate that the substantially larger and less patchy footprints of recent mass bleaching events undermine the connectivity and resilience of coral populations – even in long-distance dispersers.

Table of Contents

List of Figures

Main Text

Appendix C

Appendix D

List of Tables

Main Text

Appendix C

Appendix D

Statement of the contribution of authors

This thesis was supported by funds provided by the Australian Research Council's centre of excellence program, a Laureate Fellowship to Terry Hughes, and a James Cook University Postgraduate Research Scholarship.

The thesis was supervised by Professor Terry Hughes, Associate Professor Michael Bode and Professor Sean Connolly.

Chapter 2: Dietzel, et al. *(in review)*

- Andreas Dietzel: Concept of study, data analysis, writing of manuscript
- Michael Bode: Data analysis, concept of study, supervision
- Sean Connolly: Statistical support, supervision
- Terry Hughes: Supervision, data collection, concept of study

Chapter 3: Dietzel, et al. *(in review)*

- Andreas Dietzel: Concept of study, data analysis, writing of manuscript
- Michael Bode: Data analysis, supervision
- Sean Connolly: Data analysis, statistical support, supervision
- Terry Hughes: Supervision, data collection, concept of study

Chapter 4: Dietzel, et al. *(in prep)*

- Andreas Dietzel: Concept of study, data analysis, writing of manuscript
- Michael Bode: Concept of study, data analysis, supervision
- Sean Connolly: Statistical support, supervision
- Terry Hughes: Supervision, data collection

Chapter 5: Dietzel, et al. *(in review)*

- Andreas Dietzel: Concept of study, data analysis, writing of manuscript
- Michael Bode: Data analysis, concept of study, supervision
- Sean Connolly: Statistical support, supervision
- Terry Hughes: Supervision, data collection

Statement of Original Authorship

The work contained in this thesis has not been previously submitted to meet requirements for an award at this or any other higher education institution. To the best of my knowledge and belief, the thesis contains no material previously published or written by another person except where due reference is made.

Signature:

Date: July 10, 2020

Acknowledgements

I thank my supervisors, Terry Hughes, Michael Bode and Sean Connolly, for their continued support throughout this degree. I thank everyone who has contributed directly or intellectually to the work summarized in this thesis, in particular Michael McWilliam, James Kerry, Katie Peterson and Roberto Salguero-Gomez. I thank the members of the Australian Coral Bleaching Taskforce and other scientists around the world for making available data without which this thesis would not have been possible. Finally, I thank my family and friends for helping and guiding me along this journey.

Chapter 1: General introduction

Coral reefs in the Anthropocene

In the last 500 years, human activity has become the dominant influence on Earth's geology and ecosystems (Crutzen 2006; Lewis & Maslin 2015). This new geological epoch – the Anthropocene – is already visible in the climatic and geological record, but it is particularly marked by the diametrically opposed population trajectories of humans and the world's wild animal and plant species (Ceballos & Ehrlich 2002; Butchart *et al.* 2010; Pereira *et al.* 2010; Barnosky *et al.* 2011; Dirzo *et al.* 2014). By the end of the 21st century, 11 billion humans are expected to inhabit the planet. By comparison, since the onset of human civilization, the global abundance of fish and wild mammals has declined by a factor of two and six respectively (Bar-On *et al.* 2018), species are going extinct at a rate 1000 times the background rates of extinction (Pimm *et al.* 2014), and the International Union for Conservation of Nature (IUCN) currently lists 41% of the world's amphibian species, 25% of mammal species and 14% of bird species as threatened (IUCN 2020).

In an attempt to match the global scale of human impact on the planet, scientists study the Earth's geosphere, atmosphere and biosphere at unprecedented scales. Technological advances in remote sensing, computer modelling and big data have facilitated breakthroughs in our understanding of global climate change (IPCC 2018), the wider planetary boundaries of human development (Steffen *et al.* 2015), but also of trends in the global distribution and abundance of the Earth's flora and fauna. For instance, a recently developed map of global tree densities revealed that the global number of trees has halved since the start of human civilization – from approximately 5.6 to 3.0 trillion – and continues to decline at a rate of 15.3 billion trees per year (Crowther *et al.* 2015). Similar global scale assessments exist for a variety of taxa such as soil nematodes (van den Hoogen *et al.* 2019), Antarctic krill (Atkinson *et al.* 2009) or birds (Gaston & Blackburn 1997). However, for the vast majority of species, including many of global ecological importance, the spatial and temporal scale of available ecological data is too limited to assess and predict their demographic trends in the Anthropocene.

Reef-building corals, and the ecosystems they engineer, are of immense global ecological and economic value. The calcium carbonate skeletons of both live and dead corals build complex three-dimensional topographies that provide habitat to an estimated one million reef species (Fisher *et al.* 2015), the vast majority of which remains undiscovered or unnamed (Fisher *et al.* 2015; Brandl *et al.* 2018). Coral reef ecosystems provide a wide variety of ecosystem services to humans including food production, coastal protection and revenue from tourism (Moberg & Folke 1999). Combined, the world's coral reefs have an estimated economic value of more than $350 billion per year (Costanza *et al.* 1998, 2014). Australia's Great Barrier Reef alone contributes an estimated $56 billion to the Australian economy per year and supports 64,000 jobs (O'Mahony *et al.* 2017).

Disturbances have always shaped life on coral reefs (Connell 1978). The cumulative impact of natural and anthropogenic disturbances has, however, led to a steady depletion of coral abundances on reefs around the world (Gardner 2003; Wilkinson 2008; De'ath *et al.* 2012). Stressors include hurricanes or cyclones (e.g. Woodley *et al.* 1981), poor water quality (Fabricius 2005), outbreaks of corallivorous starfish (Pratchett *et al.* 2017) and diseases in corals (Green & Bruckner 2000) and key herbivores (Lessios *et al.* 1984), overfishing (Jackson *et al.* 2001), and, more recently, large-scale marine heatwaves caused by global warming (Hoegh-Guldberg 1999; Hughes *et al.* 2003). The increasing frequency, extent and intensity (Hughes *et al.* 2018a) of coral mass bleaching events is taking an unprecedented toll on coral populations (Hughes *et al.* 2017b) transforming coral assemblages (Hughes *et al.* 2018b) and impairing reef connectivity and recovery (Hughes *et al.* 2019a). Under a business-as-usual scenario of global greenhouse gas emissions (IPCC scenario RCP8.5), virtually all of the world's coral reefs are predicted to experience annual severe bleaching conditions before the end of the 21st century (Van Hooidonk *et al.* 2016).

Coral demography

Demographic data are statistical data collected about the characteristics of a population, including its size, density, composition, migration and vital rates. These data are essential to measuring and predicting trends in the abundance of a population or species and to detecting processes, such as reproductive failure, that may compromise its long-term viability. In humans, census data on the size of a population, its age and sex structure as well as fertility and mortality rates are routinely collected. In contrast, demographic data in wild animal and plant species are typically sparse and highly restricted in space and time. Invertebrate

(Cardoso *et al.* 2012; Régnier *et al.* 2015) and marine (Webb & Mindel 2015) taxa are particularly understudied. Instead, assessments and predictions of trends in their abundances rely typically on expert opinion and proxies of population decline such as percentage habitat lost or decline in total community abundance (McCarthy *et al.* 2001; Martin *et al.* 2012). While this approach provides rapid and inexpensive first-order approximations of population declines, it often ignores interspecific and intraspecific differences in biology and distribution and provides limited insights into the demographic and ecological processes underlying population decline.

As benthic colonial organisms with a pelagic larval phase, reef building corals have size rather than age-dependent life histories (Hughes 1984) and rely on larval dispersal to recolonize lost habitat. Colony sizes typically vary by several orders of magnitude. The few large, highly fecund colonies contribute disproportionately to future generations (Hughes *et al.* 1992; Hall & Hughes 1996), are more likely to undergo partial than whole-colony mortality, can, in some species, reach lifespans of several hundred years and thus allow species to persist despite ongoing recruitment failure (Hughes & Tanner 2000). Broadcast spawning coral species release both sperm and eggs into the water column where fertilization occurs. By contrast, in brooding species, egg fertilization and embryogenesis occur inside the colony before large, well developed planula larvae are released and disperse. As a result, brooder larvae typically settle close to their natal reef, whereas spawner larvae can disperse over distances of 10s to 100s of kilometres. While the populations of both brooders and spawners are considered open, differences in dispersal kernels determine how coral species explore space and have ramifications for their capacity to recover from disturbances. These life history characteristics, in combination with the limited spatial and temporal scope of in-water surveys, pose unique challenges to the study of coral populations. Consequently, demographic data at spatial and temporal scales that capture key demographic processes such as stock-recruitment dynamics and the response to changing reef disturbance regimes are scarce, particularly at the species level.

Conservation demography of coral reefs

As reef disturbance regimes continue to escalate, coral reef scientists and managers are tasked to study and manage phenomena at large spatial and temporal scales, at which ecological data is notoriously scarce (**Figure 1.1**). Long-term regional trends in coral abundances are typically based on measurements of the overall percentage benthic cover of hard corals. Cover

is an apt abundance metric for modular organisms like trees and corals, whose individuals compete for limited space and typically vary in size by orders of magnitude. However, it limits our ability to infer interspecific and intraspecific trends in abundances and to predict the future fate of coral populations, species and assemblages. For instance, assessments of extinction risk in corals have relied heavily on regional trends in coral cover and expert opinion in the absence of species-level abundance data at biogeographic scales (Carpenter *et al.* 2008) (**Figure 1.1**). The conclusion that one third of the world's reef-building coral species faces an elevated risk of global extinction (Carpenter *et al.* 2008), for example, has attracted criticism for not reflecting the vast geographic ranges of most Indo-Pacific coral species (Hughes *et al.* 2014).

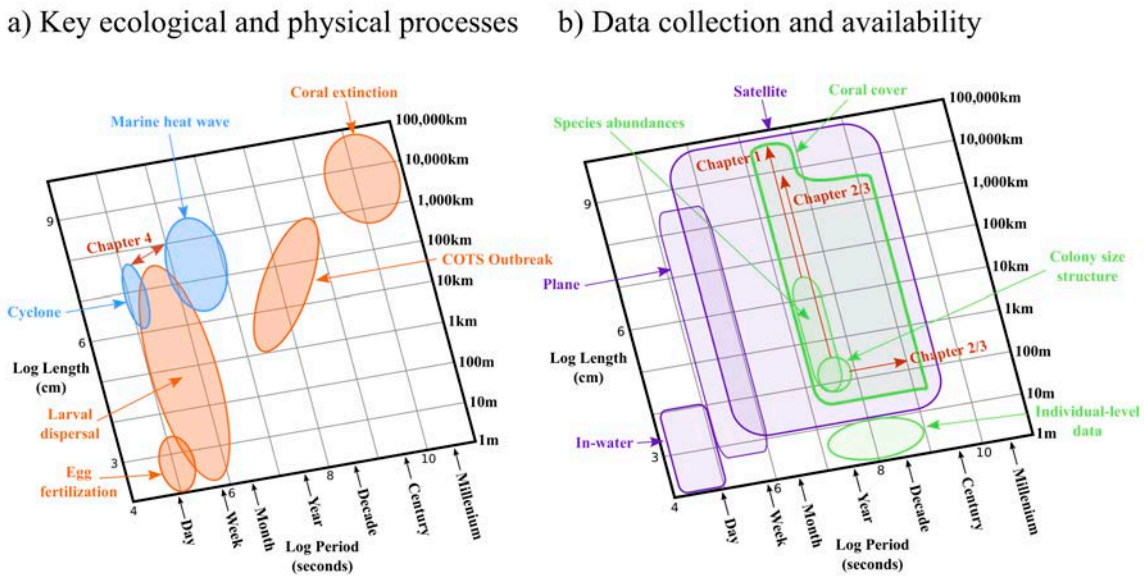

Figure 1.1 Schematic Stommel diagrams showing **a)** the spatial and temporal scales on which key ecological (orange) and physical (blue) processes determining coral demography operate; and **b)** the spatial and temporal scales at which different types of demographic data (green) are available in corals and the methods with which they are collected (purple). The spatio-temporal delineation of survey methods depicts the typical scale trade-offs of methods.

Trends in overall coral cover also provide limited insights into the demographic processes underlying population decline, likely future population trajectories, and long-term population viability. For instance, the role of reproduction and recruitment in regulating population dynamics, historically understudied due to the open nature of coral populations and intractability of larval dispersal (Caley *et al.* 1996), is increasingly shifting into focus as concerns arise over the capacity of coral populations to recover from increasingly frequent

and severe disturbances. Coral recruitment rates on Australia's Great Barrier Reef decreased by 89% relative to their historical baselines following unprecedented back-to-back mass bleaching events in 2016 and 2017 (Hughes *et al.* 2019a). While coral cover was found to be a good predictor of differences in recruitment rates, it masks potential shifts in colony size structure and their implications for the reproductive output of a population and population viability. A systematic decline in the abundance of small colonies may, for instance, indicate ongoing recruitment failure while declines in the abundance of large, highly fecund individuals implicate a decline in fecundity. Long-term regional trends in colony size structure have been reported for the Red Sea (Riegl *et al.* 2012), Kenya (McClanahan *et al.* 2008) and the Caribbean (Bak & Meesters 1998) but comparable examinations for the Great Barrier Reef are currently missing (**Figure 1.1**).

As the world's coral reefs, and the scientists studying them, enter uncharted territory, we urgently need a better understanding of the demographic challenges faced by coral populations in the Anthropocene (Edmunds & Riegl 2019). The ever expanding scope of remote sensing and computer modelling (Hedley *et al.* 2016; Madin *et al.* 2019), innovative, scalable survey methods (González-rivero *et al.* 2014; Chirayath & Earle 2016), meta-analyses (Darling *et al.* 2019), curated databases (Madin *et al.* 2016), and long-term ecological studies (Lindenmayer *et al.* 2012b) are all instrumental for the required expansion of the spatial and temporal scope of demographic data. The integration of existing demographic, ecological and biophysical data across spatial, temporal and taxonomic scales (Robinson *et al.* 2014) as well as the recycling and repurposing of historical data (Hawkins *et al.* 2013) also present promising avenues to overcome the data crisis in biodiversity conservation (Kindsvater *et al.* 2018). Historical data, for instance, can be used to examine departures from historical baselines and, in particular, slowly unfolding shifts in ecosystems (Pauly 1995; Hughes *et al.* 2011, 2013b).

Few phenomena illustrate better the novel challenges faced by reef organisms and reef scientists in the Anthropocene than large-scale marine heat waves. Three mass coral bleaching events within the past five years (2016, 2017 and 2020) have disturbed coral populations on the Great Barrier Reef and unprecedented spatial scales (Hughes *et al.* 2017b, 2019b). While the capacity for long-distance larval dispersal is an integral adaptation to life in the fragmented and frequently disturbed reef environment, disturbances that simultaneously deplete populations over large swaths of reef area may undermine the connectivity of

populations by diminishing external recruitment subsidies. Historically, cyclones have been the dominant large-scale disturbance on coral reefs. On the GBR, cyclone impact is typically patchy and limited to within 100-200km of its track (e.g. Done 1992; Beeden *et al.* 2015). In contrast, the mass bleaching event in 2016 alone affected the Northern third of the Reef severely and the Central third moderately (Hughes *et al.* 2017b). We currently know little about the differences in spatial patterns of large-scale reef disturbances, namely their extent and patchiness, and whether mass bleaching events present an unprecedented challenge the resilience of coral populations and assemblages.

Coral demography in the Anthropocene

The overarching aim of this thesis is to fill important knowledge gaps in our understanding of the large-scale demographic challenges that corals face in the Anthropocene. Each of my chapters approaches coral reef conservation with a focus on how coral demography is changing in an era of global human influences. Each of the chapters examines these questions at the wide, metapopulation to biogeographic scale that is so important to coral reef ecosystem dynamics but understudied.

In **Chapter 2**, I estimate the population sizes of more than 300 Indo-Pacific coral species at biogeographic scales. For this, I integrate ecological and physical data from different sources and across varying scales of spatial and taxonomical coverage (**Figure 1.1**). These estimates provide a novel perspective on the global extinction risk of coral species, the assessment of which has hitherto relied heavily on proxies of percentage coral habitat lost and expert opinion rather than species abundances. **Chapter 3** fills important knowledge gaps in our understanding of long-term demographic changes in coral populations on Australia's Great Barrier Reef. Specifically, I examine decadal trends in the colony size frequency distribution of coral populations, an important indicator of population viability in corals, along the length of the GBR by recycling and repurposing historical line-intercept transect (LIT) data (**Figure 1.1**). LIT data are commonly used to measure coral abundances and provide a valuable proxy for shifts in colony size structure. However, more advanced demographic inferences about, for instance, changes in the reproductive output of coral populations require knowledge of the true colony size frequency distribution of a population. In **Chapter 4**, I present a new method that allows the reconstruction of the true colony size frequency distribution that most likely underlies a measured distribution of intercept lengths. This method presents an important bridge between routinely collected monitoring data of coral abundances and size-based

demographic tools such as structured population models. I demonstrate the potential of the method for advanced demographic inference by examining decadal changes in the fecundity of coral populations on the GBR. Finally, in **Chapter 5**, I investigate differences in the spatial footprint and patchiness of large-scale reef disturbances on the GBR. Specifically, I contrast the spatial patterns of four mass coral bleaching events (in 1998, 2002, 2016 and 2017) and Severe Tropical Cyclone Yasi (in 2011), for which spatially extensive survey data of disturbance impact are available. For this chapter, I harness ecological data collected by satellites, planes and in-water surveys (**Figure 1.1**) and, subsequently, complement the empirical evidence with theoretical modelling to explore the implications of different spatial disturbance patterns for the population connectivity and recovery dynamics of coral species with different dispersal capacities.

Chapter 2: The population sizes of reef-building coral species at biogeographic scales

Currently in review in *Nature Ecology and Evolution*

2.1 INTRODUCTION

The abundance of corals on the world's coral reefs, typically measured as percent benthic cover, has declined for many decades due to a broad range of anthropogenic stressors (Wilkinson 2008; Jackson *et al.* 2014). The rate and scale of this decline is accelerating as the spatial extent and frequency of mass coral bleaching and mortality events increases due to global warming (Baker *et al.* 2008; Eakin *et al.* 2010; Hughes *et al.* 2018b, a). While some regional trends in overall coral cover are relatively well understood (Gardner 2003; De'ath *et al.* 2012), we currently know little about the numerical abundance of reef-building corals and, in particular, of individual coral species at biogeographic scales. Consequently, recent assessments of the global extinction risk of coral species have relied on expert opinion and on regional trends in overall coral cover rather than data on the abundance of individual species (Carpenter *et al.* 2008). For other ecologically important taxa (**Table 2.1**), global estimates of species-level abundances have helped to fill critical gaps in our understanding of their extinction risk (ter Steege *et al.* 2015), their role in global biogeochemical cycles (Fauset *et al.* 2015), and the ecological challenges of setting and achieving conservation and restoration targets (Crowther *et al.* 2015).

Here, I calculate the total abundance of reef-building corals, and the population sizes of more than 300 Indo-Pacific coral species on reef flats, crests and slopes between Indonesia and French Polynesia. These estimates are derived from species abundance data collected along a 10,000 km long biodiversity gradient, coral cover data from more than 900 Indo-Pacific reef sites in marine provinces stretching from Indonesia to French Polynesia, and on spatial data on reef habitats (**Figure 2.1**). Approximately 70% of the global shallow-water coral reef area and more than 600 of the estimated 800 hard coral species of the world occur in the domain of this study. To enhance comparability with estimates of global population size for other taxa

(**Table 2.1**), I follow convention and present population size estimates as total counts of colonies (Hughes & Jackson 1985; Connell *et al.* 1997) rather than the total area occupied by individual species. Individual colonies are capable of conducting independently all biological functions, including growth, reproduction and mortality (Hughes & Jackson 1985; Connell *et al.* 1997). However, I also examine the extent to which numerical abundances of colonies are representative of relative extent of coral cover. I reveal patterns of hyperdominance that are similar to those observed for the Amazonian tree flora (ter Steege *et al.* 2013), and I test for correlations between population size estimates and the current conservation status classifications of coral species under the International Union for Conservation of Nature's (IUCN) Red List.

2.2 MATERIALS AND METHODS

Because ecological data at the scale of this study are scarce, I combined data from different sources to derive estimates of the total abundance of scleractinian corals and the population sizes of 318 species. I first mapped the availability of coral habitat across the study region using data on the global distribution of the world's coral reefs (UNEP-WCMC *et al.* 2010). The total reef area in the study domain is 107,700 km^2. However, these global data provide no estimates of the availability of different habitat types and include habitats not suitable for corals. I therefore complemented these data with detailed habitat maps from 61 reef locations (**Table C-3**) to estimate the average proportion of a reef that is reef crest, flat and slope habitat dominated by live coral (rather than e.g. rubble or sand). To account for variations in overall community abundance, I then interpolated more than 900 measurements of coral cover (Bruno 2016; Bruno & Valdivia 2016) across the study region. Finally, I used species abundance data collected on reef crest, flats and slopes across the study domain to apportion the total abundance of corals in the study region to 318 species. A graphical overview of the steps in the analysis is given in **Figure C-4**.

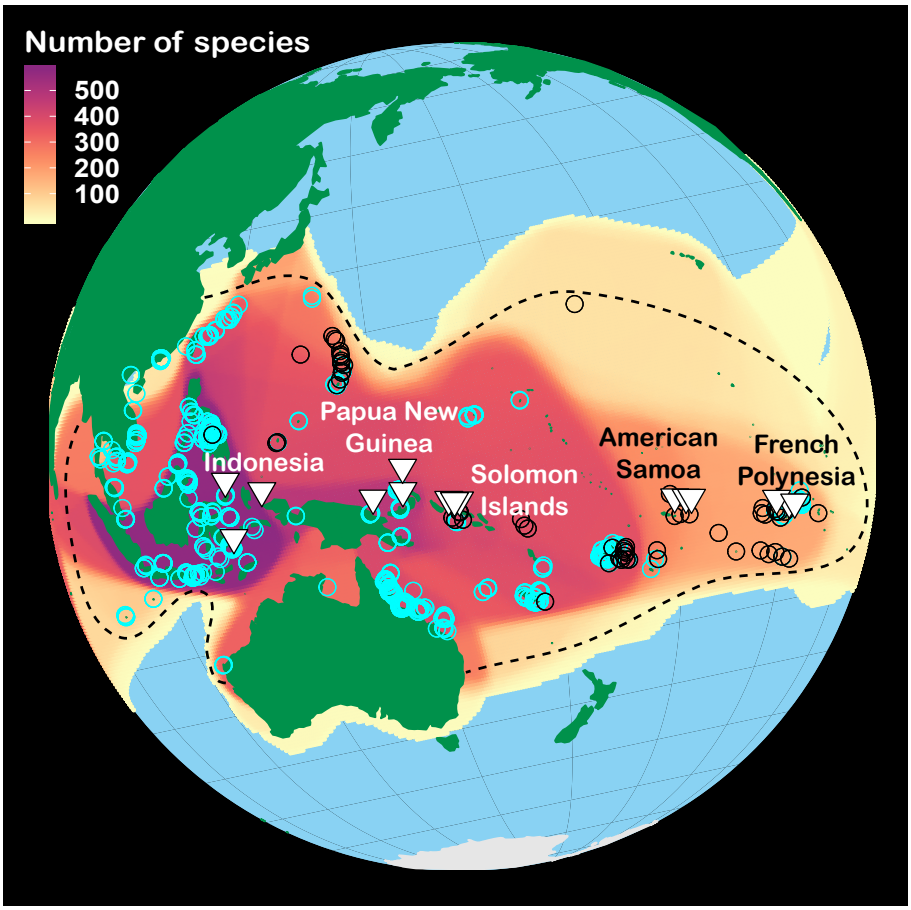

Figure 2.1 The Indo-Pacific biodiversity gradient and the locations where coral abundance and reef habitat data were collected. Shading indicates species richness of corals. White triangles (▽) indicate the location of the 15 islands across five regions where species abundances were measured, blue circles (○) show the locations of coral cover measurements, and black circles (○) indicate the location of coral reef habitat surveys.

Coral abundance data

Coral abundances were measured on reef slopes, crests and flats in five regions (Indonesia, Papua New Guinea, Solomon Islands, American Samoa, French Polynesia) along a 10,000 km gradient in species richness (**Figure 2.1** and Error! Reference source not found.). In each region, four sites were selected on each of three islands. At each of the 60 sites, ten 10 m line intercept transects were run on the upper reef slope (6-7m depth), reef crest (1-2m) and reef flat (tidal). All intercepted, physically discrete (i.e. with contiguous tissue) coral colonies larger than 1cm in diameter were identified to species in-situ by a highly trained team of coral taxonomists, with the exception of a species cluster of sub-massive *Porites* (e.g. *Porites lobata*, *P. lutea, P. solida*) which I excluded from the present analysis (Karlson *et al.* 2004;

Connolly *et al.* 2005; Hughes *et al.* 2014). When necessary, close-up high-resolution digital photographs were taken to record small-scale features, or colony samples were collected, to confirm species identifications later using taxonomic monographs or archived type specimens in the Museum of Tropical Queensland, which houses the world's largest collection of modern scleractinians. To allow for comparisons with current IUCN threat status classifications in corals (Carpenter *et al.* 2008), I adhered to the species taxonomy and phylogeny currently used by the IUCN and reconciled minor inconsistencies where necessary. I adopted recent revisions of coral taxonomy and phylogeny (Huang *et al.* 2011) which reassigned some species among genera or families. Along the total of 1,800 transects, 37,129 intercepted colonies were recorded belonging to 318 species, which represents approximately half of all known coral species that occur in the study region (n = 618). Only a subset of those species would occupy the specific habitat types that were sampled. To estimate how many such species there were, I estimated the number of unobserved species for those particular metacommunities from the multi-site species-abundance distribution, using previously-published methods (Connolly *et al.* 2017). Missing species likely also occur in additional habitats or regions that were not sampled (e.g. lagoon floors, deeper slopes). Elsewhere, these species abundance data were used to explore the size of the metacommunity species pool (Connolly *et al.* 2005, 2017) and a range of other ecological and biogeographic questions (Karlson *et al.* 2004; Cornell *et al.* 2007, 2008; Connolly *et al.* 2009; Hughes *et al.* 2014). To estimate species abundances within the domain of this study (**Figure C-5**), I complemented the species abundance data at 60 sites with an extensive dataset of more than 900 measurements of local coral cover (Bruno 2016; Bruno & Valdivia 2016) (**Figure 2.1**). Species abundance data were collected between 1999 and 2002 and coral cover data between 1997 and 2006 (Bruno 2016; Bruno & Valdivia 2016).

Reef habitat quantity, quality and composition

I collated 61 coral reef habitat maps throughout the study domain from different sources (**Table C-3**) to (a) quantify the extent of reef habitat with live coral as the dominant benthic cover (rather than e.g. sand, rubble, rock or algae) and (b) to estimate the average proportions of different reef habitat types. Reef polygons in the Global Distribution of Coral Reefs data (UNEP-WCMC *et al.* 2010) classified as "deep reef" or "shallow non reef" were excluded from the analysis. Proportional reef habitat composition for habitat maps from the Khaled bin Sultan Living Oceans Foundation (KSLOF) was calculated using the "habitat analysis tool" of

the KSLOF's online, interactive World Reef Map. For each habitat map, I identified the habitat classifications that matched the habitat types in the surveys of species abundances (reef slope, crest and flat). Reef habitat classifications with live coral as dominant benthic cover that could not be attributed to reef crest, slope or flat were identified as "others".

I calculated for each habitat map the proportion of live-coral dominated reef slope, crest, flat and "other" habitat relative to the total mapped reef. Reef parts classified as, for instance, land, mangroves or deep water were excluded. I applied a cubic root and logistic transformation of these proportions to satisfy normality, and fitted a Bayesian linear model with brms (Bürkner 2017) to the transformed (Warton & Hui 2011) proportions y_i, where habitat type (slope/fore reef, crest, flat/back reef) was the explanatory variable:

$$y_i \sim N(\mu_i, \sigma)$$

$$\mu_i = \beta_0 + \beta X_i$$

$$\beta_0, \beta \sim N(0,100)$$

$$\sigma \sim \text{cauchy}(0,5)$$

I then used the posterior distributions of the parameters to estimate uncertainty (**Figure C-6**). I assume that the estimated proportions of live-coral dominated reef habitat types at the 61 sites (**Table C-3** and **Figure 2.1**) are largely representative for Indo-Pacific reefs but acknowledge the potential for bias introduced by regional differences in geomorphology, bathymetry and mapping precision, an additional source of uncertainty that could not be formally incorporated in the confidence intervals. The ongoing improvement of reef habitat maps from around the world will help refine future analyses.

Reef habitat types differ not only in their spatial extent, or proportions of the total reef, but also in colony densities (**Figure C-6**). I accounted for differences in colony densities by calculating the relative colony densities in each habitat type and using them to rescale the proportions of the total reef classified as live-coral dominated slope, crest, flat and "other" habitat (**Figure C-6**). Because no data on colony densities in "other" habitat types were available, I assumed the average of the three surveyed habitat types. The posterior distribution of the proportion of the total reef with live coral as dominant benthic cover LC_{Total} is calculated as the sum across the four habitat classifications. The proportion of the total reef with live coral as dominant benthic cover and the proportion of the total reef classified as live-coral dominated crest were affected only marginally by the rescaling. The rescaled proportion

of live-coral dominated slope habitat increased, while the rescaled proportion of live-coral dominated flat habitat decreased (**Figure C-6**).

Estimating coral abundances and population sizes

I created a gridded base map (resolution 50km by 50km) of the domain of the study (**Figure C-5**). I interpolated coral cover data across the study domain using an inverse-distance weighted model (function idw(), R package 'gstat', inverse distance power value of 2.0) following a similar study that estimated the global conservation status of more than 15,000 Amazonian tree species (ter Steege *et al.* 2015). Using interpolated rather than raw coral cover data accounts for regional variation in sampling intensity but assumes that coral cover is spatially autocorrelated and varies predictably between regions, particularly where observations are sparse. However, as noted in the main text, the conclusions are robust even if the extreme assumption is made that there are no corals at all outside the regions where colonies were sampled. All analyses were carried out in R (R Core Team 2019) using a cylindrical equal-area projection with a custom prime meridian of 160ºW. The narrower distribution, and increased median, of interpolated cover values relative to the frequency distributions of the raw data (**Figure C-7**) likely occurs for two reasons. First, areas of sparse observations tend to have above-average cover estimates, and these estimates make a larger contribution to the spatial interpolation. Second, the inverse-distance weighted method calculates a spatial average between sample data points which reduces the influence of extreme values.

For each of the 60 sites at which species abundances were surveyed, I calculated total coral cover and colony densities following an approach (Marsh *et al.* 1984) that allows calculation of coral colony densities from line intercept transect data. I regressed colony densities against cover using a generalised additive model with normal error structure (thin-plate regression splines with 3 knots and weakly informative priors, function 'stan_gamm4', package 'rstanarm', Stan Development Team 2016). I then used the regression model to predict for each grid cell the upper and lower bound of the 95% credible interval of colony density ρ_g (**Figure C-7**). I then estimated the total number of corals in the study domain N_{Scl} as

$$1) \quad N_{Scl} = \sum_{g=1}^{n} (\boldsymbol{A_{Reef\,g}\ LC_{Total}\ \rho_g})$$

where ρ_g is the predicted colony density of coral-dominated reef habitat in grid cell g, $A_{Reef\,g}$ the reef area in grid cell g and LC_{Total} the rescaled proportion of the total reef with live coral

as dominant benthic cover (**Figure C-6**). My estimates of coral colony densities (median of 28.9 colonies per m^2, **Figure C-7**) fall well within the bounds of other reported densities (Connell *et al.* 1997).

Here I calculate and report population sizes of corals as counts of colonies rather than total area occupied, or counts of polyps or genets. Specifically, I define an individual in the analysis as a physically discrete colony. While I acknowledge that the demographic contribution of an individual colony depends on its size (Hughes 1984; Hall & Hughes 1996), estimating population sizes as counts of individuals follows the convention in conservation biology and demography, allowing a comparison with similar estimates in other organisms of global ecological importance (**Table 2.1**), including trees that resemble corals in their size-dependent life histories. I show, furthermore, that numerical abundance and total area occupied by each species are very closely correlated (**Figure 2.4**).

To estimate the population sizes of the 318 Indo-Pacific coral species in this analysis I first predicted their relative abundances in each of the five surveyed regions and three habitat types using the species abundance data described above. To each of the 15 surveyed meta-communities (3 habitats in each of 5 regions, 12 sites each) I fitted a recently developed unified model (Connolly *et al.* 2017) that captures multiple macroecological patterns in coral abundances (local species abundance distribution, interspecific variation in the strength of spatial aggregation, patterns of community similarity, species accumulation and the size of the species pool). The unified model describes the probability distribution of abundances among species and sites in a metacommunity with only four fitted parameters: Taylor's power-law scaling parameters a and b and the mean and variance of log abundance in the metacommunity μ and σ^2. The unified model also provides an estimate of the size of the species pool and thus an estimate of the number of species too rare to be sampled (the veil effect) (Connolly *et al.* 2005, 2017) (**Table C-1**).

The observed abundance of a species inevitably constitutes a biased estimate of a species' true abundance given the large proportion of rare species and intraspecific patterns of spatial aggregation. I therefore used the fitted parameters to simulate, for each surveyed meta-community, 100,000 new meta-communities to find a range of likely true species abundances that underlie a given observed species abundance, using a parametric bootstrap simulation approach from Connolly *et al.* (2017). First, I randomly drew a vector of n (n = estimated size of species pool) mean site-level abundances μ_i (henceforth referred to as simulated true mean abundance) by repeatedly sampling from a lognormal distribution described by the fitted

parameters μ and σ^2. The power-law scaling parameters a and b then specify an among-site variance in abundance that is conditional on that species-specific mean: $\sigma_i^2 = a\,\mu_i^b$. For species with greater variance than mean site-level abundance ($\sigma_i^2 > a \bullet \mu_i^b$), I randomly drew 12 site-level abundance values from a negative binomial distribution with mean μ_i and variance σ_i^2. For species with greater mean than variance in site-level abundance (where the negative binomial distribution is undefined), I randomly drew 12 site-level abundance values from a Poisson distribution fully specified by a species' simulated true mean abundance μ_i. See Connolly *et al.* (2017) for further details and justification of this parametric bootstrap simulation approach.

I thus obtained, for each surveyed meta-community with fitted parameters *a, b*, μ and σ^2, a range of simulated true species-level mean abundances μ_i that can underlie a simulated observed mean abundance (i.e., a mean of the observed counts across all sites). Finally, to derive relative abundances I divided each simulated true mean abundance by the sum of simulated true mean abundances of all species in the species pool in each simulated meta-community. I estimate the number of unobserved species in each metacommunity as the difference between the size of the species pool and the number of observed species. Note that this also allows an estimate of the proportion of colonies likely to belong to those unobserved species. Specifically, in the Monte Carlo simulations, some species that have non-zero mean abundance will nevertheless be simulated to have sampled abundance zero everywhere. I could therefore normalize the mean abundances across all species: $\rho_i = \frac{\mu_i}{\sum_{j=1}^{S} \mu_i}$, where S is the number of species in the metacommunity species pool. The proportion of the metacommunity that belongs to the unobserved species is thus the sum of the ρ_i values across all species whose simulated sampled abundances were zero. I took the average of this quantity across all Monte-Carlo simulated data sets as an estimate of the proportion of the metacommunity represented by unobserved species in the abundance data.

To estimate total population sizes for each region, I assume that the modelled range of simulated relative true mean abundances μ_{ijk} is representative of the relative contribution that a species i with observed mean abundance μ_i makes to overall metacommunity abundance in region j and habitat type k. I calculate a species' population size as

$$2) \quad N_i = \sum_{j=1}^{n} \sum_{k=1}^{m} (\boldsymbol{\mu_{ijk}}\ \boldsymbol{N_{Scl\,ijk}})$$

where μ_{ijk} is a species' mean relative abundance in region *j* and habitat *k*, $N_{Scl\ ijk}$ the total number of scleractinian corals in region *j* and habitat *k* within the geographic range of species *i*. With this approach, I obtain first-order approximations of species-level abundances based on assumptions similar to those underpinning comparable analyses in trees (ter Steege *et al.* 2013, 2015; Crowther *et al.* 2015). I fully acknowledge that these are preliminary estimates and that species-level abundances, especially of rare species, have a high degree of uncertainty.

I assigned each grid cell to one of the five geographic regions based on its proximity to the regional centroids of the species abundance survey locations. I then calculated the total number of corals $N_{Scl\ ijk}$ in region *j* and habitat *k* within the geographic range of species *I* (range data from Hughes *et al.* (2013)) by first calculating the number of corals in each grid cell for each habitat type using the rescaled proportions of live-coral dominated crest, flat and slope habitat (**Figure C-6**) and then summing across all grid cells for each region. I additionally accounted for gradients in species richness. I assume that a species' relative abundance is inversely proportional to the species richness in a grid cell: i.e. a hypothetical species *i* with relative abundance μ_i contributes twice as many individuals in a grid cell with 100 species as in a grid cell with 200 species within the same region. I calculated the species richness in each grid cell based on the number of overlapping geographic ranges (Hughes *et al.* 2013a) (**Figure 2.1**). I rescaled the total number of corals within each grid cell by its relative species richness compared to the species richness at the closest regional centroid. This allowed me to collapse the calculation of a species' global population size into a simple, spatially implicit rather than spatially explicit equation (equation 2).

Uncertainty about true metacommunity abundance, conditional on observed abundance in the samples, is formally accounted for in the Monte Carlo procedure. However, two additional sources of uncertainty cannot be formally quantified. One source is the relative abundances of coral species outside of the regions where abundances were sampled (which I assume to equal the mean relative abundance within the study region within a species' geographic range, and to be zero elsewhere). A second is the amount of reef area in the entire study area, which, given the geographically patchy distribution of relative habitat availability estimates, may differ from the estimates I used. To produce an extreme lower bound estimate, I assumed that species abundances were zero outside of the five countries that were sampled (Indonesia, Papua New Guinea, the Solomon Islands, Samoa, and French Polynesia), and I recalculated "global" population sizes. Combined, the reef area of these five countries accounts for 30.8%

of the total reef area in the study domain. I first calculated the reef area in each country from data provided by UNEP-WCMC *et al.* (2010). Assuming a spatially homogeneous colony density of 28.9 colonies per m^2 (median density, **Figure C-7**) rather than extrapolating coral cover across the spatial grid, I then calculated the total number of colonies in each country, which I apportioned to each habitat type using the estimates of live-coral dominated crest, slope and flat habitat presented in **Figure C-6**. I then projected abundances for individual species based on the estimates of species' relative abundances in the study regions as in the baseline analysis.

Coral abundances and IUCN conservation status

To examine the relationships between coral population sizes and IUCN conservation status, I log-10 transformed population sizes to satisfy the statistical assumption of normality and fitted a Bayesian linear regression model to the log-10 transformed population size data (**Figure C-3**) with brms (Bürkner 2017) using weakly informative priors:

$$y_i \sim N(\mu_i, \sigma)$$

$$\mu_i = \beta_0 + \beta X_i$$

$$\beta_0, \beta \sim N(0,100)$$

$$\sigma \sim \text{cauchy}(0,5)$$

I examined model diagnostics (chain mixing, effective sample size, convergence statistic R-hat), carried out pairwise contrasts and calculated Bayes' R2 (function 'bayes_R2', package 'rstanarm', Stan Development Team 2017) as a measure of the total variance explained by the model. I additionally compared differences between species with low (least concern or near threatened) and elevated (vulnerable or endangered) extinction risk. For all Bayesian regression models I initiated 4 MCMC chains of 17,500 steps, each with a 5,000-step warm-up and thinning rate of 5, yielding a total of 10,000 samples, which were subsequently drawn from to propagate uncertainties.

Propagation of uncertainty analysis

I provide uncertainty bounds for the population size estimates following a bootstrap resampling approach. Specifically, I repeatedly (n = 10,000) sampled from the distribution of possible values of each parameter in equations 1 and 2 (ρ_g, $N_{Scl\ ijk}$, LC_k and μ_i), solved

equations 1 and 2 for each bootstrap run and summarised across all runs to calculate the composite uncertainty of N_{Scl} and N_i. To capture the uncertainty in LC_k, I used the respective posterior distributions of the fitted parameter estimates. To reconstruct the posterior distribution of $N_{Scl\ ijk}$ I sampled from the posterior distribution of LC_k, and from the upper and lower bound of the 95% credible interval of predicted coral colony densities in each grid cell ρ_g. Lastly, to propagate the uncertainty in μ_i, I randomly sampled for each species i with a given observed mean site-level abundance a simulated true mean site-level abundance μ_i from the previously derived range of simulated pairs of true and observed abundances in each of the 15 surveyed meta-communities. The composite uncertainties of N_{Scl} and N_i were then calculated as the mean and 95% confidence intervals across the 10,000 bootstrap runs.

2.3 RESULTS AND DISCUSSION

I estimate that approximately half a trillion (95% Bayesian credible interval (CI): 0.3 x 10^{12} – 0.8 x 10^{12}) coral colonies inhabit the shallow-water coral reefs in the marine provinces extending between Indonesia and French Polynesia, comparable in magnitude to the estimated number of trees in the Amazon rainforest (ter Steege *et al.* 2013), or to the estimated number of birds in the world (Gaston & Blackburn 1997) (**Table 2.1**). Together, the acroporid, poritid and favid (now mostly reclassified as merulinid) corals comprised two-thirds of the 318 species that were encountered, and they accounted for three-quarters of the combined abundance of all species (**Figure 2.2a**). Massive, branching and encrusting growth forms are the most common (**Figure 2.2b**), whereas functionally important tabular corals that provide understory habitat(Kerry & Bellwood 2015) and other growth forms are less prevalent.

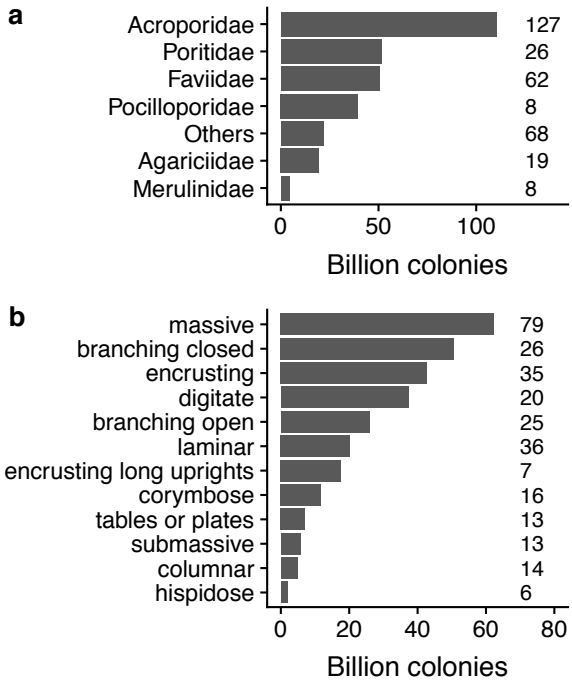

Figure 2.2 Taxonomic and morphological composition of the Pacific coral fauna. **a**, The total abundance of coral colonies by family (summed across species). **b**, The total abundance of coral colonies by colony growth form (summed across species). Sample sizes (number of species) are given on the right plot margin.

Table 2.1 Global and regional abundances of Earth's flora and fauna.

Taxa	No. of species	No. of individuals
Prokaryotes in the world (Bar-On *et al.* 2018)	400,000	10^{31}
Soil nematodes in the world (van den Hoogen *et al.* 2019)	-	4.4×10^{20}
Birds in the world (Gaston & Blackburn 1997)	9,946	3.0×10^{11}
Trees in the world (Crowther *et al.* 2015)	45,000	3.0×10^{12}
Trees in the Amazon (Hubbell *et al.* 2008)	15,200	4.0×10^{11}
Corals in the Pacific (present study)	618	5.9×10^{11}
Individual species		
Antarctic krill (Atkinson *et al.* 2009)		7.8×10^{14}
Humans (May 2020 estimate (Worldometer 2020))		7.8×10^{9}
Individual tree species in the Amazon (ter Steege *et al.* 2013, 2015)		10^{4} - 10^{9}
Individual coral species in the Indo-Pacific		10^{5} - 10^{10}
California condor (US Fish and Wildlife Service 2017)		4.6×10^{2}
Tigers (wild) in the world (Goodrich *et al.* 2015)		3.1×10^{3}

The estimated population sizes of individual coral species differ by five orders of magnitude (**Figure 2.3**). While the population sizes of each of the eight most common coral species exceed the global human population size of 7.8 billion, the six rarest species each have population sizes below one million. The majority (65%) of the examined species, however, number in excess of 100 million colonies, with one out of every five species exceeding one billion colonies. Given that the geographic ranges of most of the examined species extend to varying degrees beyond the spatial extent of this study (**Figure C-1**), with 81% extending westwards into the Indian Ocean, their global population sizes are even larger. Patterns of commonness and rarity varied substantially between the five regions where species abundance data were collected. That is, both the overall variance in species abundance, and the relative abundances of different species, changed from one region to another in the species abundance data. For example, the species *Isopora palifera* was relatively rare on replicate reefs and sites in American Samoa (compared to regions to the west and east) despite ranking among the 20 globally most common species, with an estimated global population size of about 3.6 billion colonies (**Figure C-2**). The numerical abundance of each species explained over 90% of the variation among species in benthic cover (**Figure 2.4**), with a slope of approximately 1, indicating that numerically abundant corals tended to dominate space occupancy in proportion to their numerical advantage (i.e., a species 10 times more abundant than another will also tend to occupy about 10 times as much space, on average).

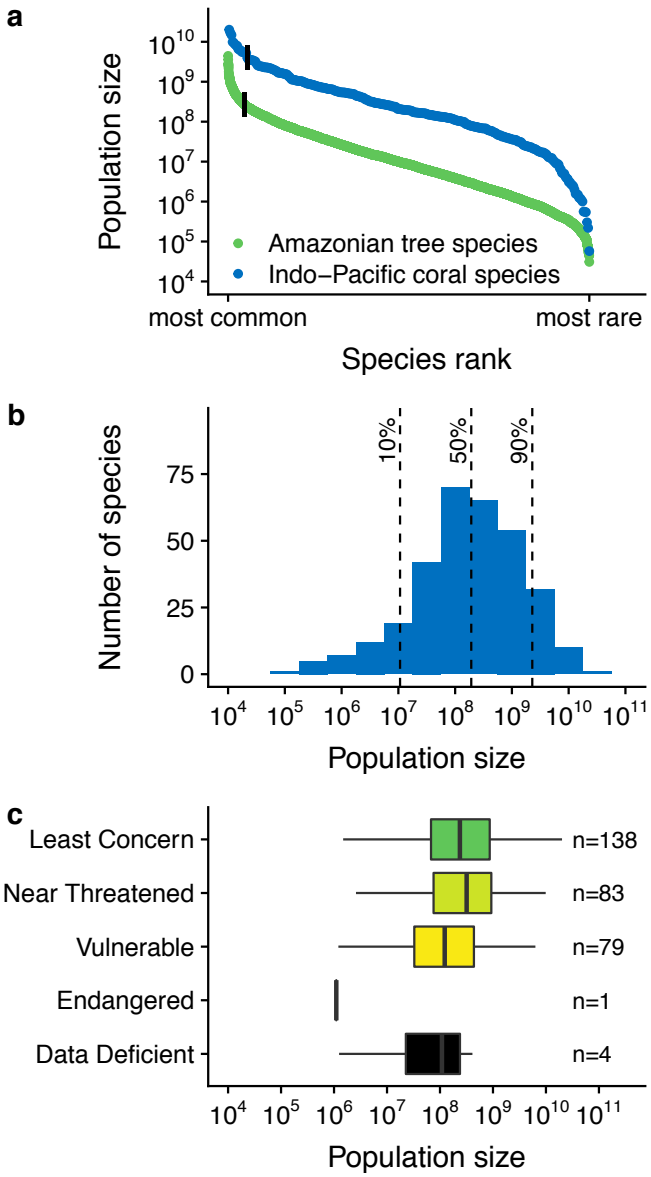

Figure 2.3 The population sizes of Indo-Pacific coral species and their conservation status. **a**, Rank abundance distribution for 318 Indo-Pacific coral species (●) and 4953 Amazonian tree species (●) (ter Steege *et al.* 2015). Vertical lines demarcate the small fraction of hyperdominant tree species (227 out of 4953) and coral species (17 out of 318) respectively. **b**, Species abundance distribution of 318 Indo-Pacific coral species. **c**, The distribution of coral population sizes by IUCN conservation status. Boxplots show centre line (median), box limits (upper and lower quartiles) and whiskers (×1.5 interquartile range). Note that the much higher abundances of Indo-Pacific corals relative to Amazonian trees in panel a, despite the similar total number of individuals, arises because there approximately an order of magnitude fewer coral species than tree species.

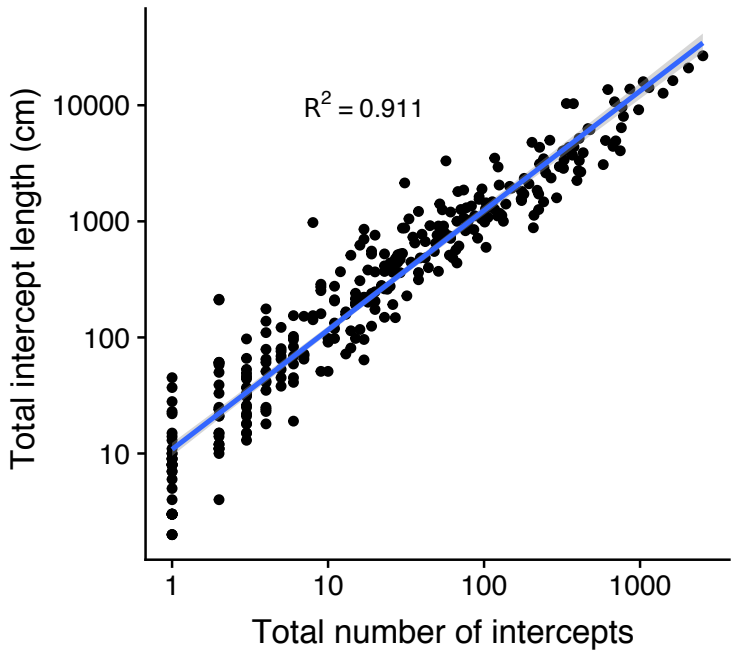

Figure 2.4 Correlation between numerical abundance and the area occupied by each species. The total number of intercepts and total intercept length is shown of each of 318 Indo-Pacific coral species sampled across the five regions and three habitat types. Ten thousand centimetres of intercept length on 1,800 transects equates to 1.8% benthic cover.

Patterns of hyperdominance

A small fraction of the examined species (17 out of 318) numerically dominates the Indo-Pacific coral fauna (**Figure 2.3a, b**). Combined, these 17 hyperdominant species (defined as the species whose pooled abundance accounts for half of total community abundance(ter Steege *et al.* 2013)) account for as many coral colonies as the remaining 301 species, indicating their disproportionate contribution to the assemblage structure and ecological functioning of shallow-water Indo-Pacific coral reef ecosystems. I estimate that in each metacommunity between 7 and 66 rare species were undetected in the samples of species abundances (Connolly *et al.* 2005, 2017) (the veil effect)). Combined, these missing species accounted for 0.2% to 3.5% of the combined abundance of all species in the species pool of each metacommunity (**Table C-1**).

Hyperdominant species are generally characterised by both high local abundances and vast geographic ranges, although some rank among the rarest in some regions within their ranges (**Figure C-2**). Poritid, pocilloporid, favid and acroporid taxa, as well as taxa with encrusting, digitate or closed branching growth form were overrepresented among the 17 hyperdominant

species. In contrast, the 50% of sampled species with lower than the median abundance accounted for less than 4% of the combined abundance of all species. These comparatively rare species nevertheless can have population sizes of up to 200 million colonies. Even *Stylocoeniella cocosensis* – a species that is both range-restricted and numerically rare – has an estimated population size of approximately 23 million colonies (95% CI: 20.2 – 25.5 x 10^6).

Whereas the Indo-Pacific coral fauna exhibits hyperdominance (**Figure 2.3a**), hyperrare coral species (defined as species with population sizes < 1000 individuals (Hubbell 2015)) are unlikely to be prevalent in the five regions that were examined. Hyperrare tropical tree species comprise more than a third (5800 out of 16,000 species) of the Amazonian tree flora (ter Steege *et al.* 2013). These tree species are highly endemic, whereas the geographic ranges of Indo-Pacific coral species are typically very large (Hughes *et al.* 2002), with few species facing the double-jeopardy of being both range-restricted and locally rare (Hughes *et al.* 2014). Even for coral species restricted to the Coral Triangle, range sizes of these endemics are close to the area of the continental United States of America (Hughes *et al.* 2002). Consequently, the hypothetical population densities of an evenly dispersed hyperrare species in the Coral Triangle hotspot would be unviably low, averaging approximately one colony per 8,000 km^2. Similarly, an aggregated hyperrare species of 1,000 colonies, with a higher density of one colony per $10m^2$, would have a range size of just 1 km^2 of reef habitat, making it highly vulnerable to local disturbances. These discrepancies in hyperrarity and endemicity between corals and trees are likely due to fewer barriers to dispersal in the sea, and the dispersal capacity of marine larvae (Kinlan & Gaines 2003).

Extinction risk

The presented estimates of population size provide a new perspective on the extinction risk of Indo-Pacific coral species. Currently, one third of the world's reef-building coral species and about one quarter of the 318 species examined in this study are listed by IUCN as either vulnerable to extinction (VU), endangered (EN) or critically endangered (CR) (Carpenter *et al.* 2008). The overlap in population sizes between risk categories was considerable (**Figure 2.3c**) and differences in IUCN conservation status explained only a small proportion of the overall variance in population sizes (Bayes $R^2 = 0.04$), although pairwise comparisons revealed that the population sizes of species with elevated (VU, EN or CR) extinction risk

were significantly different from those with low extinction risk (near threatened: NT, least concern: LC) (**Figure C-3**).

Remarkably, of the 80 species in the analysis that are considered by IUCN to have an elevated extinction risk (listed as vulnerable, endangered or critically endangered), twelve have estimated population sizes exceeding 1 billion colonies. For instance, *Porites nigrescens* ranks among the 10 most abundant species I examined, is not considered to be highly susceptible to coral bleaching (Carpenter *et al.* 2008), and yet is currently listed by IUCN as vulnerable to global extinction. Conversely, one third of the rarest species in the analysis that comprise the bottom 10% of species abundances, are listed by IUCN as of Least Concern. Notably, many species currently listed by IUCN as Data Deficient also have the smallest population sizes (**Figure 2.3c**), indicating that our poor knowledge of their ecology and abundance is reflective of their rarity and that their extinction risk may be relatively high and unrecognized.

The presented population size estimates inform and refine earlier estimates of extinction risk in Indo-Pacific corals, which relied heavily on qualitative expert opinion (Carpenter *et al.* 2008). In particular, my findings call into question earlier inferences that a considerable proportion (one quarter) of the examined Indo-Pacific coral species could go globally extinct within the next few decades. For typically widespread, highly abundant Indo-Pacific coral species, local depletion and functional extinction are likely to pose more tangible and imminent threats, and large-scale shifts in assemblage structure (Hughes *et al.* 2018b) and mass rarity (Hull *et al.* 2015) present more likely scenarios than global extinction. A major revision of current Red List classifications of corals (Carpenter *et al.* 2008) is urgently needed, based on an adaptation of Red List criteria that better reflect the life histories and population sizes of invertebrates (Cardoso *et al.* 2011, 2012) like corals.

Local depletion of functionally important coral species may trigger cascades of extinctions in associated organisms long before the global extinction of the depleted coral species itself (Gaston & Fuller 2008; Säterberg *et al.* 2013). For instance, my findings highlight the comparative rarity of tabular corals, both in terms of total numbers and species richness. Declines in their abundance may compromise their ability to provide important shelter habitat (Kerry & Bellwood 2015) and food resources for obligate corallivores such as butterflyfishes, some of which (e.g. *Chaetodon trifascialis*) feed almost exclusively on tabular corals (Pratchett 2005). The capacity of a numerically and functionally impoverished reef

community to provide vital ecosystem services to people will also likely be severely compromised.

Estimates of the global abundance of organisms, while inevitably uncertain, can provide robust insights into their biology, global ecological role and extinction risk. I have formally accounted for some sources of uncertainty, such as uncertainty about the metacommunity-scale mean abundances of coral species. In other cases, a formal accounting of uncertainty is not feasible. In particular, I suspect that the areal extent of different types of reef habitat, and variation in species' relative abundances outside the regions where those abundances were directly sampled, are likely to be important additional sources of uncertainty. Indeed, our knowledge of the biology, ecology and abundance of individual coral species at large spatial scales is notoriously limited, as illustrated by ongoing revisions of the taxonomy of scleractinian corals (Knowlton & Jackson 1994; Huang *et al.* 2011). The presented population size estimates are therefore preliminary, similar to comparable estimates for other organisms (ter Steege *et al.* 2015). However, the estimated total number of coral colonies in the Pacific and presented range of population sizes are plausible. In particular, they are several orders of magnitude larger than sizes that would put them at risk of global extinction, a conclusion that is unlikely to be materially altered by improvements in the precision of the estimates due to, e.g., higher-resolution or more spatially extensive measurements of habitat area. Indeed, even an extreme lower-bound scenario where I assume that the abundances of all of the sampled coral species is zero outside of the five regions where species abundance data were collected (which excludes approximately 70% of the total reef area in the study domain) yields estimates of population sizes that range from approximately one million colonies for the rarest species to more than a billion colonies for the most common species. (Note that this estimate also makes the pessimistic assumption that the study species are not present in habitat types other than the three where sampling was conducted.)

Table 2.2 Exemplary rates of decline in population size and coral cover. Calculations are based on an initial population size of 200 million colonies, or a moderately high total coral cover of 30%, with each declining by half every decade.

Years	Population size (million colonies)	Coral cover (%)
0	200.0	30.0
10	100.0	15.0
20	50.0	7.5
30	25.0	3.8
40	12.5	1.9
50	6.3	0.9

The presented results suggest that global extinctions of Indo-Pacific corals will likely unfold over a much longer timeframe than local or regional-scale depletions, because of the broad geographic ranges and huge population sizes of many coral species. While regional-scale data on species-level abundances are scarce, coral cover for all species combined has declined in recent decades in many parts of the Caribbean (Gardner 2003) and on the Great Barrier Reef (De'ath *et al.* 2012), but has remained relatively stable in the wider Pacific (Moritz *et al.* 2018). A simple depletion model illustrates how a halving of coral cover each decade would reduce a moderately high cover of 30% to close to 1% after 50 years (**Table 2.2**). A collapse in coral abundances of such magnitude would no doubt be ecologically devastating, but the global extinction of coral species would remain unlikely. A single species with an initial modest population size of 200 million colonies, would still retain 6.25 million colonies after half a century (**Table 2.2**). The results highlight the opportunity for action to mitigate the threats to reef species, well before climate change could cause global extinctions, to make possible an eventual recovery of reef coral assemblages (Hughes *et al.* 2017a).

Chapter 3: Long-term shifts in the colony size structure of coral populations along the Great Barrier Reef

Currently in review in *Proceedings of the Royal Society B*

3.1 INTRODUCTION

Population biology is fundamentally concerned with changes in population size and structure, and with rates of birth and death that depend on sex, size and/or age. Shifts in population structure arise from temporal and spatial variation in the underlying demographic processes. Human demographers have long used the age structure of populations to reveal the impact of past mortality events such as wars or famines, and to forecast future population growth or declines (Graunt 1662; Franklin 1751). Changes in the population structure of keystone taxa affect not only their demographic performance but can have cascading effects on community composition and ecosystem functioning. The global decline in large, old trees (Lindenmayer *et al.* 2012a), for instance, implies a loss of critical habitat, food and carbon storage (Lindenmayer & Laurance 2017). Such detailed demographic data are, however, rarely available for populations of wild animal and plant species, which limits our ability to identify the processes underlying population decline and to assess long-term population viability.

Reef-building corals resemble trees in their pivotal role as primary habitat providers, and in the importance of the size of individuals for population dynamics (Hughes 1984; Hall & Hughes 1996; Madin *et al.* 2014). Consequently, changes in the size structure of coral colonies have major implications for demographic performance, and for the structural complexity of the reef environment, which in turn affects fish abundance and the productivity of coral reef fisheries (Graham 2014). The size structure of coral colonies often differs markedly between species (Meesters *et al.* 2001) and is sensitive to environmental conditions (Bauman *et al.* 2013) and disturbances (Bak & Meesters 1998, 1999). However, the size

structure of local populations rarely attains a stable equilibrium due to stochastic pulses of recruitment and disturbance (DeAngelis & Waterhouse 1987; Hughes & Tanner 2000). Non-equilibrial, transient dynamics are particularly likely to be prevalent in long-lived species with highly persistent life stages (Koons *et al.* 2005).

Coral population biology and demography is commonly based on measurements of recruitment and of the size-specific survivorship, growth, fecundity and mortality of colonies (Hughes 1984; Hall & Hughes 1996). While declines in coral cover have been well documented on many reefs (Gardner 2003; De'ath *et al.* 2012), trends in the size structure of coral populations, particularly over long temporal and large spatial scales, are rarely examined. Existing studies of long-term changes in size structure have been both consistent (Miller *et al.* 2016) and inconsistent (McClanahan *et al.* 2008; Riegl *et al.* 2012) with an early hypothesis that coral populations will respond to changing disturbance regimes with shifts towards relatively more larger colonies due to reduced recruitment (Bak & Meesters 1999). These studies have, however, been constrained in their spatial scale (McClanahan *et al.* 2008; Miller *et al.* 2016) or taxonomic scope (Riegl *et al.* 2012). A better understanding of long-term and regional shifts in the colony size structure of coral taxa with different life history strategies is urgently needed. Declines in the abundance of large, highly fecund colonies (Hall & Hughes 1996) would compromise a population's fecundity, reducing its viability and ability to provide structurally complex reef habitat for other reef organisms. Conversely, a reduced abundance of small colonies may indicate declines in recruitment (Hughes & Tanner 2000; Miller *et al.* 2016).

Here, I document decadal changes in the colony size structure of coral populations in 2016 and 2017 relative to their historic baselines in 1995 and 1996, on reef crests and slopes along the 2,300 km length of the Great Barrier Reef. I examine changes in colony size structure as changes in size-class abundances and as changes in the mean, standard deviation and 10^{th} and 90^{th} percentiles of colony size on a logarithmic scale to allow for comparison with similar studies in other regions (Bak & Meesters 1999; McClanahan *et al.* 2008; Riegl *et al.* 2012; Miller *et al.* 2016). I explore these shifts in latitudinal regions with different disturbance histories, and in all major coral taxa. I place particular emphasis on changes in the abundance of large, fecund colonies and of very small colonies, as indicators of declines in reproductive output and recruitment.

3.2 MATERIALS AND METHODS

Survey locations

Coral communities and their colony size structure were assessed on the reef crest and reef slope using a nested sampling design, on replicate sites and reefs in five sectors along the length of the Great Barrier Reef (**Figure 3.1a**). Crest communities were surveyed at 1-2 m depths on 15 mid-shelf reefs, three per sector, in 1995 and again in 2017. Reef slope communities were assessed at 6-7 m depths on 15 additional mid-shelf reefs in 1996 and in 2016. At each of the 30 reefs, eight to ten 10 m line-intercept transects were run at each of four sites. All intercepting colonies were identified using the following 12 morpho-functional benthic groups of hard corals: *Isopora*, *Montipora*, tabular *Acropora*, other *Acropora*, favids (species and genera from the formerly recognized family Faviidae, now mostly reclassified as merulinids (Huang *et al.* 2011)), *Porites*, *Pocillopora damicornis*, *Stylophora*, *Seriatopora*, Mussidae, other *Pocillopora* and other scleractinians. A total of 40,105 intercepts was recorded across all years, habitats, taxa and sectors. Elsewhere, spatial patterns in the taxonomic composition of these coral assemblages (Hughes *et al.* 2012) and long-term shifts in coral recruitment onto settlement panels on the 30 reefs were examined (Hughes *et al.* 2019a).

Statistical analyses

To examine trends in colony size structure, I used colony intercept lengths as a proxy for colony size (McClanahan *et al.* 2008; Riegl *et al.* 2012). I examined trends in the colony size structure of individual taxa and entire communities (i.e. pooled across all taxa), both in terms of changes in size-class abundances and as changes in the mean and standard deviation, as well as the 10^{th} and 90^{th} percentile of colony size as indicators of changes in the relative abundance of small and large colonies (**Figure 3.1b**). Notably, an increase in the 10^{th} percentile of colony size indicates a decline in the relative abundance of small colonies. Colony size frequencies typically follow a lognormal distribution (Bak & Meesters 1998). I therefore log-transformed intercept data for all analyses. Because sample sizes of some taxa were small at the scale of individual reefs and sectors, I pooled and analysed taxon-specific trends at the scale of the GBR. To examine changes in size-class abundances, I binned log-transformed intercept lengths into quintiles (1^{st} quintile: small, 2^{nd} to 4^{th} quintile: medium-sized, 5^{th} quintile: large) (**Figure 3.1b**). Colony size structures often vary widely between

taxa, habitats and regions (Meesters *et al.* 2001). Bin boundaries were therefore allowed to vary between taxa, habitats and sectors, but fixed across survey years. I used bootstrap resampling (n = 1000) to assess uncertainties in size-class abundances.

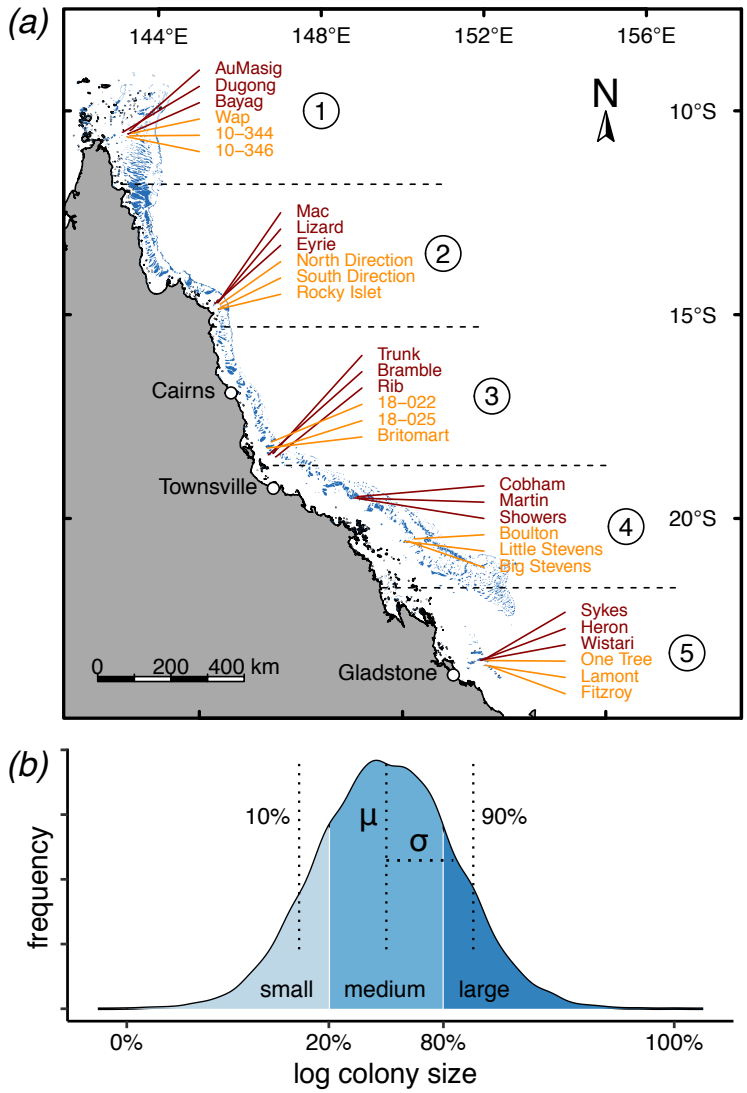

Figure 3.1 Map of survey locations and colony size metrics. *(a)* Map showing locations of reefs on which crest (red) and slope (orange) communities were surveyed in five sectors along the length of the Great Barrier Reef. Blue polygons show the locations of individual reefs. *(b)* Size structure metrics used to measure changes in size-class abundances (small, medium, large: based on quintiles) and changes in the moments of colony size structure (mean (μ), standard deviation (σ), 10th percentile, 90th percentile).

To examine changes in the mean (μ), standard deviation (σ), and the 10th and 90th percentile of colony size, both in communities and individual coral taxa, I fitted multi-level multiple linear regression models to the log-transformed intercept data, in which μ and σ of size structure were modelled as functions of year, habitat and sector (and their interactions) for community-level analyses, and as functions of year, habitat and taxon (and their interactions) for taxon-specific analyses (pooled across sectors). All modelling analyses were carried out in a Bayesian framework with brms (Bürkner 2017). This procedure allowed me to estimate 95% Highest Posterior Density Intervals (HPDI) for μ and σ, and to derive HPDIs for the 10th and 90th percentiles of colony size using the posterior draws of μ and σ. All models were run with weakly informative priors, 2000 iterations (warmup = 200) in each of three chains, and with a thinning rate of 5. I examined chain mixing, carried out posterior predictive checks to examine model fit, and used the Gelman-Rubin convergence statistic (R-hat) to examine model convergence.

3.3 RESULTS

The abundance of coral colonies declined sharply across all size classes in all sectors, with the exception of the far south, on both the reef crest and slope, and in almost all taxa (**Figure 3.2** and **Figure 3.3**). These declines were accompanied by declines in coral cover, on average (mean ± SD, n = 30), from 41.0% (± 15.6%) to 16.3% (± 15.3%) on reef crests and from 34.6% (± 12.5%) to 22.3% (± 13.8%) on reef slopes. At the scale of the Great Barrier Reef, the abundance of small colonies (in the first quintile in 1995 or 1996) declined by 76.1% (95% CI: 74.3% - 77.7%) on the crest and 57.2% (54.2% - 60.1%) on the slope (**Figure 3.2b**). The overall abundance of large colonies (in the 5th quintile) also decreased sharply, by 62.7% (59.9% - 65.1%) on the crest and 30.7% (26.3% - 35.6%) on the slope. The overall abundance of medium-sized corals (in the 2nd to 4th quintile) also declined, on crests by 52.2% (50.4% - 54.0%) and on slopes by 27.5% (24.4% - 30.2%) (**Figure 3.2b**).

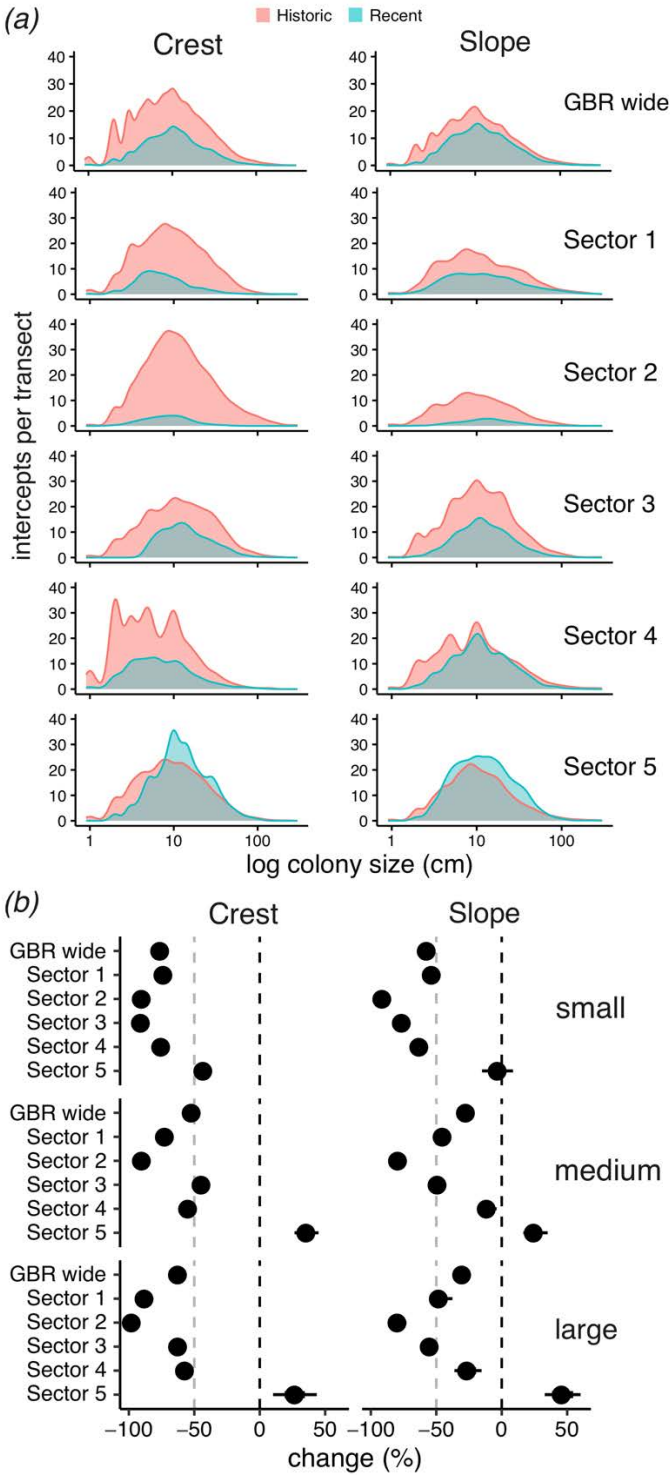

Figure 3.2 Changes in the colony size structure of crest (left) and slope (right) communities by sector. *(a)* Coral colony size structure of historic (1995/1996) and recent surveys (2016/2017) are shown for each of five sectors (1: Far North to 5: Far South) and pooled across all sectors (top). *(b)* Changes in the abundance of small, medium-sized and large colonies by sector and habitat. Percentage changes in reef-level abundances are defined as changes in the number of intercepts in the 1st quintile (small), 2nd to 4th quintile (medium) and

5th quintile (large) of colony size. All estimates are shown as 95% highest density intervals. The point indicates the median, the thick line the 66% confidence interval and the thin line the 95% confidence interval.

Declines in size-class abundances were most pronounced on all reefs in sectors 1-3 in the northern half of the Great Barrier Reef (**Figure 3.2a**), which experienced extreme thermal stress in 2016 and 2017. In these three sectors, the abundance of large colonies (in the 5th quintile) on the crest dropped by 88.2% (95% CI: 85.1% - 91.1%), 97.9% (96.7% - 98.9%) and 62.0% (55.0% - 68.1%) respectively, and by 48.1% (38.6% - 56.6%), 86.4% (73.9% - 86.4%) and 55.3% (47.4% - 61.4%) on the slope (**Figure 3.2b**). The declines were less severe on reefs in sector 4 where large colonies declined by 57.1% (50.5% - 62.7%) on the crest and by 24.5% (14.3% - 35.5%) on the reef slope. In marked contrast, on southern reefs in sector 5 the abundance of large colonies increased by 25.8% (10.1% - 41.1%) on the crest and by 46.9% (28.4% - 66.4%) on the slope (**Figure 3.2b**).

Similar geographic patterns emerged in trends in the abundances of small colonies (in the 1st quintile). On the reef crest, the abundances of small colonies declined consistently across all sectors. In sectors 1 to 4 the abundance of small colonies dropped by 74.3% (95% CI: 69.5% - 78.5%), 90.1% (87.8% - 92.2%), 91.0% (88.5% - 93.4%) and 75.2% (71.9% - 78.5%), respectively (**Figure 3.2b**). Although reefs in the far south recorded the lowest declines, small colonies were still 43.6% (36.2% - 50.1%) less abundant on crests in 2016 than in 1996. On the reef slope, the abundances of small colonies declined by 54.3% (46.7% - 61.6%) in sector 1, 91.5% (87.6% - 94.5%) in sector 2, 76.1% (71.8% - 79.9%) in sector 3, and 62.7% (57.6% - 67.1%) in sector 4 (**Figure 3.2b**), and remained stable in sector 5 (95% CI: -15% - +9.1%).

The decline in numbers of small, medium and large colonies was remarkably consistent across all major taxa, on both crests and slopes (**Figure 3.3**). The abundance of small colonies on the reef crest declined by at least 50% in 11 of the 12 major taxa, with half of them losing >75% of their small colonies (**Figure 3.3b**). The exception was other *Pocillopora*, which lost 28.0% (1.7% - 52.0%) of its small colonies. Declines were less severe on the reef slope, where 9 out of 12 taxa lost at least half of their small colonies. Small colonies of tabular *Acropora* and other *Pocillopora* were comparatively less affected, but still declined, on average, by 12.2% (-32.9% - +13.6%) and 30.2% (-71.6% - +18.9%) respectively (**Figure 3.3b**).

Changes in the abundances of large colonies (in the 5th quintile) varied between taxa. Numbers of large colonies declined by > 50% in 8 out of 12 of the taxa on the crest and in 5 taxa on the reef slope (**Figure 3.3b**). Slow-growing, long-lived groups like the Poritidae and Mussidae suffered comparatively minor losses of large colonies. Large colonies of Poritidae declined by 14.9% (-30.6% - +1.6%) on crests, and 23.8% (10.3% - 35.2%) on slopes. Large Mussidae increased by 8.8% (-41.4% - +81.3%) on crests but declined by 50.5% (28.1% - 71.1%) on slopes. Large colonies (in the top quintile) of the genus *Seriatopora* declined by 100% (100% - 100%) on the reef crest, and by 49.6% (29.6% - 87.9%) on the reef slope.

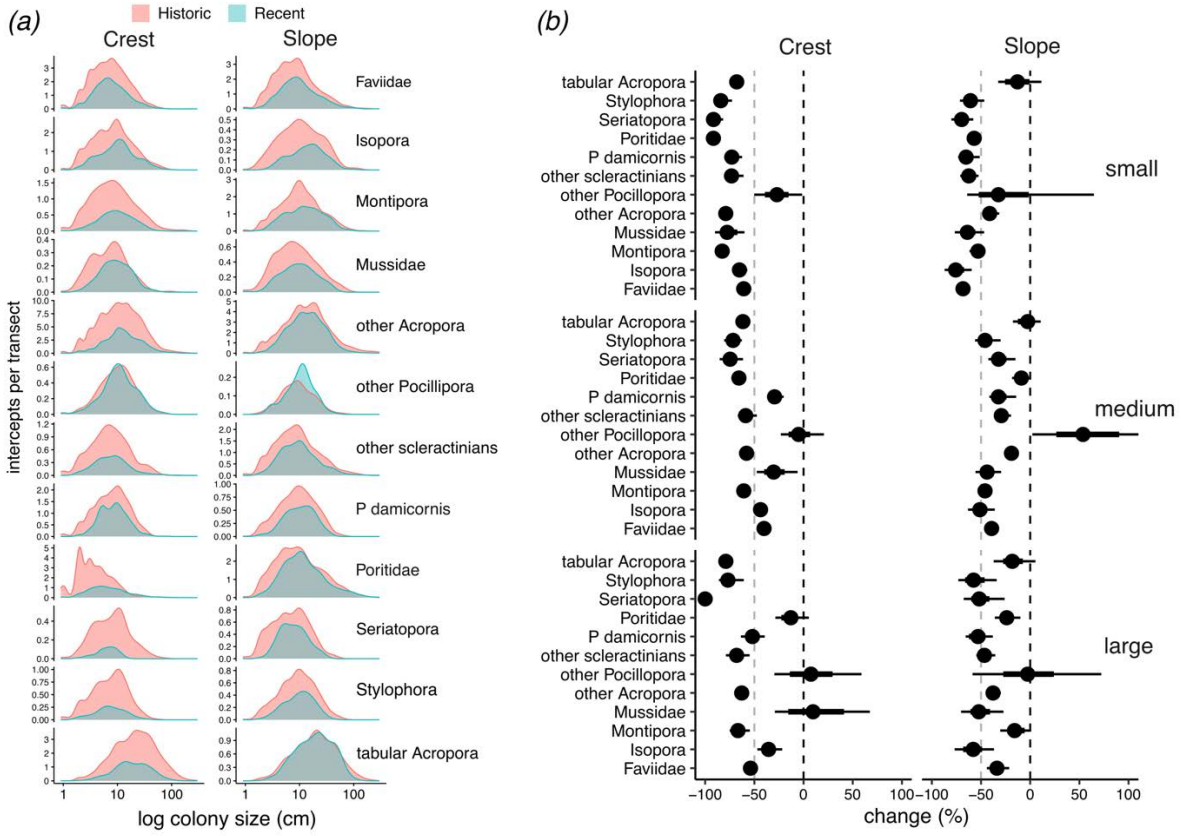

Figure 3.3 Changes in the colony size structure of major coral taxa. *(a)* Colony size structure of historic (red, 1995/1996) and recent surveys (blue, 2016/2017) are shown for each of 12 coral taxa on reef crests (left) and reef slopes (right). *(b)* Changes in the abundance of small, medium-sized and large colonies by taxa and habitat. Percentage changes in absolute abundances are defined as changes in the number of intercepts in the 1st quintile (small), 2nd to 4th quintile (medium) and 5th quintile (large) of intercept lengths. All estimates are shown as 95% highest density intervals. The point indicates the median, the thick line the 66% confidence interval and the thin line the 95% confidence interval.

The abundance of medium-sized colonies (2nd to 4th quintile) also declined in most taxa and habitats. On the crest, 7 of the 12 examined taxa lost at least half of their medium-sized colonies. Medium-sized colonies of the genera *Seriatopora* (-63.9% - -86.1%) and *Stylophora* (-62.5% - -78.5%) were the most affected. On the slope, the abundance of medium-sized colonies approximately halved in 4 of the 12 taxa, remained stable in tabular *Acropora* (-17.5% - 11.3%) and Poritidae (-17.6% - +0.8%), and increased by 55.1% (-6.2% - +134.3%) in other *Pocillopora* (**Figure 3.3b**).

While before-after coral abundances on both the reef crest and reef slope declined across all size classes (**Figure 3.2** and **Figure 3.3**), colonies in the 10th percentile were larger in 2016 and 2017 (Figure 3.4), due to the disproportionate loss of small colonies. In contrast, colonies in the 90th percentile of colony size remained stable in size. The disproportionate decline in small colonies resulted in a systematic narrowing of colony size structures, across habitats, sectors and taxa (**Figure 3.4**), as indicated by declines in the standard deviation (sigma) of colony size. For both crest and slope communities the standard deviation of colony size was remarkably similar between sectors in 1995 and 1996 but was consistently lower across all sectors and more variable between sectors in the recent surveys. Increases in the 10th percentile of colony size, indicating declines in the relative abundance of small colonies, were particularly pronounced in the central and southern regions of the GBR (sectors 3 to 5), and changed comparatively little in crest communities of sectors 1 and 2 (**Figure 3.4**).

The size of the largest colonies (90th percentile) remained stable on reef slopes in all sectors and on crest communities in sectors 3 to 5 (**Figure 3.4**). Combined with the disproportionate loss of small colonies, this resulted in consistent increases in mean colony size across all sectors and habitats, with the exception of crest communities in sector 1 and 2, where mean colony size decreased by 20.0% (14.7% - 24.7%) and 27.7% (21.9% - 32.9%) respectively. On the crests in sectors 3 to 5, mean colony size increased by 23.3% (16.5% - 29.8%), 21.0% (14.5% - 28.2%) and 30.4% (24.6% - 36.3%) (**Figure 3.4**). On the reef slope, mean colony size increased consistently across sectors, by up to 32.1% (17.5% - 48.2%) (sector 2). A North-South gradient was particularly evident on the reef crest, where size structures shifted more in the south towards larger mean colony sizes, with relatively fewer small and more large colonies (**Figure 3.4**). By contrast, shifts in colony size structure were consistent across sectors on the reef slope.

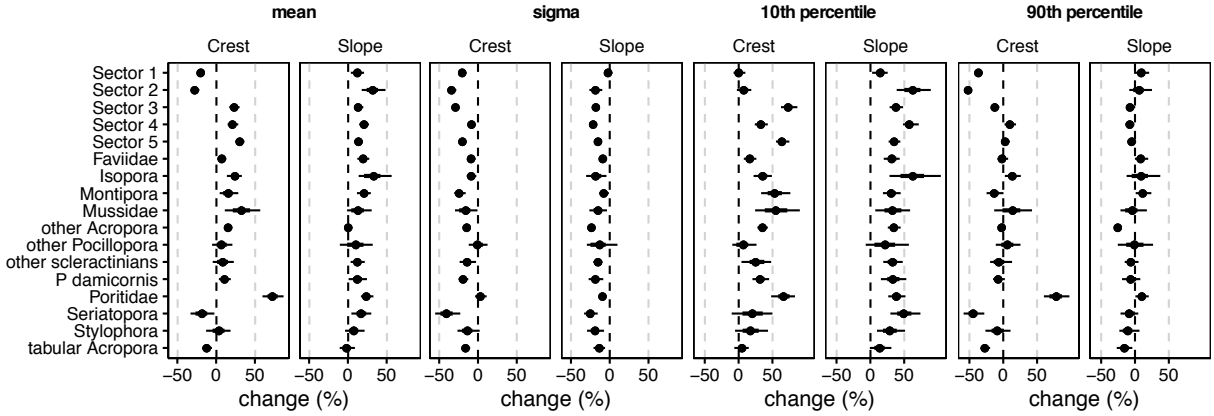

Figure 3.4 Changes in the mean, standard deviation (sigma) and 10th and 90th percentile of the colony size structure of crest and slope communities in five sectors, and of individual taxa (pooled across sectors). Percentiles are indicators for the relative abundance of small (10th) and large (90th) colonies, where an increase in the 10th percentile indicates a decrease in the relative abundance of small colonies. All estimates are shown as 95% highest posterior density intervals (HPDI) where the point indicates the median, the thick line the 66% credible interval and the thin line the 95% credible interval.

The size structure of individual taxa also changed markedly (**Figure 3.4**). The size of the smallest colonies (10th percentile) increased consistently across all taxa and habitats (**Figure 3.4**), while the size of the largest colonies (90th percentile) remained comparatively stable except for crest populations of tabular *Acropora* and *Seriatopora* (**Figure 3.4**). As a result, mean colony size increased, and the standard deviation of colony size (sigma) decreased in most taxa and habitats. Changes were particularly pronounced in corals of the genus *Seriatopora* and the family Poritidae. The colony size structure of Poritidae shifted towards larger colonies indicated by increases in mean colony size (crest: 72.7% (60.6% - 88.9%), slope: 24.1% (15.3% - 32.2%)), increases in the size of large colonies (90th percentile, crest: 78.2% (60.2% - 95.8%), slope: 11.0% (-0.8% - +20.9%)), and by marked increases in the size of small colonies (10th percentile, crest: 67.5% (49.5% - 85.9%), slope: 38.0% (26.2% - 51.3%)). Corals of the genus *Seriatopora* suffered sharp declines in the relative abundance of both small and large colonies, as indicated by increases in the 10th percentile of colony size (crest: 21.5% (-10.8% - + 54.2%), slope: 50.2% (28.2% - 70.0%)) and decreases in the 90th percentile (crest: 44.8% (29.1% - 57.4%), slope: 9.8% (-20.7% - +4.1%)), resulting in a pronounced narrowing of their colony size structure (**Figure 3.4a**). Large colonies of tabular

Acropora declined in size by 26.7% (19.3% - 33.2%) on the reef crest and by 16.0% (4.7% - 25.5%) on the reef slope (**Figure 3.4**).

3.4 DISCUSSION

This study documents the systematic decline of absolute coral abundances across size classes, habitats, sectors and taxa on the Great Barrier Reef over the last two decades. Sharp declines in the abundances of medium-sized and, in particular, highly fecund large colonies signal the depletion of coral brood stock required to replenish diminished populations (**Figure 3.2** and **Figure 3.3**). The simultaneous, disproportionate decline in the abundance of small colonies, by 76.1% on the crest and 57.2% on the slope (**Figure 3.2** and **Figure 3.3**), corroborates findings that the depletion of coral brood stocks impaired coral recruitment rates on the Great Barrier Reef following mass coral bleaching in 2016 and 2017 (Hughes *et al.* 2019a).

Here I used colony line-intercept lengths as proxy for colony size to estimate shifts in colony size structure from commonly collected line-intercept transect data. This quantity is not a direct measure of colony size, in the sense that a larger colony could theoretically have a smaller line intercept than a smaller colony, depending on which part of the colony is intersected by the transect. However, the conclusion that the colony size structure of coral populations has fundamentally shifted along the Great Barrier Reef over the last decades is robust because (1) I examine relative rather than absolute changes in size-class abundances and size structure, (2) because a long intercept is always statistically more likely to stem from a large colony than a shorter intercept, and thus locations where intercept lengths tend to be longer, on average, will also tend to have larger colonies on average, and (3) because, for studies of this kind, sampling biases are unlikely to vary systematically between taxa, or over space and time, given sufficient sample size (McClanahan *et al.* 2008).

The presented results support the hypothesis that, in deteriorating reef environments, coral populations can exhibit a disproportionate loss of small coral colonies due to the depletion of brood stocks and the resulting decline in recruitment rates, as witnessed on reefs in the Caribbean (Bak & Meesters 1999). In contrast, my findings are inconsistent with alternative suggestions that naturally higher recruitment rates on many Indo-Pacific (compared to

Caribbean reefs (Smith 1992)) may instead effect increases in the relative abundance of small colonies, as reefs recover, as well as decreases in mean colony size and in the abundance of large colonies, as found in the Red Sea (Riegl *et al.* 2012) and Kenya (McClanahan *et al.* 2008). In the Red Sea, recruitment rates remained constant following coral mass bleaching (Riegl *et al.* 2012) but declined by 89% compared to historic baselines on Australia's Great Barrier Reef in the aftermath of back-to-back mass bleaching events in 2016 and 2017 (Hughes *et al.* 2019a). In demographically open populations, the relationship between brood stocks and recruitment may be obscure at local scales but emerges at the scale of larval dispersal (Hughes *et al.* 2000, 2019a). Discrepancies in post-disturbance changes in recruitment between reefs in the Red Sea and on the GBR may reflect differences in the severity, extent or patchiness of disturbance impact.

Geographic patterns in trends in size-class abundances are likely to reflect the history of recent reef disturbances on the Great Barrier Reef. Changes were most pronounced in the Northern and Central sectors of the Reef, which experienced extreme thermal stress in 2016 and 2017. Size-class abundances on reefs in the far South remained comparatively unchanged (**Figure 3.2** and **Figure 3.3**). Although crest communities in sectors 1 and 2 shifted towards relatively more small colonies, declines in their absolute abundances of 74.3% and 90.1% respectively (**Figure 3.2b**) indicate that this outcome should not be misconstrued as signs of resilience or recovery. Shifts towards smaller colonies may be attributable to the lower bleaching susceptibility of recruits (Mumby 1999) and juveniles (Álvarez-Noriega *et al.* 2018), and to the partial mortality of medium-sized and large colonies.

As reef disturbance regimes continue to change and escalate (Hughes *et al.* 2018a), with virtually all reefs in the world projected to experience annual severe bleaching conditions before the end of the century under current emission trajectories (Van Hooidonk *et al.* 2016), the window for the recovery of populations and assemblages between consecutive mass mortality events is shrinking. Populations, in particular of slow-growing and late-maturing taxa, may no longer be afforded sufficient time to recover pre-disturbance brood stocks and population-levels of reproductive output (Hall & Hughes 1996). Allee effects at low densities of sexually-mature conspecific colonies may further impair the successful fertilization of eggs, particularly in rare and severely depleted species (Oliver & Babcock 1992; Teo & Todd 2018). Lower mortality rates of large individuals may provide temporary refuge from population decline and recruitment failure, but may mask the erosion of population viability if

trends in the decline in smaller colonies are overlooked (Hughes & Tanner 2000). For instance, the abundance of large slow-growing, long-lived poritid and mussid corals changed comparatively little in this study, but both taxa suffered dramatic losses of small colonies, particularly on the reef crest (poritids: 91.3%, mussids: 77.6%) (**Figure 3.3b**).

The implications of shifts in colony size structure extend beyond demography because they also affect the ability of corals to perform ecological functions. Most notably, the largest colonies in a population or community contribute disproportionately to reproduction (Hall & Hughes 1996), and therefore to the genetic make-up of future generations (Hughes *et al.* 1992), but also provide essential habitat for other reef organisms like fish (Kerry & Bellwood 2015). Declines in the abundance of large colonies thus reduce the productivity of reef ecosystems, and fisheries (Graham 2014), both directly, through declines in the availability of coral gametes, larvae and recruits, which constitute important sources of food for fish (Pratchett *et al.* 2001) and other reef organisms including corals (Fabricius & Metzner 2004), and indirectly, through the loss of structural complexity and habitat. In the Caribbean, the abundance of *Acropora cervicornis* and *Acropora palmata*, two branching coral species with complex morphology, has declined steeply, especially since the 1980s (Bruckner 2002; Gardner 2003), indicating that the historical baseline of what constitutes the colony size structure of an "undisturbed" population or assemblage has likely shifted on many reefs for decades, if not centuries or millennia (Jackson *et al.* 2001). Large-scale long-term trends in the abundance of large old corals and their unique ecological roles remain largely under-explored, compared to similar studies in trees (Lindenmayer *et al.* 2012a; Lindenmayer & Laurance 2016, 2017).

This study demonstrates the importance of examining the abundance of colony sizes beyond the traditional focus on coral cover (Dornelas *et al.* 2017), to improve our understanding of the demographic processes underlying declines in coral cover, such as recruitment failure and the depletion of brood stock, and our ability to predict the likely trajectories of coral populations. As the depletion of coral populations and the erosion of the structural complexity of reef habitat continues, and the frequency of reef disturbances increases (Hughes *et al.* 2018a), we urgently need better data on demographic trends in corals (Edmunds & Riegl 2019).

Chapter 4: Beyond cover: reconstructing the population size structure from line-intercept data for demographic inference

Manuscript in preparation

4.1 INTRODUCTION

Measuring the abundance and characteristics of organisms requires trade-offs between the quantity (spatial and temporal coverage and replication) and quality (accuracy, detail, taxonomic resolution, invasiveness) of the data collected. Technological advances have expanded the scope of what is measurable and alleviated, or eliminated, some trade-offs in sampling design. However, as measurement methods proliferate, are continuously refined and replaced, the compatibility of methods and data becomes an increasing problem. For instance, alterations to the sampling protocol of a long-term study or comparisons to historical data require careful consideration of the backward compatibility of methods and data. Similarly, data collected on the same study system but by different methods can only be integrated if measurement units are compatible or convertible.

Ecologists traditionally gather data on the abundance of organisms to examine trends in populations and ecosystems. The abundance of solitary organisms like mammals and birds is commonly measured as counts of individuals, the abundance of sessile organisms like plants and benthic invertebrates as percent cover, particularly for monitoring purposes. Detailed studies of population dynamics are typically too time-consuming and costly to conduct at spatial and temporal scales relevant for the conservation of populations and species. For instance, data on trends in demographic composition (e.g. age and sex structure), which have long informed projections of population growth in humans (Graunt 1662; Franklin 1751), are rarely available for wild animal and plant species. Changes in population structure and density can have profound implications on population dynamics by affecting growth, mortality and reproduction, and thus population viability. Such demographic shifts can be masked by invariant abundance data, which makes it hard to predict long-term population viability, and

can lead to unjustified optimism about the conservation status of species and ecosystems. For example, population changes in the abundance of organisms in capture fisheries has often proven much less dramatic than reductions in their size distributions, even though the latter is a better prediction of collapse (Pauly *et al.* 2013; Clements *et al.* 2017).

The line intercept transect method

The line-intercept transect (LIT) method (Canfield 1941) has been widely used for decades to measure the percent cover of sessile organisms like plants and benthic invertebrates (Loya 1978). A transect tape is extended to create a transect across the study site. Individuals intercepted by the tape are identified and intercept lengths are recorded. By dividing the sum of all intercept lengths by the total length of the transect an estimate of percent cover is derived. Both basal and canopy cover can be measured. The LIT method thus implies a sequential reduction in dimensionality from the three-dimensional habitat to the one-dimensional intercept length to the typically reported 0-dimensional estimate of percent cover (**Figure 4.1**). Percent cover is an efficient and effective way to measure the abundance of organisms that compete for limited space and light and typically vary widely in individual size, but does not capture population size structure and density, important indicators of reproductive output (e.g. Hall and Hughes 1996) and fertilization success (e.g. Oliver and Babcock 1992) in modular sessile organisms.

The distribution of intercept lengths can be used as a proxy for the distribution of individual colony sizes, with longer intercepts statistically more likely to be contributed by larger individuals. However, because most demographic quantities tend to be measured as functions of projected area (or less commonly surface area or volume) (Madin *et al.* 2014; Álvarez-Noriega *et al.* 2016; Dornelas *et al.* 2017) LIT data need to be transformed into these latter dimensions in order to quantitatively assess the demographic implications of changes in size structure. Simply squaring the linear measurement, or treating it as the diameter (e.g. Connolly et al. 2005) or radius (e.g. Zawada et al. 2019) of a circle, may introduce biases for several reasons. First, linear intercepts of colonies are secants, not necessarily diameters, and the probability distribution of secant lengths, relative to diameter, may be complex and size-dependent. Second, because the likelihood of an individual being intercepted by the transect tape is proportional to its size, larger individuals will be statistically overrepresented in the distribution of intercept lengths. Consequently, attempts to reconstruct the distribution of

individual sizes underlying a measured distribution of intercept lengths that fail to address these biases are unlikely to produce reliable results.

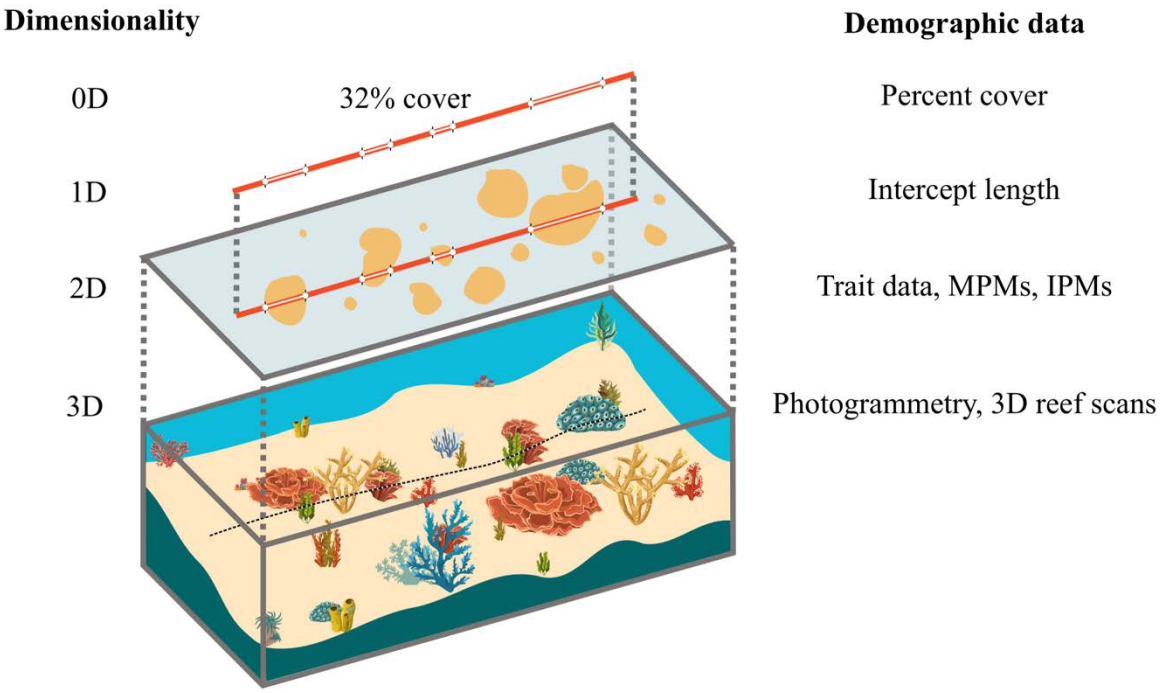

Figure 4.1 The spatial dimensionality of line intercept transects and demographic data. Line intercept transects reduce the three-dimensionality of the environment to zero-dimensional estimates of percent cover via one-dimensional measures of intercept length. In contrast, more detailed demographic data are usually based on two-dimensional estimates of individual size (planar area). Such data include matrix projection models (MPMs) and integral projection models (IPMs) and size-dependent trait data like the size-fecundity relationship. New survey methods capture the full three-dimensionality of the habitat.

Here I present a new method that allows the size structure of individuals in a population or community to be reconstructed from line-intercept transect data. The method explicitly accounts for the two statistical biases through an optimisation algorithm that reverse-engineers the sampling process of the LIT method. I demonstrate how this method can leverage the potential of routinely collected LIT data for demographic inference using the example of reef-building corals on Australia's Great Barrier Reef (GBR). I first reconstruct the colony size structure of coral populations from LIT data collected along the length of the GBR, across a period of unusual and substantial population disturbances, including mass bleaching events, severe tropical cyclones, and outbreaks of the crown-of-thorns starfish *Acanthaster planci*. I

then use the reconstructed colony size structures to examine decadal changes in the reproductive output of different coral taxa per m^2 reef habitat, using knowledge of a taxon's size-fecundity relationship (Hall & Hughes 1996). I contrast changes in colony size structure, fecundity and colony density with changes in coral cover to emphasise the value of understanding changes in coral size, and to provide a more comprehensive overview of long-term demographic trends in corals on the GBR.

4.2 MATERIALS AND METHODS

Survey data

Crest and slope communities were repeatedly surveyed using LIT methods, on 30 reefs along the entire length of the Great Barrier Reef. Crest communities were surveyed on 15 reefs both in 1995 and again in late 2017 and slope communities on 15 reefs in 1996 and again in late 2016. In between these two surveys, the region experienced a series of large-scale disturbances including several cyclones, four mass bleaching events (in 1998, 2002, 2016 and 2017) as well as two outbreaks of the crown-of-thorns starfish *Acanthaster planci*. In response, coral abundances declined significantly (De'ath *et al.* 2012), community composition shifted (Hughes *et al.* 2018b) and coral recruitment rates declined by 89% (Hughes *et al.* 2019a). The exception was reefs at the far southern end of the Great Barrier Reef, which escaped recent mass mortality events relatively unscathed, but were heavily impacted by a recent bleaching event in 2020.

At each reef, eight to ten 10m line-intercept transects were conducted at each of four sites. All intercepted colonies were identified using the following key of 12 morpho-functional groups of benthic hard corals: *Isopora*, *Montipora*, tabular *Acropora*, other *Acropora*, favids (species and genera from the formerly recognized family Faviidae but now largely reclassified as merulinid corals), *Porites*, *Pocillopora damicornis*, *Stylophora*, *Seriatopora*, mussids, other *Pocillopora* and other scleractinians. In total, 41,105 intercepted colonies were recorded across all years, habitats, taxa and sectors.

Reconstruction of size structure from LIT data

This LIT data describes the intersection of several line transects with an underlying distribution of non-overlapping polygons in the plane (**Figure 4.2a**). The goal of this method

is to reconstruct the size distribution of the underlying polygons from a recorded distribution of intercept lengths. This inverse problem is a geometric and statistical challenge not unique to the survey of coral communities. The process (illustrated in **Figure 4.2**) involves five major steps:

(1) A theoretical population of circular coral populations is simulated, with planar areas that follow a lognormal distribution defined by initial parameter guesses of the mean (μ) and standard deviation (σ) of the lognormal distribution.
(2) Line intercept transects are simulated through this population by randomly intersecting each colony in the population to obtain a simulated distribution of intercept lengths F_{sim}.
(3) The divergence between the simulated distribution of intercept lengths F_{sim} and the empirical distribution of intercept lengths recorded in the field F_{emp}. is statistically examined.
(4) The divergence between F_{sim} and F_{emp} is minimized to find the parameters μ and σ of the lognormal distribution that are most likely to underlie a measured distribution of intercept lengths F_{emp}.
(5) The goodness of fit is examined.

In this process, I make two major assumptions. First, that coral colonies can be approximated by non-overlapping circles in the plane. This assumption arguably oversimplifies the often complex three-dimensional coral morphologies, and reef topographies consisting of canopies, understories and cryptic habitats (Goatley & Bellwood 2011) and disregards growth-form dependent departures from roundness, particularly in taxa with frequent partial colony mortality events.

My second major assumption is that the distribution of colony areas follows a lognormal distribution. I opt for the lognormal distribution because the distribution of log-transformed colony sizes, commonly measured as their planar or projected areas (Hughes 1984; Hall & Hughes 1996; Bak & Meesters 1998; Madin *et al.* 2014; Dornelas *et al.* 2017), typically follows a normal distribution (e.g. Vermeij & Bak 2000). The lognormal distribution commonly arises in other natural phenomena including the distribution of coral abundances (Connolly *et al.* 2005), is a flexible model that can take a variety of shapes and has only two parameters. However, the method is flexible with regard to assumptions about the underlying distribution of individual sizes. Alternative distributions commonly used to describe size

spectra include the exponential distribution, the heavy-tailed Weibull distribution and the power law probability distribution (e.g. Muller-Landau *et al.* 2006; White *et al.* 2008).

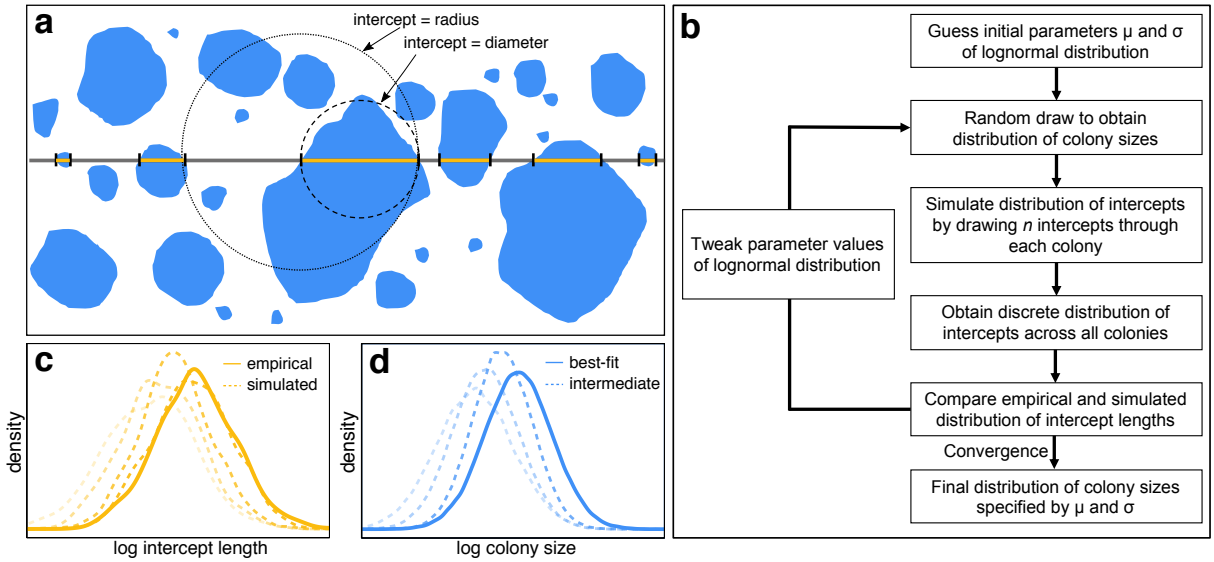

Figure 4.2 Reconstructing population size structure from line intercept transect data. **(a)** Schematic representation of the line-intercept transect method. Blue polygons indicate contours of coral colonies, the grey line the transect tape, the orange lines the intercepts of each colony with the transect tape and the dashed circles the approximation of colony sizes by using the intercept as the radius (Zawada *et al.* 2019) or diameter (Connolly *et al.* 2005) of a circle. **(b)** Optimisation algorithm used to reconstruct the colony size structure from recorded LIT data. Best-fit parameters μ and σ of the lognormal distribution of colony sizes are determined by minimizing the Kullback-Leibler divergence between the empirical distribution of intercept lengths and the simulated distribution of intercept lengths, which is generated by drawing n (proportional to colony diameter) random intercepts through each colony drawn from a lognormal distribution of colony sizes. **(c)** Density plot showing the distribution of intercept lengths recorded in the field (empirical) and the distribution of intercept lengths iteratively simulated by the optimisation routine. **(d)** Density plots showing the best-fit distribution of colony sizes and intermediate steps.

I adopted and modified an approach proposed by Pandi & Ranade (2016) to estimate the colony size structure from the measured distribution of intercept lengths (the method was developed to estimate particle sizes from focused beam reflectance measurements). Pandi & Ranade (2016) applied an optimisation routine to solve the inverse problem of finding the distribution of circle geometries that is most likely to underlie a measured distribution of

intercept lengths. I adapt it as follows. I start with an initial guess of the parameters μ and σ of a lognormal distribution (**Figure 4.2b**). I randomly draw 1,000 samples from a lognormal distribution with random initial parameters μ and σ to obtain a sample distribution of colony sizes *LN* (μ, σ). For each of these colonies, I generate *n* random intercepts where *n* is proportional to the diameter of the colony. This addresses the sampling bias of the LIT method that the likelihood of an individual intercepting with the transect tape is proportional to its size.

To address the second bias, the generation of random intercepts, I consult Bertrand's probability paradox (Bertrand 1889), according to which three methods exist for generating the chord length distributions that result from a random intersection with a circle of a given radius: the random endpoints method, the random radius method and the random midpoint method. Bertrand's paradox is that these methods are all equally valid but produce different results. I followed an approach (Aerts & de Bianchi 2014; Li 2017) that treats each method as equally likely or plausible to generate a joint distribution of chord lengths through a circle with a unit diameter (**Figure 4.3**). I randomly draw from this chord distribution *n* times for each simulated colony, where *n* is proportional to colony diameter and chosen to be 1 for the smallest colony in the sample, and multiply each drawn intercept by the actual diameter of the colony. The result is a distribution of intercept lengths F_{sim} that results from the initial parameter choices $LN(\mu, \sigma)$.

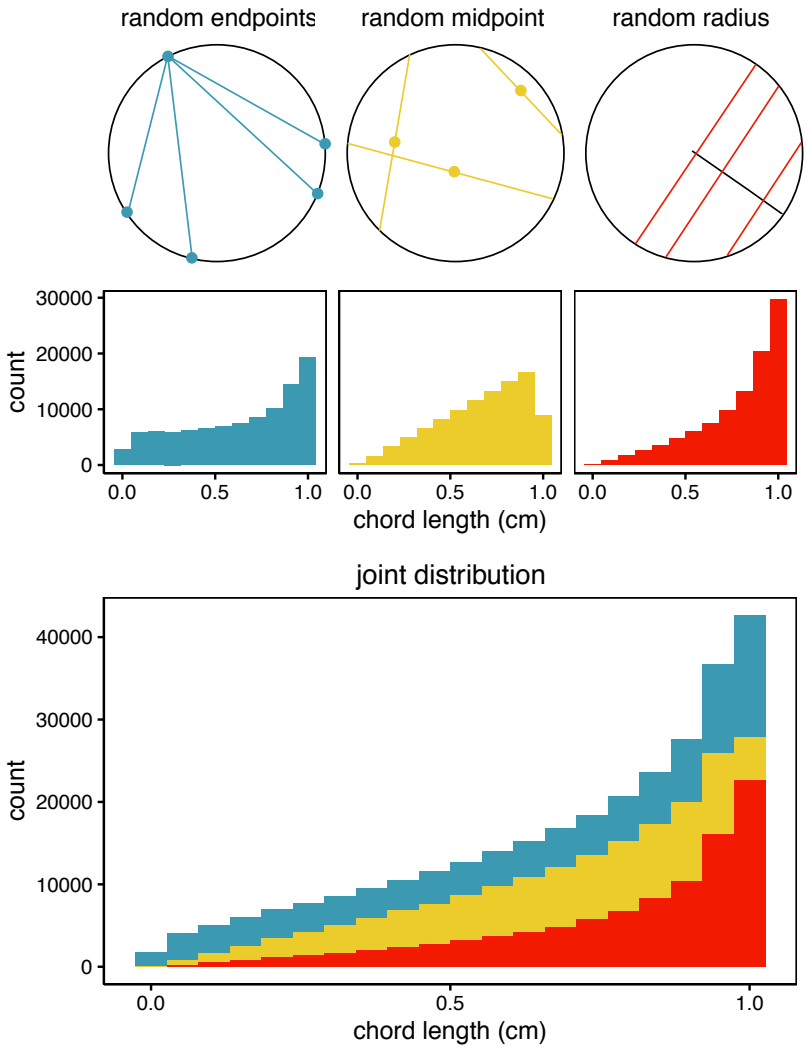

Figure 4.3 Random intercept generation. Distribution of intercept or chord lengths randomly generated using the random endpoint, random midpoint and random radius method (top) and the joint distribution of the three methods combined (bottom).

I then use a Nelder-Mead optimisation algorithm to search for values of μ and σ that minimize the Kullback-Leibler divergence (Kullback & Leibler 1951) between the empirical and the simulated distribution of intercept lengths. This algorithm was chosen because it is robust to noisy reward surfaces and does not require the function to be continuous or differentiable (an important factor, given that the theoretical distributions $LN(\mu, \sigma)$ are generated by Monte Carlo sampling).

To validate the reconstructed distribution of colony sizes I inspected quantile-quantile-plots of the empirical and simulated distribution of intercept lengths. I also compared the actual coral cover at a survey site, readily calculated as the sum of intercept lengths relative to the total transect length, with the coral cover predicted by combining the best-fit distribution of colony sizes with estimates of local colony density, which can be estimated from LIT data (Marsh *et al.* 1984). I compared the predictive accuracy of the presented approach with the predictive accuracy of two simplified approaches that assume that treating the intercept as the diameter (Connolly *et al.* 2005) or the radius (Zawada *et al.* 2019) of a circle provide reasonable first-order approximations of the distribution of colony sizes (**Figure 4.2a**).

I applied this method to reconstruct the colony size structure of coral populations on the Great Barrier Reef. Specifically, I investigated decadal changes in the colony size structure of coral communities and individual taxa on reef crest and slopes. Changes in community size structure were examined at the scale of sectors for each habitat. For taxon-specific analyses data were pooled at the scale of the Great Barrier Reef for each habitat due to insufficient sample sizes at the scale of individual sectors. Only the results of the taxon-specific analysis are presented here but community-level analyses were included for validation purposes. I compare trends in size structure derived from the reconstruction method with trends based on raw LIT data.

I demonstrate how the reconstructed colony size structures can be used for demographic inference by estimating changes in the reproductive output of coral populations on the GBR. For this, I first estimate the colony density of each taxon using a method developed by Marsh et al. (1984). I then use estimates of a species' size fecundity relationship to calculate the reproductive output of each colony in the population and sum across all colonies to derive an estimate of reproductive output per m^2 reef. For the taxa Faviidae, other *Acropora*, *Stylophora* and tabular *Acropora* I used published estimates of size-dependent colony fecundity (Hall & Hughes 1996). I modified the approach of Hall and Hughes (1996) to simulate a linear increase in the percentage of fecund colonies from 0% to 100% between the reported minimum size of a fecund colony and the size at which all colonies were fecund using the equation

$$\log y = \log 10^{a+b\ \log_{10} x}\ \frac{(\log x - \log x_{min})}{(\log x_{all} - \log x_{min})}$$

where y is the fecundity of a colony measured as the total volume of testes produced (mm^3), x is the size of the colony measured as its projected area (cm^2), x_{min} the minimum size of a fecund colony, x_{all} the size at which all colonies were fecund, and a and b are the coefficients of models fitted by Hall and Hughes (1996). For Poritidae, *Pocillopora damicornis* and other *Pocillopora*, I calculated the total number of eggs produced by a colony of a given size using published estimates of size at maturity, polyp density and polyp fecundity. I assume that once a colony reaches sexual maturity 90% of its polyps are mature. The resulting size-fecundity relationships are indicated in **Figure 4.5**.

Because both colony density estimates (Marsh *et al.* 1984) and reconstructed size structures constitute approximations prone to deviations, estimates of colony densities were standardized by coral cover as follows:

$$\hat{\rho} = \rho_{LIT} * \frac{C_{LIT}}{C_{pred}}$$

where $\hat{\rho}$ is the standardized or corrected estimate of colony density, ρ_{LIT} the colony density estimated from the LIT data following Marsh et al. (1984), C_{LIT} the percent coral cover estimated from the LIT data and C_{pred} the cover predicted by combining estimates of colony densities and colony size structure (see method validation). This standardization ensures that estimates of changes in the reproductive output of populations are not an artefact of overestimates or underestimates of coral abundance due to errors underlying estimates of colony densities and size structure.

4.3 RESULTS

Method validation

The presented method performs significantly better at reconstructing the likely colony size distribution underlying a measured distribution of intercept lengths than two alternative approaches, which use each intercept as either the radius or diameter of a circle. Both alternative approaches, but in particular the radius method, overestimate the frequency of large colonies (**Figure 4.4a**), and as a result perform poorly at predicting coral cover (**Figure 4.4b**). While the optimisation routine exhibits minor, non-systematic deviations between predicted and true coral cover (mean ± SD = +13% ± 21%), the diameter and radius methods systematically overestimate coral cover, on average by a factor of 2 (+90% ± 119%) and 8 (+677% ± 501%) respectively (**Figure 4.4b**).

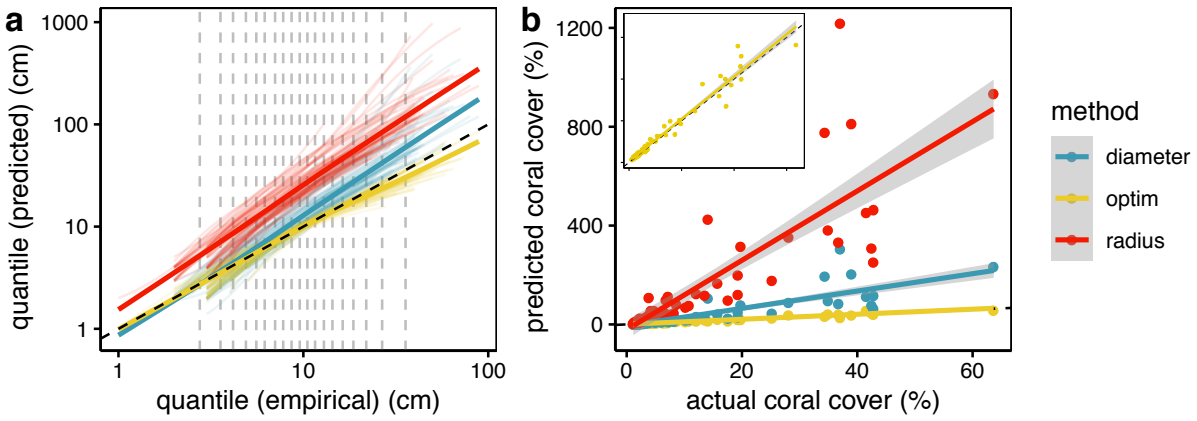

Figure 4.4 Validation of reconstruction method. Quantile-quantile plot showing the correlation between the quantiles of the empirical line-intercept data and the quantiles of the distribution of intercept lengths predicted by the optimisation algorithm and the intercept-as-diameter and intercept-as-radius methods. Thin lines indicate the q-q correlation for each taxon, thick lines the q-q correlation across all predictions, the dashed diagonal the unity-line and vertical dashed lines the position of the average empirical quantile across all taxa. **(b)** Correlation between actual coral cover of taxa, calculated as the sum of all intercept lengths divided by the length of the total transect, and the 2-dimensional estimate of coral cover derived from estimates of colony density and the reconstructed colony size structures. The dashed diagonal line indicates the unity line. The inset plot shows the predictive accuracy of the optimisation routine in more detail.

Table 4.1 Predictive accuracy of size structure approximation methods across range of sizes measured as the mean percent deviation of the predicted percentiles of intercept length from the corresponding empirical percentiles of intercept length.

Percentile	Intercept as diameter	Intercept as radius	Optimisation routine
5%	-17% (±19%)	54% (±36%)	-21% (±17%)
10%	-5% (±23%)	88% (±41%)	-6% (±17%)
15%	8% (±28%)	111% (±52%)	3% (±19%)
20%	15% (±28%)	124% (±52%)	2% (±14%)
25%	19% (±26%)	134% (±51%)	4% (±14%)
30%	24% (±29%)	146% (±55%)	7% (±13%)
35%	26% (±32%)	149% (±61%)	5% (±10%)
40%	30% (±32%)	157% (±65%)	6% (±10%)
45%	34% (±35%)	163% (±68%)	5% (±9%)
50%	35% (±36%)	169% (±71%)	3% (±9%)
55%	40% (±38%)	175% (±75%)	3% (±7%)
60%	44% (±44%)	186% (±87%)	2% (±6%)
65%	47% (±45%)	191% (±89%)	0% (±7%)
70%	51% (±51%)	201% (±100%)	-1% (±7%)
75%	54% (±56%)	207% (±111%)	-3% (±7%)
80%	61% (±69%)	220% (±138%)	-5% (±8%)
85%	69% (±93%)	238% (±186%)	-9% (±9%)
90%	79% (±119%)	257% (±238%)	-12% (±12%)
95%	94% (±154%)	286% (±306%)	-17% (±16%)

Quantile-quantile plots corroborate these differences in predictive accuracy (**Figure 4.4a**). The optimisation routine tends to underestimate the frequency of very small and very large colonies, indicated by minor deviations at the smallest and largest percentiles between the empirical and predicted distribution of intercept lengths (**Table 4.1**). In contrast, the percentiles of the intercept distributions simulated by the diameter and radius methods deviate systematically across the range of empirical percentiles (**Figure 4.4a**). Trends in reconstructed colony size structures were highly consistent with trends in raw intercept length distributions (see chapter 3, **Figure 3.4**).

Demographic trends beyond cover

Changes in colony size structure varied markedly between taxa. Corals of the families Poritidae and Mussidae and of the genera *Isopora* and *Montipora* experienced pronounced

shifts towards relatively more large colonies on both the crest and slope (**Figure 4.5**). In contrast, the disproportionate loss of both small and large seriatoporids resulted in a narrowed distribution, particularly on the reef crest. Faviids experienced a similar narrowing of the colony size distribution on the crest but shifted towards relatively more large colonies on the slope. The relative distribution of colony sizes of tabular acroporids remained comparatively unchanged (**Figure 4.5**).

Shifts in size structure resulted in marked shifts in the reproductive output of populations (**Figure 4.5**). While the fecundity of faviids, other *Acropora*, tabular *Acropora* and *Stylophora* decreased consistently across habitats, by up to 50% relative to their historical baselines (*Stylophora*), the fecundity of pocilloporid and poritid corals remained stable or even increased (**Figure 4.6b**). Declines in the abundance and reproductive output of large *P. damicornis* corals were compensated by increases in the abundance and reproductive output of medium-sized, or small mature colonies. In contrast, shifts in the size structure of poritid corals resulted in lower abundance and reproductive output of medium-sized colonies but increases in the abundance and reproductive output of large colonies. Other *Pocillopora* experienced declines in abundance and reproductive output on the crest but increases on the slope (**Figure 4.5**). Declines in the fecundity of favids, acroporids and *Stylophora* were driven by declines in the abundance of large fecund colonies. This trend was particularly pronounced in *Stylophora*, whose fecundity exhibits the steepest increase with colony size (**Figure 4.5**).

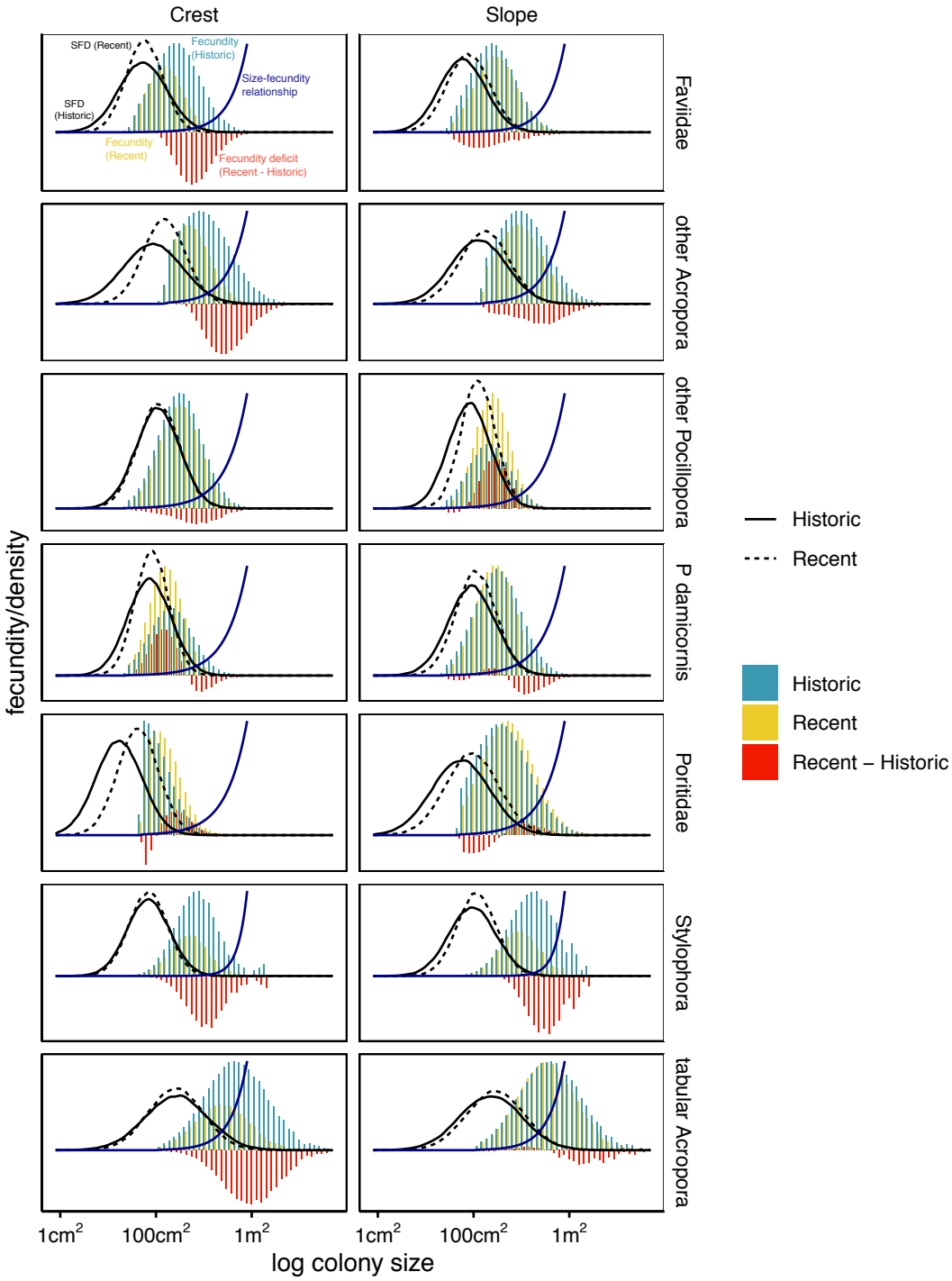

Figure 4.5 Change in cumulative size-class fecundities by taxa and habitats. Histograms show for different taxa the total reproductive output of different size classes in historic (blue) and recent (yellow) surveys, as well as the deficit or gain in fecundity (recent-historic, red). Density plots (black lines) indicate the colony size structure in historic (solid) and recent (dashed) surveys. The blue line indicates the size-fecundity relationship, with fecundity on the arithmetic scale.

At the community-level, the combined volume of testes produced by faviids, acroporids and *Stylophora* declined from 0.32 litres to 0.17 litres per m^2 on the crest and from 0.3 litres to 0.22 litres on the slope (**Figure 4.6**). In contrast, the combined number of eggs produced by poritids and pocilloporids remained comparatively stable, with 0.8 million eggs produced per m^2 on the crest and 2.0 million eggs per m^2 on the slope.

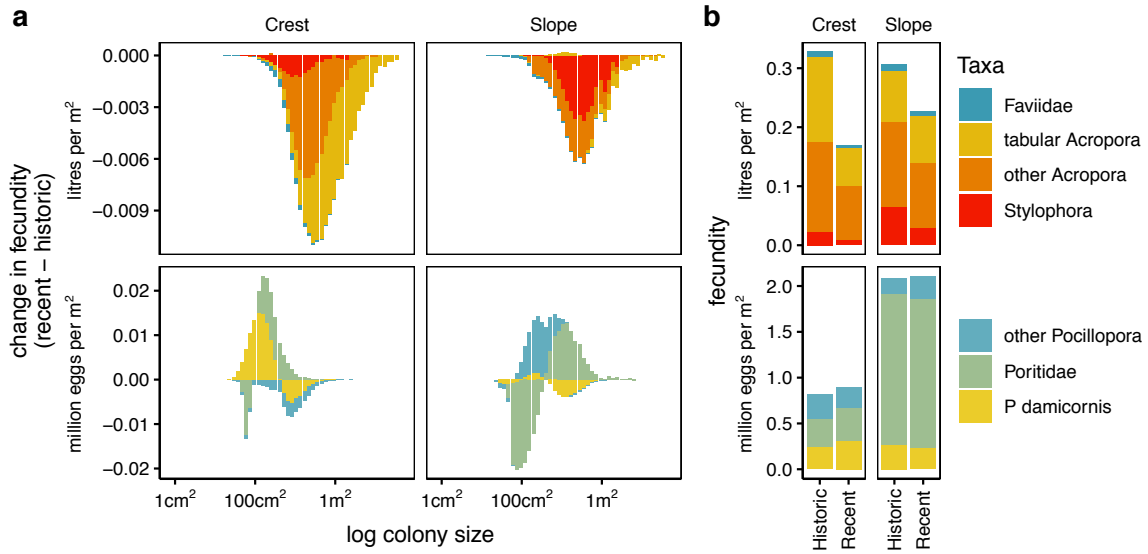

Figure 4.6 Community-level changes in fecundity. **(a)** Stacked barplots show the change in size-class fecundities (recent – historic) of different taxa on the reef crest and reef slope. **(b)** Stacked barplots show the total fecundity of taxa in historic and recent surveys.

Trends in coral cover, the most widely used measure of demographic trends in corals, can differ markedly from trends in colony densities and population fecundity (**Figure 4.7**). For instance, the moderate decline of poritid cover on the crest (-20%) and slope (-5%), masked steep declines in colony densities (-64% and -38%) caused by shifts towards relatively more large colonies while declines in fecundity were less pronounced (-6% and -19%). Similarly, the density and fecundity of faviids, other *Acropora* and *Stylophora* declined faster than their cover on the reef crest. The reproductive output of *Stylophora* declined by 56%, whereas cover declined by only 33%. In contrast, tabular acroporids suffered similar losses in cover and fecundity on the crest and even experienced increased reproductive output despite minor declines in cover on the slope due to shifts towards larger colonies. Similar shifts towards relatively more large colonies in crest and slope populations of the genus *Isopora* resulted in pronounced declines in densities (-24% and -44%) despite stable cover (-2% and +3%). While

the cover of mussid corals remained constant, they experienced disproportionate declines in colony densities on both the reef slope and the reef crest, concomitant with a shift towards larger colonies (**Figure 4.7**).

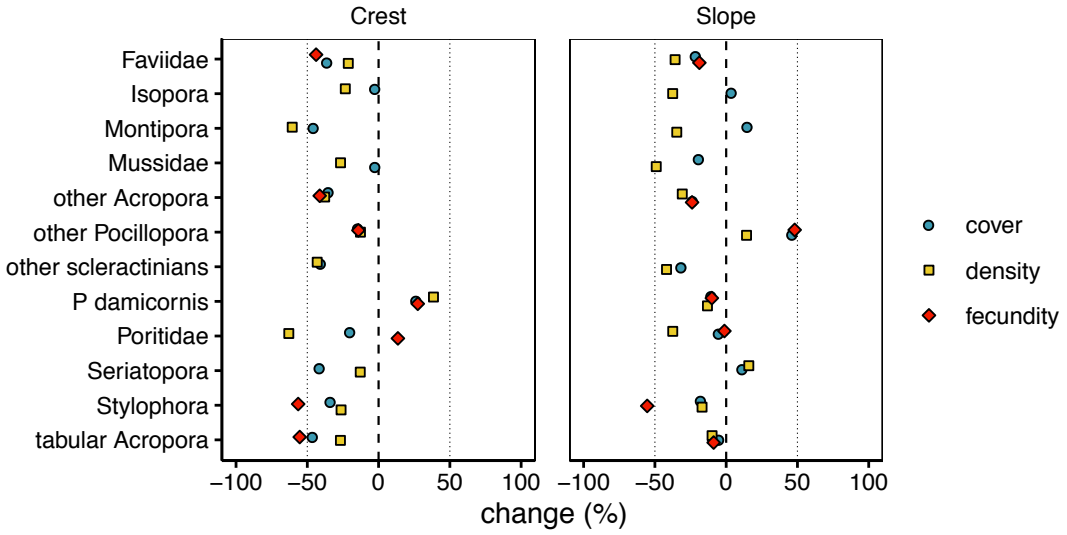

Figure 4.7 Demographic trends beyond cover. Changes in coral cover, colony density and fecundity of major taxa on the crest and slope. Colony densities are calculated as colonies per m^2 and fecundity as egg volume per m^2 (tabular *Acropora*, *Stylophora*, other *Acropora* and Faviidae) or eggs per m^2 (Poritidae, *P. damicornis*, other *Pocillopora*).

4.4 DISCUSSION

Discrepancies between trends in coral cover, colony densities and population fecundity demonstrate the importance of examining demographic trends beyond coral cover alone, and the importance of data on trends in colony size structure (**Figure 4.7**). For instance, an examination of trends in the abundance of poritid corals based on trends in cover alone would fail to detect steep declines in colony density, pivotal for egg fertilization success (Oliver & Babcock 1992). However, the reproductive output of poritid populations, measured as eggs produced per m^2 reef habitat, remained stable or increased (**Figure 4.7**) due to the increased abundance and reproductive output of large colonies (**Figure 4.5**). The ability to store past gains in population growth, commonly referred to as the storage effect (Chesson 2000), allows, in particular, slow-growing, long-lived taxa like poritid corals to persist despite

ongoing recruitment failure but masks the gradual erosion of their population viability if only trends in cover are examined (Hughes & Tanner 2000).

Changes in the reproductive output of coral populations illustrate the demographic importance of large, highly fecund colonies, and the necessity of reliable estimates of colony size structure. Taxa with steep size-fecundity relationships like *Stylophora* (Hall & Hughes 1996) are particularly sensitive to declines in the abundance of large colonies, and even minor changes in colony size structure can result in marked changes in population fecundity (**Figure 4.5**). Consequently, while the presented method tends to underestimate the abundance of both small and large colonies (**Figure 4.4**) and the lognormal distribution is light-tailed, estimated changes in fecundity are sensitive to deviations from (log-)normality, particularly in the right tail. The alternative approaches of using the intercept of a colony as its diameter (Connolly *et al.* 2005) or radius (Zawada *et al.* 2019) consistently deviate from the true size structure (**Figure 4.4a**) and overestimate coral cover (**Figure 4.4b**). They are thus likely to overestimate the reproductive output of populations.

Declines in the abundance of large colonies disproportionately affect the reproductive output of coral populations (**Figure 4.5**) but also diminish their capacity to provide important ecological functions. Large table corals, for instance, provide important shelter habitat for fish species (Kerry & Bellwood 2015). The erosion of reef structural complexity has been linked to shifts in energetic dynamics and reef productivity (Morais *et al.* 2020). Further, while most coral species reproduce only once per year, coral propagules constitute an important food source for fish (Pratchett *et al.* 2001) and other reef organisms including corals (Fabricius & Metzner 2004). Declines in the fecundity of coral populations (**Figure 4.6b**) may therefore have unrecognized consequences for the productivity of reef communities, similarly to the overlooked role of cryptobenthic fish species for reef trophodynamics (Brandl *et al.* 2019).

The presented method allows colony size structure to be reconstructed from traditional LIT data. While further validation using extensive field data on coral cover and colony size frequency distributions is required, the new method performs significantly better than two alternative methods, and exhibits comparatively minor, non-systematic biases in its predictive accuracy (**Figure 4.4**). Neither of the two alternative methods accounts for the two biases underlying the collection of line intercept transect data: (1) the size-dependent detectability of coral colonies and thus the under-representation of small colonies in the intercept data, and (2)

the distribution of randomly drawn intercepts through approximately round planar colony shapes. Using the intercept as the diameter of a circle consistently underestimates the likely size of each intercepted colony because and intercept an approximately round colony is always at least as long as its diameter but typically longer. This method thus compensates, to a degree, for the under-representation of small colonies, and, as a result, performs better than the radius method.

By reverse-engineering population size structure using knowledge of the underlying sampling processes and corrections of their inherent geometrical and statistical biases, the optimisation routine can be adapted to reflect different sampling designs. Similarly, it allows users to examine whether statistical distributions such as the exponential, the power-law or the Weibull distributions, frequently used to describe size spectra (White *et al.* 2008; Gillespie 2015), provide better fits to their data than the lognormal distribution commonly used to describe the distribution of coral colony sizes (e.g. Bak & Meesters 1998).

The presented method bridges the gap between routinely collected monitoring data and data required for demographic inference beyond trends in coral cover. I illustrated its usefulness at the example of examining trends in fecundity of coral population on the Great Barrier Reef. Knowledge of a population's colony size structure can, however, also be used to project population dynamics into the future using structured population models which have been published for a range of coral taxa (e.g. Hughes 1984; Done 1988; Babcock 1991; Hughes & Tanner 2000; Edmunds 2015; Kayal *et al.* 2018) but also various other animal and plant species with size-dependent life histories (Jones *et al.* 2015; Salguero-Gómez *et al.* 2016a). Interesting research questions include the investigation of transient population dynamics under ongoing recruitment failure, impacts on and implications of density-dependent gamete fertilization success (Oliver & Babcock 1992), time to (quasi-) extinction, or recovery to pre-disturbance abundances and size structures. Similarly, the identification of shifts in the morphological composition of coral communities and its implications for topographical reef complexity rely on sound data on colony sizes (Zawada *et al.* 2019).

Technological advances in reef survey methods are likely to complement or replace LIT methods in the near future. These include photogrammetry (Ferrari *et al.* 2017), remote sensing (Hedley *et al.* 2016), drones (Chirayath & Earle 2016) and robotics (González-rivero *et al.* 2014). These new tools not only help overcome the scarcity of ecological data on coral

populations (Kindsvater *et al.* 2018; Madin *et al.* 2019), but may also help alleviate the mismatch between routine monitoring data and data required by demographic tools. However, the legacy of historical LIT survey data provides an invaluable resource for the examination of long-term demographic trends and departures from historic baselines. Baselines are particularly important for the detection of slow transient dynamics such as the gradual erosion of the viability of long-lived taxa due to recruitment failure (Hughes & Tanner 2000), tipping points or impending regime shifts (Hughes *et al.* 2013b).

In times of declining coral abundances (Gardner 2003; De'ath *et al.* 2012) and escalating reef disturbance regimes (Van Hooidonk *et al.* 2016; Hughes *et al.* 2018a), I urgently need a better understanding of demographic trends in corals (Edmunds & Riegl 2019). The role of reproduction and recruitment in shaping coral population dynamics was historically neglected due to the open nature of coral populations and the intractability of larval dispersal (Caley *et al.* 1996), but increasingly attracts the attention of coral biologists. Severely suppressed recruitment rates (Hughes *et al.* 2019a) following unprecedented back-to-back regional mass bleaching events on Australia's Great Barrier Reef in 2016 and 2017 (Hughes *et al.* 2017b, 2019b) testify that the cumulative impact of natural and anthropogenic disturbances increasingly jeopardizes the capacity of coral populations to replenish between bouts of disturbance. Our ability to track and predict population recovery depends on the collection of more detailed demographic data that better reflect the size-dependent life histories of corals (Dornelas *et al.* 2017; Edmunds & Riegl 2019).

Chapter 5: The spatial footprint and patchiness of large-scale disturbances on coral reefs

Currently in review in *Global Change Biology*

5.1 INTRODUCTION

Disturbances are recurrent pulses of mortality that shape the structure and dynamics of ecosystems on both ecological and evolutionary time scales (MacArthur & Wilson 1967; White & Jentsch 2001). The emergence of novel disturbance regimes due to climate change and other anthropogenic impacts can overwhelm recovery processes, reshuffle the composition of communities and accelerate species extinction (Turner 2010; Urban 2015; Hughes *et al.* 2018b; Turner *et al.* 2020). For example, populations of slow growing, late maturing species may be unable to recover fully if the interval between consecutive disturbances becomes too short (Hansen *et al.* 2018). Similarly, species with limited dispersal capacity may fail to recolonize damaged habitat following an unusually large and spatially homogeneous disturbance (Moloney & Levin 1996). To understand the short and long-term effects of disturbances on a species or ecosystem, we need to examine the spatial extent and patchiness of their impacts – particularly for those disturbances whose spatiotemporal patterns are rapidly changing.

The impact or severity of a disturbance is generally measured as the area affected, the reduction in the size of the population, or the proportion of the biomass lost. Other critical dimensions of disturbances include their selective impacts on different species, genotypes, size or age classes, their spatial and temporal characteristics, as well as potential interactions between different disturbance events (White & Jentsch 2001). Conceptual models tailored to the system or species of interest can help to explore, for example, how disturbance characteristics interact to influence population dynamics (e.g. Moloney & Levin 1996), species coexistence (Liao *et al.* 2016) and species extinction thresholds (Liao *et al.* 2015). However, the paucity of spatially extensive, long-term empirical data on recurrent

disturbances means that our understanding of their spatial patterns is limited, particularly in marine ecosystems where remote sensing (e.g. aerial or satellite) is restricted.

On most coral reefs, recurrent hurricanes (or cyclones) are the dominant large-scale acute disturbance that has shaped the structure and evolution of reef communities (Connell 1978). Different species of corals have a range of strategies to resist hurricane damage, or to rebound quickly afterwards. However, the long-term decline of corals on reefs around the world (Gardner 2003; Bruno & Selig 2007) indicates that the cumulative impact of chronic human impacts and acute disturbances has often outstripped reef recovery processes. Local, chronic stressors such as water pollution and overfishing, and recurrent cyclones are increasingly compounded by bouts of thermal stress causing mass coral bleaching. Severe mortality due to thermal extremes can transform the composition of coral communities (Baker *et al.* 2008; Hughes *et al.* 2018b), impair stock-recruitment dynamics (Hughes *et al.* 2019a) and is increasingly unfolding at unprecedented spatial scales and frequencies (Hughes *et al.* 2018a; Eakin *et al.* 2019). To date, we have witnessed three pan-tropical mass bleaching events in 1997/1998, 2010/2011 and 2015/2016, each of which severely affected 50-70% of the world's coral reefs (Hughes et al. 2018a).

Cyclones and mass bleaching events differ markedly in spatial and temporal scale. On average, one or two cyclones cross the 2,300km length of the Great Barrier Reef (GBR) each year, with individual reefs experiencing an average return time of about 1-3 decades (Puotinen *et al.* 2016). The return-time and severity of cyclones has not changed on the GBR in recent decades (Puotinen *et al.* 2016). In contrast, regional-scale mass bleaching of corals on the Great Barrier Reef was first recorded in 1998, the hottest year then on record, which triggered an unprecedented global bleaching event (Berkelmans & Oliver 1999; Hughes *et al.* 2018a). A second bleaching episode occurred on the GBR in 2002 (Berkelmans *et al.* 2004), then a 14 year gap, before unprecedented back-to-back bleaching occurred in 2016 and 2017 (Hughes *et al.* 2019b). So far, approximately 94% of the world's coral reefs have bleached severely (>30% of corals bleached) at least once since 1980, on average 3-4 times, and the interval between recurrent events is shrinking (Hughes *et al.* 2018a). Without rapid acclimation and reductions in greenhouse gas emissions, virtually all reefs are projected to experience annual bleaching by the end of the century (van Hooidonk *et al.* 2013).

The responses of coral assemblages to disturbances vary between habitats due to differences in exposure, assemblage structure, and other variables. For example, bleaching rates of many coral taxa decrease with depth due to the attenuation of heat and light (Baird *et al.* 2018). Similarly, physical forcing during storms affects communities in shallow-water habitats disproportionately (e.g. Woodley *et al.* 1981). Environmental background conditions as well as past disturbances (Middlebrook *et al.* 2008; Hughes *et al.* 2019b) can modulate the impact of a disturbance by selecting both species and individuals better acclimated to local conditions. Corals adapted to extreme thermal conditions such as intertidal reef flats are typically more tolerant to heat stress than corals in more thermally stable habitats, but the benefits of acclimation are limited under extreme heat stress conditions (Schoepf *et al.* 2015).

Cyclones and mass bleaching are both highly selective, disproportionately affecting susceptible species (Pratchett 2007; Madin *et al.* 2014; Hughes *et al.* 2018b) and, within species, vulnerable genotypes and size classes (Madin *et al.* 2014; Álvarez-Noriega *et al.* 2018). Coral species with encrusting or massive morphologies are relatively resistant to wave damage compared to branching species, and rates of recovery also vary among taxa depending on their life histories (Hughes & Jackson 1985). Mild and moderate levels of heat exposure are also selective, affecting so-called "winners" more than "losers", depending on their thermal tolerance (Marshall & Baird 2000; Loya *et al.* 2001). However, the disparity between winners and losers is diminished during temperature extremes, when even the toughest species have high rates of mortality (Hughes *et al.* 2018b).

The spatial extent and patchiness of large-scale disturbances is important for subsequent population connectivity (Hughes *et al.* 2019a), recovery dynamics (Turner *et al.* 2020) and extinction risk (Johst & Drechsler 2003; Kallimanis *et al.* 2005; Liao *et al.* 2015). However, the patchiness of multiple disturbance is rarely quantified due to the scarcity of spatially extensive data over long time periods. On coral reefs, patterns of cyclone impact are often inferred from proxies such as cyclone tracks (Wolff *et al.* 2016) or models of wave height (Puotinen *et al.* 2016). Direct observations on the Great Barrier Reef show that the effects of cyclones on corals is typically very patchy among local sites, and among adjoining reefs close to the cyclone's track (Done 1992; Beeden *et al.* 2015). Similarly, on the GBR, the spatial footprints of each of four mass bleaching events have now been documented (Berkelmans & Oliver 1999; Berkelmans *et al.* 2004; Hughes *et al.* 2018b), allowing a direct comparison of the spatial characteristics of each event.

Larval dispersal allows corals and other sessile organisms to recover and persist in highly fragmented and frequently-disturbed habitat. Corals release either well-developed brooded larvae (brooders), or eggs and sperm that fertilize externally (broadcast spawners). Brooding species settle predominantly locally and are largely self-seeding at the scale of an individual reef (Ayre & Hughes 2000). In contrast, broadcast larvae can disperse over markedly greater distances of 10s-100s of km (Jones *et al.* 2009; Figueiredo *et al.* 2013). Consequently, their ability to recolonize damaged habitat is likely to be less sensitive to the scale and spatial heterogeneity of a disturbance. The recruitment rates of both brooding and spawning corals were severely depressed on GBR following the recent back-to-back mass bleaching events in direct proportion to the loss of adult breeding stocks (Hughes *et al.* 2019a), suggesting that mass coral bleaching events deplete coral populations at spatial scales that exceed even the dispersal capacity of spawning coral species.

We currently lack a quantitative comparison of the spatial footprint and patchiness of different events and types of disturbance. Here, I quantify and contrast the spatial footprint of four mass bleaching events and a Severe Tropical Cyclone on Australia's Great Barrier Reef. Specifically, I quantify their spatial extent, the magnitude of their impact (which I define as spatial extent weighted by impact severity) and the spatial distribution or patchiness of their impact. I then use a model of reef disturbance and recovery dynamics to demonstrate how the spatial patterns of disturbances can modify the dynamics of reef recovery, and how a species' dispersal capacity alters its vulnerability to disturbance.

5.2 MATERIALS AND METHODS

Spatial data on disturbance impacts

In order to quantify the spatial footprint of different large-scale reef disturbances, I examined the spatial extent, magnitude and patchiness of five coral mass mortality events on the Great Barrier Reef. Detailed and spatially-extensive survey data are available for four mass coral bleaching events in 1998, 2002 (Berkelmans *et al.* 2004), 2016 and 2017 (Hughes *et al.* 2017b, 2018c, 2019b) and for Severe Tropical Cyclone Yasi in 2011, a Category 5 system, and one of the most severe tropical storms on the GBR in recent decades (Beeden *et al.* 2015, 2016).

Each bleaching episode was assessed on 540 to 1156 individual reefs (Hughes *et al.* 2017b). The severity of coral bleaching in each event was recorded using aerial surveys of reefs along the length and breadth of the GBR. Bleaching was recorded from the air using the following five categorical scores: no bleaching, 0-10% of colonies affected, 10-30%, 30-60%, and >60% (**Table D-1**). Bleaching scores were recorded separately for major habitats – reef crests, flats and upper slopes. The accuracy of the aerial scores was ground-truthed during the bleaching event in 2016, on 168 reefs that were assessed extensively underwater as well as from the air (Hughes *et al.* 2017b).

The impact of Cyclone Yasi was measured by surveys on 71 reefs at varying distances from the cyclone's track, along a 350km section of the central Great Barrier Reef (Beeden *et al.* 2015). More than 800 damage scores were recorded across a range of different habitat types. The following six damage levels were distinguished: no damage, minor, moderate, high, severe, and extreme coral damage (**Table D-1**, for more details see Beeden *et al.* (2015)). A further 13 tropical cyclones of category 3 or higher have occurred on the GBR since 1998 (**Figure 5.1c**), but in each case surveys of coral communities afterwards were too sparse to quantify large-scale spatial patterns (Done 1992; Fabricius *et al.* 2008). Over the study period, cyclones of category 3 or higher were more than three times more frequent than larger-scale bleaching events (i.e. 14 versus 4).

Data analyses

I began by calculating the overall magnitude of a disturbance, which I define as the area it affected weighted by its severity. I represent the overall magnitude as the proportion of the total reef area of the Great Barrier Reef affected by different severities of each of the five disturbance events, following a similar approach devised by Beeden *et al.* (2015). For this calculation, I created a gridded base map of the GBR (50 x 50 km), and calculated the area of reef (UNEP-WCMC *et al.* 2010) and the frequency of different severity levels for each disturbance event in each grid cell. I then apportioned reef area in each grid cell to the different severity levels based on their relative frequency. Grid cells without a survey score were treated as unaffected. To assess the cumulative magnitude of the back-to-back bleaching event in 2016 and 2017, I used the scores from 590 reefs that were surveyed in both years. I calculated for each reef the average proportion of corals bleached in 2016 and 2017 using the interval mid-points (**Table D-1**) of the bleaching categories. I then calculated for each reef the

cumulative bleaching across the two events as the sum of the proportion of corals bleached in 2016 and the proportion of the corals that survived the 2016 bleaching but bleached in 2017. I acknowledge that the ordinal severity scores for bleaching and cyclone are based on different methodologies and are not equivalent (Table S1). Nonetheless, the consistent changes in coral cover at sites with different severity levels suggest that their impacts on coral abundance were broadly comparable (**Figure D-1**).

Measuring spatial disturbance patterns

I followed three approaches to quantify and contrast the patchiness or spatial clustering of the five disturbance events, and the combined 2016 and 2017 bleaching events. First, I produced for each disturbance event a spline cross-correlogram, a common geostatistical tool that estimates the spatial dependence of observations, based on an index of spatial autocorrelation such as Moran's I. A correlogram provides a visual representation of the decay in the similarity or autocorrelation of observations as the distance between them increases. A value of Moran's I of zero indicates a random spatial distribution of damage severity, positive scores signify that damage levels are more similar at a particular distance than expected by random chance, and negative scores indicate that values which are a given distance apart are more different than random.

The two types of disturbance data are represented at different spatial scales because bleaching severity was scored from the air at the scale of kms, while cyclone damage severity was scored in-water at the scale of 10s to 100s of meters. To minimise potential biases due to the different scales of observation (Levin 1992), I calculated an average severity score for each individual reef using the mid-points of the severity score intervals (proportion bleached and cyclone damage score, **Table D-1**) as a continuous measure of disturbance severity. I binned ordinal severity scores for bleaching or cyclone damage into two categories with approximately equal sample size: highly disturbed (severity level ≥ 3) and lightly disturbed or undisturbed (severity level < 3).

I produced spline cross-correlograms for each disturbance event using the ncf package in R, which is suitable for binary data (Bjørnstad & Falck 2001). I used the default degrees of freedom for the spline cross-correlograms calculated as the square root of the sample size of each event. Correlograms quantify the distance decay in the similarity of observations but do not discriminate between spatial clusters of affected and clusters of unaffected reefs. To

reduce the influence of unaffected regions on the autocorrelation analysis, I limited the analysis to the part of the GBR that experienced destructive or very destructive winds during Cyclone Yasi (see Beeden *et al.* (2015) for delineation) and the latitudes most affected during the bleaching events in 2016 (9-20°S), 2017 (14-22°S), 2002 (14-23°S) and 1998 (15-23°S) (Hughes *et al.* 2019b). To explore the sensitivity of cross-correlograms to the binning threshold (**Table D-1**) and to averaging of severity scores at the scale of individual reefs, I also produced cross-correlograms based on the original ordinal and interval mid-point data as well as site-level observations. Patterns of spatial autocorrelation were highly consistent (**Figure D-3** and **Figure D-4**).

As a complementary, ecologically more intuitive approach to measuring spatial clustering, I measured the degree to which severely disturbed reefs were spatially isolated from reefs that escaped severe damage. For each severely disturbed reef, I calculated (1) the distance to the nearest relatively undamaged reef and (2) the proportion of relatively undamaged reefs within 100 km of a severely disturbed reef. These two metrics of spatial isolation are sensitive to the density of survey locations and the relative proportion of severely disturbed sites, which complicates comparisons between events. I therefore constructed for each event and each metric a null model of the expected distance to the nearest undisturbed or moderately disturbed reef and the proportion of relatively undisturbed reefs within 100 km of a severely disturbed reef, with a random spatial distribution of damage scores. I calculated null expectations by randomly resampling from the observed distributions of damage scores (n = 100). I fitted a Bayesian linear model to the log-transformed minimum distance data and a Bayesian multi-level model with variance structure to the logistically transformed proportion data, using the six disturbance events as predictors. I divided the obtained posterior distributions for minimum distances and proportions by the corresponding average null expectations (mean across 100 permutations) to calculate how many times greater are (1) the distance to the nearest undamaged reef and (2) the proportion of undamaged reefs within 100 km of a severely disturbed reef, than expected by chance.

I also produced spline cross-correlograms separately for each of the three dominant habitat types, the reef slope, reef crest and reef flat, for the 2017 bleaching event and Cyclone Yasi, the two disturbances for which habitat-specific observations were available. All statistical analyses were conducted in R (R Core Team 2019) and all statistical models were fit with Stan (Stan Development Team 2019) and brms (Bürkner 2017).

Model of reef recovery dynamics

I used a spatially explicit cellular automata model, parameterised to mimic the population dynamics of coral species with different dispersal capacities, to examine how differences in the spatial patterns of large-scale reef disturbances may alter recovery dynamics. I modelled a reefscape that consists of a network of local coral populations (a grid of 100 by 100 cells) connected by propagule dispersal. Local coral cover changes through deterministic growth, random background mortality, local recruitment through larval retention in each cell and external recruitment from adjacent cells (**Table D-2**). I assumed density-dependent fertilisation success (Oliver & Babcock 1992; Teo & Todd 2018), and therefore allowed local propagule production to scale quadratically with local coral cover. I repeated the model simulations using two species with different dispersal kernels, to mimic the different dispersal capacities of brooding and broadcast spawning corals. One kernel simulates the local retention of larvae, with short-distance dispersal to adjacent cells, and the other mimics long-distance dispersal to second-degree neighbours (**Figure D-8**). Local recovery can occur even in the absence of a recruitment subsidy, via growth of remnant corals. The model was written and run in MATLAB (version 9.4.0.813654; MathWorks 2018).

After the model system attains its dynamic equilibrium, I subjected it to a catastrophic mortality event (60% loss of cover) with varying degrees of spatial autocorrelation and magnitude. I used fractal structures (Lennon 2000; Yearsley 2016) to generate spatial disturbance patterns with varying degrees of spatial autocorrelation, ranging from randomly distributed to highly spatially autocorrelated (**Figure D-7**). I did not vary the level of disturbance severity but rather I varied the overall magnitude of a catastrophic disturbance event by changing the proportion of cells affected.

The impact of a disturbance is often reported as its spatial extent E or (as above) its overall magnitude M (e.g. proportion of reefs or reef habitat affected, often weighted by some measure of disturbance severity S, or its impact, such as percentage decline in coral cover). Here, I used the integral of suppressed community abundance $N(t)$ over time as an ecologically meaningful measure of the impact of a disturbance, assuming that this abundance increases asymptotically towards some maximum K:

$$M = S \cdot E$$

$$I = \int_{t_0}^{\infty} [K - N(t)] \cdot dt$$

I ran the model 25 times for each combination of degree of spatial autocorrelation, magnitude of a disturbance and short- and long-distance dispersal type.

5.3 RESULTS

The spatial extent and magnitude of large-scale reef disturbances

Each of the four recorded mass bleaching events extended over much larger spatial scales than severe Cyclone Yasi, one of the largest category-5 cyclones on the Great Barrier Reef in recent decades (Beeden *et al.* 2015) (**Figure 5.1**). The bleaching in 1998 affected mainly inshore reefs in the central and southern regions. The 2002 event damaged many inshore and mid-shelf reefs in the centre and south, and the north was again unaffected. In 2016, the northern third of GBR experienced an unprecedented heat wave that caused the most spatially extensive and severe bleaching event recorded so far on the GBR. Less severe bleaching, comparable to levels in 2002, also occurred in the central region in 2016. In 2017, bleaching was most severe in the central region and to a lesser extent in the north already affected in 2016. Across all four bleaching events, the southern GBR experienced the least damage. In comparison, category 5 Tropical Cyclone Yasi affected a smaller region of the GBR, within 100-200 km of its track.

The overall spatial extent of individual bleaching events, across all bleaching severity categories, was 28% of the GBR's total reef area in 1998, 37% in 2002, 83% in 2016, and 68% in 2016 (**Figure 5.1b**). In combination, the two back-to-back bleaching events in 2016 and 2017 affected 89% of the GBR. In contrast, Cyclone Yasi affected 13% of the GBR in 2011, or about one sixth the reef area of the most extensive bleaching event in 2016. Severe bleaching disturbance (affecting >30% of colonies) was experienced by 50% of the GBR in 2016 (**Figure 5.1b**). In contrast, severe disturbance recorded from Cyclone Yasi was restricted to 5% of the GBR, generally on reefs that were less than 100-200 km from the track of the cyclone's eye (**Figure 5.1**).

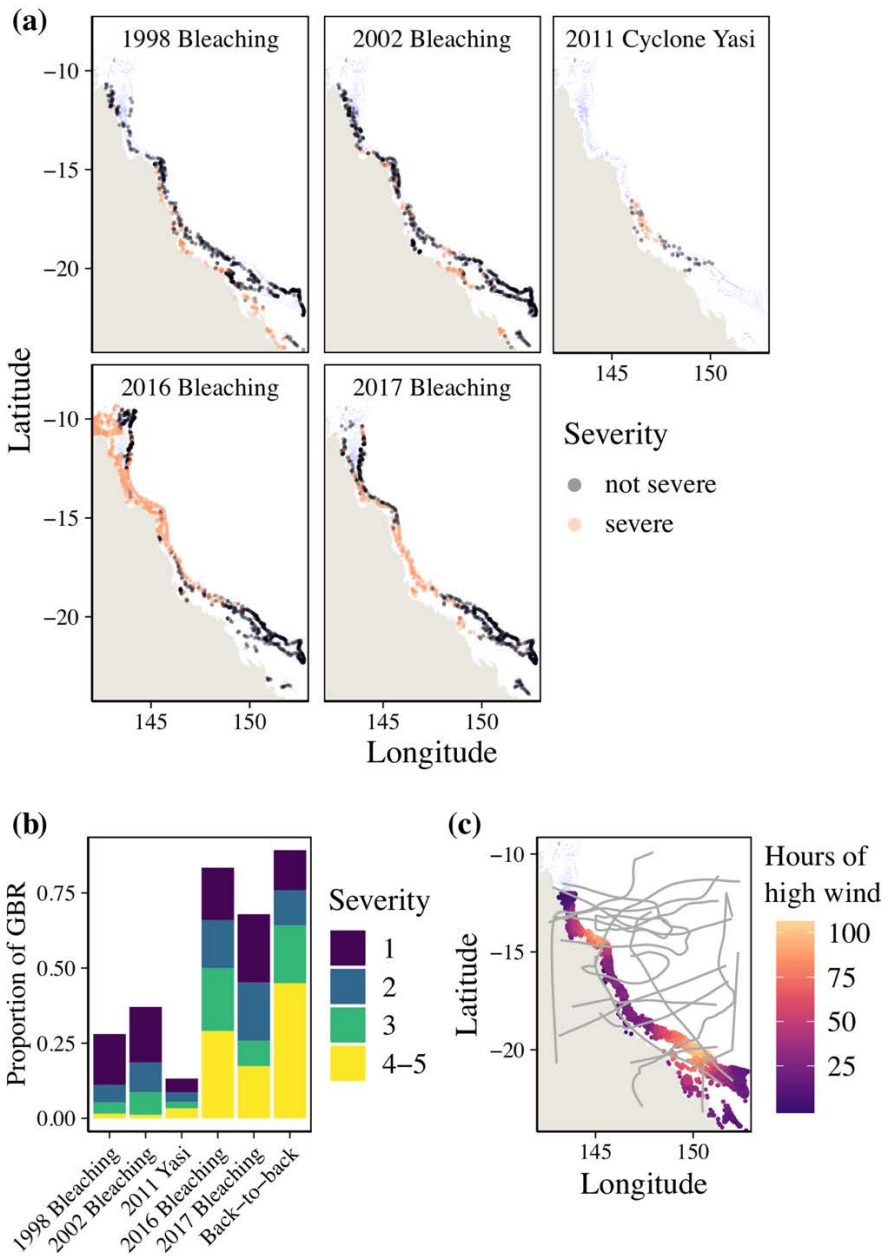

Figure 5.1 The spatial extent and magnitude of large-scale reef disturbances. **(a)** The spatial footprint of four coral mass bleaching events (1998, 2002, 2016 and 2017) and Cyclone Yasi (2011) on the Great Barrier Reef. Impact severity was grouped into not severe (scores 0-2) and severe (scores > 2). **(b)** The proportion of the total reef area on the Great Barrier Reef affected by different levels of damage for each of four bleaching events (1998, 2002, 2016, 2017), Cyclone Yasi (2011), as well as the back-to-back mass bleaching event (cumulative impact of 2016 and 2017). **(c)** Approximate tracks of the eye of 14 cyclones that reached category 3 or higher and crossed the Great Barrier Reef since 1998, as well as the cumulative hours (1998 to 2017) that each reef experienced wind speeds with elevated damage potential are shown. For details on generation of wind speed data see (Matthews *et al.* 2019).

The spatial clustering of large-scale reef disturbances

Bleaching events are not only larger, but within the affected regions their impacts are also substantially less patchy between reefs than Cyclone Yasi. The correlograms reveal that bleaching damage is spatially autocorrelated at distances over 100s of kilometres (Figure 5.2a). For example, the 2017 mass bleaching event exhibited patterns of spatial clustering up to distances of 300 km. In comparison, damage by Cyclone Yasi exhibited only weak signals of local-scale autocorrelation (**Figure 5.2a**). Notably, when site-level observations rather than reef averages were used to construct the correlograms, local patterns of spatial autocorrelation in Cyclone Yasi disappeared (**Figure D-4**). In contrast, the scale and extent of spatial autocorrelation of bleaching was less sensitive to pooling data from replicate sites per reef (Figure S4). For the 2017 bleaching event, patterns of spatial autocorrelation were consistent across three major habitat types (upper reef slope, crest and flat), indicating that the spatial extent of bleaching was similar across habitats (**Figure D-2**).

The distance of a severely disturbed reef to its nearest undisturbed or lightly disturbed neighbour (**Figure 5.2c**), and the proportion of relatively undamaged reefs within 100 km of a severely disturbed reef (**Figure 5.2b**), both corroborate the patterns of patchiness revealed by the correlograms. More than a quarter of the severely bleached reefs were isolated from the closest unbleached or lightly-bleached reef by at least 75 km in 2016, and by more than 100 km in 2017 (**Figure 5.2c**). The shorter distance in 2016 reflects an inshore-offshore gradient in the severity of bleaching in the worst affected, northern region (**Figure 5.1a**). In 2017, severe bleaching – most of it in the central region - was spread more uniformly across the continental shelf. The cumulative impact of the back-to-back bleaching event in 2016 and 2017 resulted in average distances of almost 70 km to the nearest unbleached or lightly bleached neighbour (**Figure 5.2c**), whereas the most isolated severely bleached reefs were >400 km away from the closest undisturbed or lightly-bleached reefs. In comparison to 2016 and 2017, estimated mean distances to the closest relatively undisturbed neighbours (**Figure 5.2b**) were substantially shorter for the bleaching events in 1998 (17 km), for bleaching in 2002 (15 km), and Cyclone Yasi (20 km). Distances to the nearest unbleached or lightly bleached reef were, on average, more than eight times greater (8.3 times) for the back-to-back bleaching than expected by chance, i.e. under a random spatial distribution of impact (**Figure D-6b**). In contrast, distances following Cyclone Yasi were, on average, less than double the

distance expected (1.5 times) (**Figure 5.2d**) and the posterior distribution overlapped with the null expectation (**Figure D-6b**).

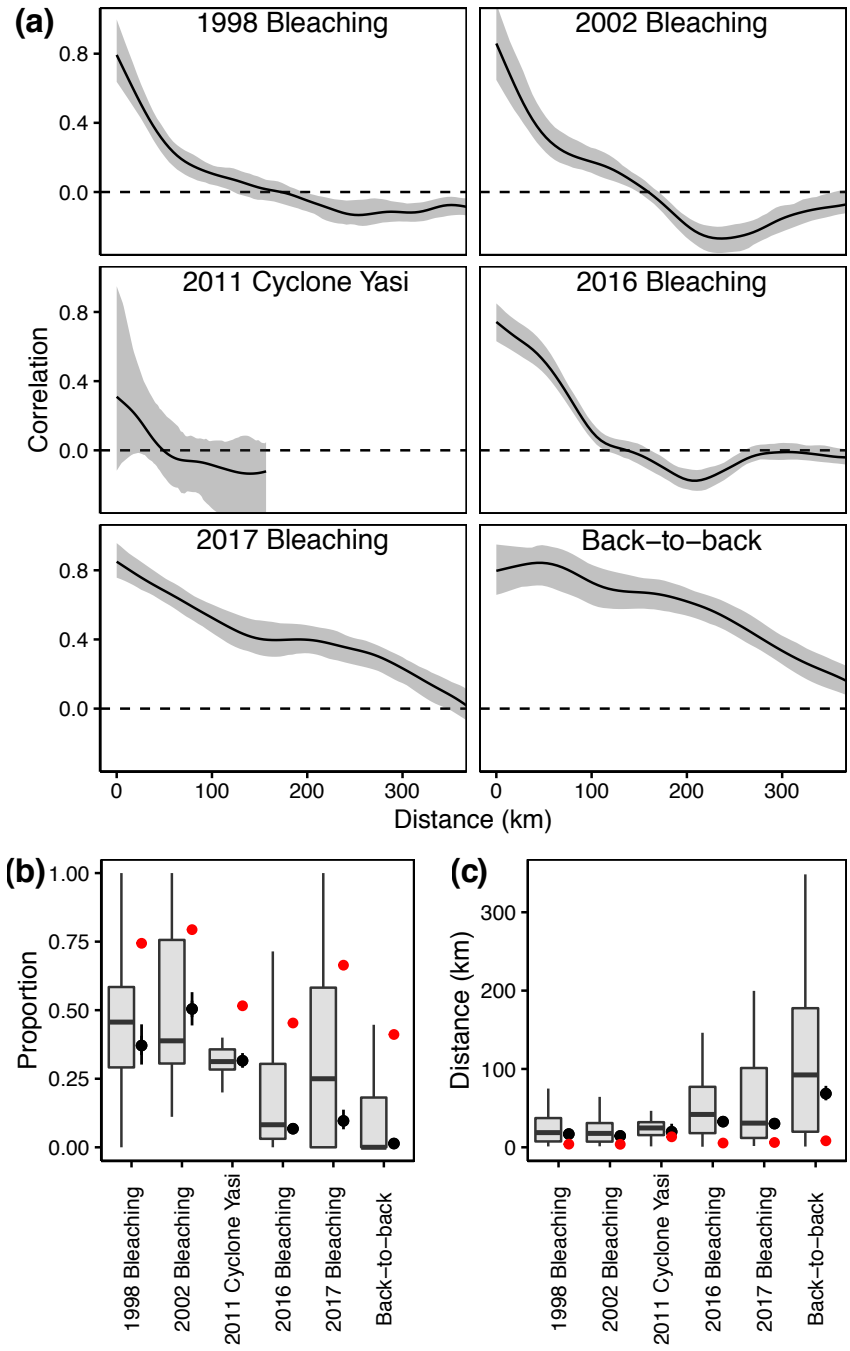

Figure 5.2 Spatial heterogeneity of large-scale reef disturbances. **(a)** Spline cross-correlograms showing the spatial dependence or similarity of damage scores with increasing distance for each disturbance event. **(b)** Distribution of distances to nearest undisturbed neighbour across all disturbed sites. **(c)** Distribution of the proportions of undisturbed sites within 100km of a disturbed site. In (b) and (c), boxplots show the medians and quartiles of observations, black circles the posterior medians, black lines the 95% credible intervals and

red circles the average null expectations under random spatial distribution of impact (mean across all permutation runs).

Similarly, the proportions of unbleached or lightly bleached reefs within 100 km of a severely bleached reef were the lowest for the 2016 bleaching event (**Figure 5.2b**). The modelled proportion was higher for the 2017 bleaching (1.4 times), Cyclone Yasi (4.7) and the 1998 (5.5) and 2002 (7.4) bleaching events (**Figure 5.2b** and **Figure D-5**). For a quarter of the reefs that bleached in 2016 or 2017 the proportion of unbleached and lightly bleached reefs within a 100 km radius dropped to 3%, and 0% respectively (**Figure 5.2b**). Only southern reefs largely escaped the two latest bleaching events. When I combined the impact of the 2016 and 2017 bleaching events, proportions of unbleached and lightly bleached reefs within 100 km were consistently low over a vast proportion of the GBR, stretching for 1,400 km over the northern and central regions (**Figure 5.3**), with an estimated mean proportion of 1.4% (**Figure 5.2c**). Modelled mean proportions of unbleached or lightly-bleached reefs within 100 km of a severely disturbed reef were 2.0, 1.6 and 1.6 times, lower than expected by chance for the 1998 and 2002 bleaching events and Cyclone Yasi respectively (**Figure D-6a**). In contrast, modelled mean proportions were 6.9, 6.7 and 30.1 times lower for the 2017, 2016 and back-to-back bleaching events than expected under a random spatial distribution of impact (**Figure D-6a**).

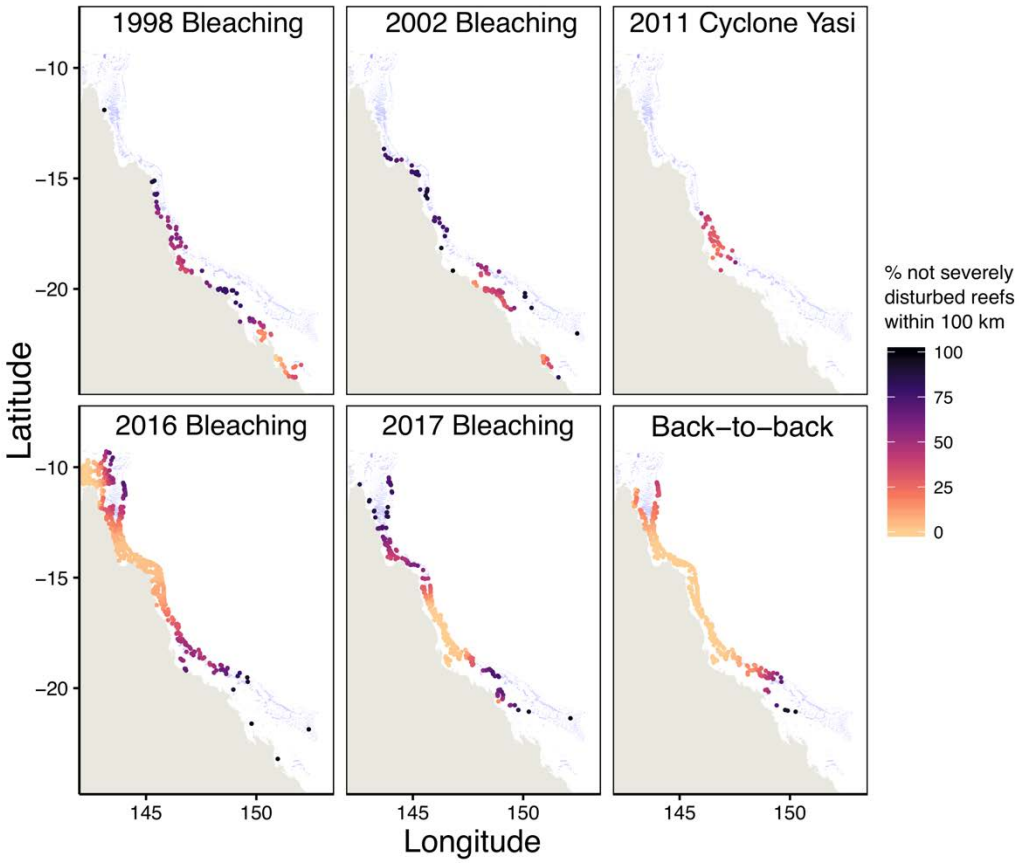

Figure 5.3 Map showing the spatial isolation of severely disturbed reefs from not severely disturbed reefs. For each severely disturbed reef the proportion of not severely disturbed reefs within a radius of 100km is shown for each of the six examined disturbance events. Shaded blue polygons indicate location of reefs on the Great Barrier Reef.

Modelling post-disturbance recovery

The model illustrates how the spatial footprint and autocorrelation of a disturbance (**Figure 5.1**, **Figure 5.2** and **Figure 5.3**), can combine to shape the recovery trajectories of affected populations (**Figure 5.4**). In the model, two disturbance events of equivalent magnitude, that differ only in the spatial distribution or clustering of mortality (**Figure 5.4a** and **Figure 5.4b**), elicit markedly different metapopulation responses (**Figure 5.4c**). Specifically, populations subjected to a randomly distributed disturbance event recover to dynamically stable pre-disturbance conditions more quickly than when mortality is spatially clustered (**Figure 5.4c**). As the magnitude and degree of spatial autocorrelation intensifies, the proportion of disturbed cells outside the dispersal range of undisturbed populations increases. The recovery of spatially isolated populations is particularly protracted in the model and depends on the slow recovery of local coral cover through growth, followed by the recovery of recruitment rates through multi-step dispersal processes.

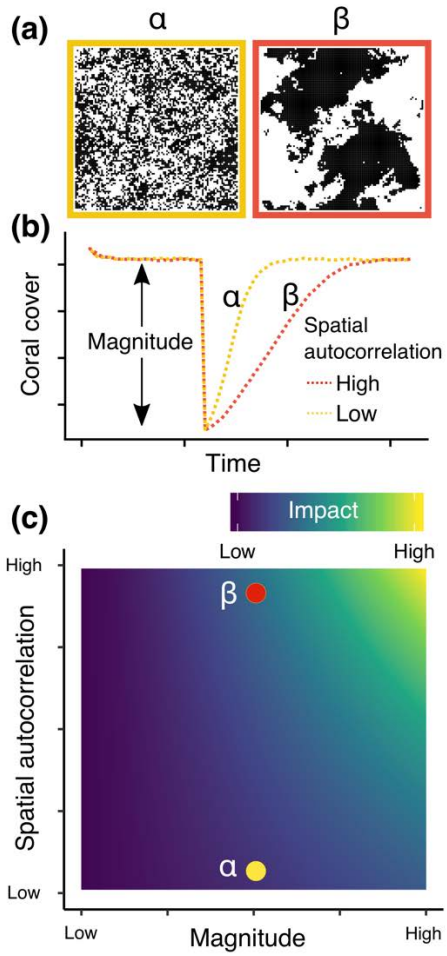

Figure 5.4 Conceptual illustration of how spatial clustering modifies the impact of a disturbance. **(a)** The spatial footprint of two hypothetical disturbances α (random spatial distribution or low spatial autocorrelation) and β (high spatial autocorrelation). **(b)** The response of the modelled metapopulation to disturbances of equivalent magnitude (% coral cover lost) but different spatial autocorrelation and subsequent recovery. Recovery is protracted if the spatial distribution of disturbance impact is spatially autocorrelated (β) rather than random (α). I used the area under the recovery curves to quantify and compare the true impact of a disturbance on the reef system. **(c)** Magnitude and spatial autocorrelation combine to determine the overall impact of a disturbance on the recovery of community abundance. The two disturbances α and β have markedly different impacts on the recovery of community abundance.

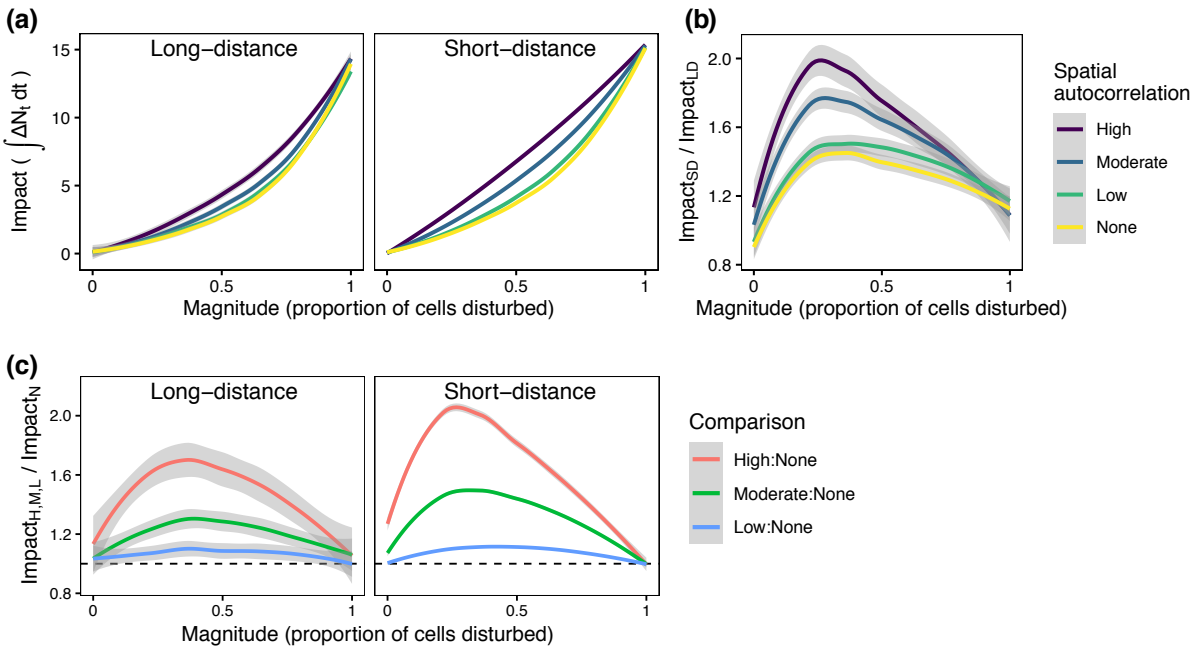

Figure 5.5 Spatial autocorrelation and larval dispersal distance. **(a)** For both long-distance and short-distance dispersers, the correlation between the impact of a disturbance, measured as the integral of suppressed community abundance over time (**Figure 5.4**), and its magnitude - the proportion of cells disturbed - is shown for disturbance events with different degrees of spatial autocorrelation. **(b)** Division of the impact of disturbances with varying degrees of spatial autocorrelation on short-distance and long-distance dispersers illustrates their differential susceptibilities to disturbances of varying magnitudes and spatial clustering. **(c)** Division of the impact of a disturbance with low, moderate or high degree of spatial autocorrelation relative to a disturbance with random spatial distribution illustrates the amplification potential of spatial clustering for varying proportions of disturbed cells.

The effect of spatial clustering on recovery trajectories is greatest for intermediate magnitudes of disturbance, and is negligible for very small and very large disturbances (**Figure 5.5a**). A greater amount of spatial clustering exacerbates the degree of isolation of affected sites from unaffected sites, which are potential sources of larvae. Shorter-distance dispersers are generally more vulnerable to large-scale disturbances, reflected by the greater impact on their community abundance, particularly under modelled scenarios of high spatial autocorrelation (**Figure 5.5b**).

Species with greater long-distance dispersal are less affected by spatial clustering than species whose propagules are predominantly retained more locally (**Figure 5.5c**). Under scenarios of

high spatial autocorrelation, however, the degree of spatial isolation exceeds even the dispersal capacity of long-distance dispersers, protracting recovery. Disturbances with a high degree of spatial clustering had up to two times greater impact on the abundance of short-distance dispersers compared to a randomly distributed disturbance. Even for long-distance dispersers, spatial clustering exacerbated the impact of a disturbance by up to 60% (**Figure 5.5c**).

5.4 DISCUSSION

Coral reef ecosystems are profoundly shaped by recurrent large-scale disturbances and mass-mortality events (Connell 1978; Woodley *et al.* 1981). The increasing frequency of regional and global-scale mass coral bleaching events presents an unprecedented threat to corals and other reef organisms. On the Great Barrier Reef, the spatial footprint of each of four mass bleaching events in 1998, 2002, 2016 and 2017 is much larger than the footprint of a severe tropical cyclone (**Figure 5.1**). Furthermore, the high degree of spatial clustering during bleaching also means that large parts of the ecosystem are affected simultaneously during each event, leaving fewer interspersed pockets of unaffected reef habitat compared to the patchier outcomes of a major cyclone (**Figure 5.2** and **Figure 5.3**).

The spatial isolation of severely disturbed reefs from potential sources of larvae was particularly severe during the two most recent mass bleaching events in 2016 and 2017, after which damaged locations were as far as 400 km away from the closest relatively undisturbed reef (**Figure 5.2c**) and proportions of unbleached reefs within the vicinity of severely disturbed reefs were consistently low over a vast stretch of reef reaching over 1,400 km (**Figure 5.3**). The frequency of mass bleaching events is increasing rapidly throughout the tropics due to anthropogenic warming (Hughes *et al.* 2018a), and the return times of recurrent events is projected to be annual (i.e. every summer) at most locations by mid-century, depending on future emissions of greenhouse gasses (Van Hooidonk *et al.* 2016).

Consistent patterns of spatial autocorrelation of bleaching and cyclone impact occurred across the three major habitat types, reef flats, crests, and upper slopes (**Figure D-2**), indicating that habitat-specific responses are synchronized at large spatial scales. On the Great Barrier Reef, bleaching in most taxa decreased gradually with depth, likely due to the attenuation of light (Baird *et al.* 2018). Coral species in deep water are, however, unlikely to significantly

contribute to re-seeding badly damaged coral populations in shallower habitats at the scale of the GBR (Bongaerts *et al.* 2017).

The frequency and intensity of cyclones has not increased on the GBR in recent decades (e.g. Callaghan & Power 2011). Moreover, the lower patchiness and larger footprint of regional and global-scale bleaching events indicates that they now pose a much more severe threat to reef connectivity, recovery and resilience. Most cyclones that affect the GBR – including Cyclone Yasi – form offshore in the Coral Sea and travel westwards towards the Queensland coast, leaving a relatively narrow track of damage. Reefs damaged by Cyclone Yasi were not significantly more isolated from not severely disturbed reefs than expected under a random spatial distribution of damage (**Figure 5.2c** and **Figure D-6**). The proportion of not severely disturbed reefs within 100 km of a severely disturbed reef, while lower than expected by chance and lower than for the bleaching events in 1998 and 2002, was on average substantially higher than for the more recent bleaching events in 2016 and 2017 (**Figure 5.2c**).

After a cyclone event, nearby undamaged reefs provide a source of larvae to aid a rapid recovery (Torda *et al.* 2018). In contrast, the mechanisms of recovery of severely damaged reefs following regional-scale bleaching may be similar to the protracted rebound of naturally isolated oceanic reefs after severe disturbance (Gilmour *et al.* 2013): In the short-term, recovery may be due largely to the re-growth of remnant survivors, followed later by recovery of pre-disturbance levels of reproduction and recruitment. Allee effects due to low colony densities, particularly in rare species and those most vulnerable to thermal stress, will likely hamper reproductive success (e.g. Oliver & Babcock 1992) and increase per-capita rates of predation (Knowlton *et al.* 1990). This scenario is particularly likely for reefs in the central and Northern section of the Great Barrier Reef that experienced spatially extensive, severe bleaching during the back-to-back bleaching events in 2016 and 2017 (**Figure 5.3**). Severely disturbed reefs can still act as sources of larvae, but their reproductive output is typically suppressed (Gilmour *et al.* 2013; Hughes *et al.* 2019a). The future capacity of distant undisturbed reefs to significantly supplement the larval pool settling on isolated disturbed reefs may be undermined by the higher rates of local retention and coral larval mortality predicted for warming oceans (Figueiredo *et al.* 2014), increasing the risk of metapopulation collapse and extinction (Riegl *et al.* 2018).

The simple model illustrates mechanistically how the spatial extent and patchiness of disturbance can affect recovery pathways: wide-spread events pose a greater recovery challenge, and a longer recovery timescale. These findings parallel similar studies in other systems (Moloney & Levin 1996; Kallimanis *et al.* 2005; Liao *et al.* 2015). Liao *et al.* (2015), for instance, found that spatially autocorrelated disturbances exacerbated the extinction risk of short-distance dispersers but not species with long-distance dispersal. Similarly, Moloney & Levin (1996) showed that plant species with local dispersal faced an elevated extinction risk under more severe disturbance regimes.

The model captures only one axis of variation between species, their dispersal capacity, and thus neglects the full spectrum of coral life history strategies and important demographic trade-offs. For instance, brooding coral species have a comparatively limited dispersal capacity compared to mass spawners, but many brooding species reproduce multiple times per year. The potential advantages of short-distance dispersal such as higher rates of local retention in naturally isolated reefs (Keith *et al.* 2015), lower larval mortality rates due to shorter pelagic larval durations, and local adaptation (Warner 1997; Ayre & Hughes 2000; Burgess *et al.* 2016) are typically omitted from conceptual models (Moloney & Levin 1996; Kallimanis *et al.* 2005; Liao *et al.* 2015). Ultimately, the implications of reduced connectivity on assemblage structure and the persistence of individual species will depend on the complex interactions between a species' entire life history, intra- and interspecific differences in disturbance susceptibility, and shifts in the extent, severity and frequency of recurrent disturbances.

The study of ecological patterns requires careful consideration of the different spatial, temporal and organisational scales across which they can vary (Levin 1992), particularly when examining the spatial patterns of disturbances. The perceived homogeneity or heterogeneity of a disturbance can vary across spatial scales, and thus depends on the scale of observation. For my analysis, I aggregated scores at the scale of individual reefs to standardize the scale of observation of both the bleaching and cyclone surveys. While the reef-scale is appropriate for studying regional patterns along the length of the Great Barrier Reef and impacts on reef connectivity, the heterogeneity of disturbances at finer spatial scales affects many ecological processes, such as gamete fertilization success (10s to 100s of metres) (Oliver & Babcock 1992; Teo & Todd 2018) and natural selection (micro-habitat scale) (Hoogenboom *et al.* 2017). Although consistent patterns of spatial clustering across habitat

types (**Figure D-2**) and sites within reefs (**Figure D-4**) suggest that between-reef patterns of spatial clustering were not sensitive to the local-scale patchiness of disturbances (e.g. Green *et al.* 2019), the cross-scale spatial patterns of reef disturbances merit further exploration.

As the Great Barrier Reef enters uncharted territory, characterised by record-low coral cover (Australian Institute of Marine Science 2019) and an increasing shift towards more frequent, larger and more intense disturbances, our ability to predict the response of individual species, communities and the entire ecosystem will depend on a comprehensive understanding of the multi-faceted shifts in reef disturbance regimes. Clearly, the larger spatial footprint and clustering, of mass coral bleaching events, and their increasing frequency, poses an unprecedented threat to coral reef ecosystems, superimposed on a pre-existing disturbance regime that is also changing. The simultaneous depletion of coral populations at the scale of hundreds of kilometres undermines the connectivity of populations, even of long-distance dispersers, and is already fundamentally altering reef recovery dynamics (Hughes *et al.* 2019a).

Chapter 6: General discussion

Much has changed on the world's coral reefs since the first detailed studies of coral population dynamics revealed the peculiarities of their colonial life histories (Hughes & Jackson 1980, 1985; Hughes 1984). Coral abundances have declined dramatically in many parts of the world (Gardner 2003; Wilkinson 2008; De'ath *et al.* 2012) and the effects of global warming are taking an increasing toll on coral populations and coral reef ecosystems (Hughes *et al.* 2017b, 2018b, a). Australia's Great Barrier Reef, the world's largest coral reef ecosystem, has experienced three mass coral bleaching events within the last five years (2016, 2017 and 2020). The effects have devastated coral populations, depleting brood stocks at spatial scales that undermine the connectivity and recovery of affected populations (Hughes *et al.* 2019a). Thermal conditions that induce heat stress in corals causing bleaching and mass mortality are expected to occur annually on most reefs around the world by the end of the 21st century. The unprecedented spatial scale, and frequency, of reef disturbances poses severe challenges to the resilience of coral populations, and the need for large-scale coral demography is greater than ever (Edmunds & Riegl 2019).

This thesis explores multiple dimensions of the threats facing the viability of coral populations and species in the Anthropocene, by filling gaps in our understanding of demographic trends at large spatial and temporal scales (**Figure 1.1**). To overcome the scarcity of ecological data at such scales, I integrated ecological and biophysical data from various sources and devised a method that allows leveraging the potential of routinely collected monitoring data for demographic inference. I first estimated the total number of coral colonies inhabiting shallow-water coral reefs in the Pacific Ocean, as well as the population sizes of more than 300 Indo-Pacific coral species at biogeographic scales. These estimates show that while local and ecological extinctions may be plausible scenarios for the Indo-Pacific coral fauna, their risk of global extinction is lower than previously estimated (Carpenter *et al.* 2008) (chapter 2). For the remaining chapters I shifted my attention to Australia's Great Barrier Reef. In chapter 3, I examined decadal shifts in the colony size structure of coral populations along the Great Barrier Reef. This study revealed a systematic depletion of coral brood stocks and a disproportionate decline in the abundance of small colonies, indicative of declines in recruitment rates. In chapter 4, I developed a method that reconstructs the true colony size structure underlying a distribution

of measured intercept lengths. By facilitating the integration of routinely collected LIT data with size-dependent demographic traits (e.g. size-fecundity relationship) and tools (e.g. structured population models), this method allows demographic inference beyond changes in coral cover or relative shifts in colony size structure (chapter 3), which I demonstrated by calculating decadal changes in the reproductive output of coral populations on the GBR. Finally, in chapter 5, I contrasted the spatial footprint and patchiness of four mass coral bleaching events (in 1998, 2002, 2016 and 2017) and a severe tropical cyclone (Yasi, in 2011). This comparison revealed that mass bleaching events pose an unprecedented challenge to the connectivity and recovery of coral populations. These events deplete coral populations across wide spatial scales and thus undermining the resilience conferred by external recruitment.

The findings of this thesis emphasize the urgent need to study demographic trends in corals beyond changes in total coral cover. Specifically, I examined interspecific (chapter 2), intraspecific (chapters 3 and 4) and spatial patterns (chapter 5) in coral abundance to reveal important insights into the viability of species and populations. While the collection of species-level abundance data goes beyond the scope of most monitoring programs, abundance data that allow the examination of changes in colony size structure in major taxa would greatly enhance our ability to assess demographic trends such as trends in recruitment and fecundity not captured by changes in cover. Severely depleted populations are susceptible to Allee effects due to the density-dependent fertilization success of coral gametes (Oliver & Babcock 1992). In chapter 4, I demonstrated how commonly collected line-intercept data can be used to estimate the density of conspecific colonies, and the density of their gamete production. Colony size data will become increasingly important as coral populations continue to decline (Dornelas *et al.* 2017; Edmunds & Riegl 2019). The implications of spatial disturbance patterns and habitat fragmentation for population connectivity, recovery and viability have long been recognized in landscape and disturbance ecology (Moloney & Levin 1996). The capacity for long-distance larval dispersal and external recruitment subsidy allows corals to persist in the naturally fragmented and frequently disturbed reef habitat. However, the spatial footprint of mass bleaching events increasingly depletes coral populations at scales that exceed even the dispersal capacity of broadcast spawning corals. Consideration of the spatial patterns of these recent mass mortality events may improve our understanding of post-disturbance recovery.

The results presented in this thesis provide interesting avenues for further research. The approach outlined in chapter 2 may, for instance, be used to assess temporal trends in the

numerical abundance of metacommunities or species, or to estimate the total number of corals inhabiting the Great Barrier Reef or the total number of colonies lost during recent mass bleaching events in 2016, 2017 and 2020. Such estimates could inform the scalability of reef restoration projects, similar to comparable studies in trees (Crowther *et al.* 2015; Bastin *et al.* 2019). They can also serve as benchmarks for DNA-based estimates of effective population sizes, an important parameter in population genetics and conservation biology (Frankham 1995). The effective population sizes of marine invertebrates like corals are typically many orders of magnitude smaller than their census population sizes (Hughes *et al.* 1992; Ovenden *et al.* 2007). The presented method to reconstruct the colony size structure from line-intercept data (chapter 4) could be used, in combination with structured population models, to project likely population trajectories including recovery of pre-disturbance population sizes or size structures, or to estimate the time to extinction of different species. Beyond demography, this method may find application in studies of changes in the morphological composition of communities (Zawada *et al.* 2019) or of ecological processes and functions that depend on colony size such as the provision of structural habitat complexity. Further, a revision of analyses based on biased approximations of colony size, such as using the intercept as the radius (Zawada *et al.* 2019) or diameter (Connolly *et al.* 2005) of a circle, may also be worthwhile.

Expanding the toolbox of coral reef ecologists

Coral reefs are entering an uncertain future, marked by escalating disturbance regimes (Hughes *et al.* 2018a) causing frequent mass mortality events (Hughes *et al.* 2017b), shifts in assemblage structure (Hughes *et al.* 2018b), and impaired reef recovery processes (Hughes *et al.* 2019a). Our ability to predict the fate of these coral populations and communities will depend on the availability of ecological data (Edmunds & Riegl 2019). Advances in marine monitoring technologies (Hedley *et al.* 2016), curated databases of existing data (Madin *et al.* 2016; Salguero-Gómez *et al.* 2016a), the development of new quantitative tools, and the integration of data from different sources present promising new avenues for coral reef research at large spatial and long temporal scales. For instance, at the local scale, reef photo-mosaics provide an unprecedented resolution of the structure and dynamics of reef populations and communities (e.g. Edwards *et al.* 2017). At the regional to global scale, remote sensing data have become integral to the study and management of coral reef ecosystems, for instance, by facilitating the monitoring and forecasting of marine heatwaves (Liu *et al.* 2014) and the mapping of the global distribution of coral reefs in unprecedented detail (Allen Coral Atlas 2020).

Detailed studies of coral population dynamics have been conducted since the 1980s (Hughes 1984) but are time-consuming and hence cost-prohibitive for the purpose of monitoring populations at large spatial scales. However, structured population models have been published for a wide variety of coral species and present a hitherto under-explored source of demographic data for corals. In other organisms structured population models have been used to discern patterns in life history strategies (Salguero-Gómez *et al.* 2016b; Healy *et al.* 2019), to identify life history characteristics that confer demographic resilience (Stott *et al.* 2010; Capdevila *et al.* 2020) or to identify more easily measurable functional traits that can be used as proxies of life history strategy, such as wood density or seed mass in plants (Adler *et al.* 2014). Frameworks of coral life history strategies have thus far relied on functional traits such as corallite diameter and skeletal density and other ecological data such as depth range (Darling *et al.* 2012). A new quantitative framework of coral life history strategies based on available demographic data is urgently needed to cross-validate and complement trait-based approaches and would enhance our understanding of patterns in coral life history strategies and of trends in population and community changes.

Conclusions

In summary, this thesis provides new insights into demographic trends in corals at large spatial and long temporal scales. At such scales, studies have largely relied on trends in total coral cover (De'ath *et al.* 2012) and expert opinion (Carpenter *et al.* 2008) rather than quantitative analyses that reflect the size-dependent life histories of corals, their vast geographic ranges and their capacity for, but also dependence on, long-distance larval dispersal. While my analyses have shown that the long-term viability of coral populations is increasingly jeopardized, particularly due to the increasing frequency (Hughes *et al.* 2018a) and unprecedented spatial footprints (chapter 5) of mass coral bleaching events, the risk of global extinction within the next few decades is low for the vast majority of Indo-Pacific coral species. This highlights the urgent need and potential of curbing greenhouse gas emissions to mitigate anthropogenic global warming, to allow for an eventual recovery of coral reef assemblages.

Bibliography

Adler, P.B., Salguero-Gomez, R., Compagnoni, A., Hsu, J.S., Ray-Mukherjee, J., Mbeau-Ache, C., *et al.* (2014). Functional traits explain variation in plant life history strategies. *Proc. Natl. Acad. Sci.*, 111, 740–745.

Aerts, D. & de Bianchi, M.S. (2014). Solving the hard problem of Bertrand's paradox. *J. Math. Phys.*, 55, 083503.

Allen Coral Atlas, A. (2020). *Allen Coral Atlas*. Available at: https://allencoralatlas.org. Last accessed 18 June 2020.

Álvarez-Noriega, M., Baird, A.H., Bridge, T.C.L., Dornelas, M., Fontoura, L., Pizarro, O., *et al.* (2018). Contrasting patterns of changes in abundance following a bleaching event between juvenile and adult scleractinian corals. *Coral Reefs*, 37, 527–532.

Álvarez-Noriega, M., Baird, A.H., Dornelas, M., Madin, J.S., Cumbo, V.R. & Connolly, S.R. (2016). Fecundity and the demographic strategies of coral morphologies. *Ecology*, 97, 3485–3493.

Atkinson, A., Siegel, V., Pakhomov, E.A., Jessopp, M.J. & Loeb, V. (2009). A re-appraisal of the total biomass and annual production of Antarctic krill. *Deep Sea Res. Part I Oceanogr. Res. Pap.*, 56, 727–740.

Australian Institute of Marine Science. (2019). *Long-term Reef Monitoring Program - Annual Summary Report on coral reef condition for 2018/2019*.

Ayre, D.J. & Hughes, T.P. (2000). Genotypic diversity and gene flow in brooding and spawning corals along the Great Barrier Reef, Australia. *Evolution*, 54, 1590–1605.

Babcock, R.C. (1991). Comparative demography of three species of scleractinian corals using age- and size-dependent classifications. *Ecol. Monogr.*, 61, 225–244.

Baird, A., Madin, J., Álvarez-Noriega, M., Fontoura, L., Kerry, J., Kuo, C., *et al.* (2018). A decline in bleaching suggests that depth can provide a refuge from global warming in most coral taxa. *Mar. Ecol. Prog. Ser.*, 603, 257–264.

Bak, R.P.M. & Meesters, E.H. (1998). Coral population structure: The hidden information of colony size-frequency distributions. *Mar. Ecol. Prog. Ser.*, 162, 301–306.

Bak, R.P.M. & Meesters, E.H. (1999). Population Structure as a Response of Coral Communities to Global Change. *Am. Zool.*, 39, 56–65.

Baker, A.C., Glynn, P.W. & Riegl, B. (2008). Climate change and coral reef bleaching: An ecological assessment of long-term impacts, recovery trends and future outlook. *Estuar. Coast. Shelf Sci.*, 80, 435–471.

Bar-On, Y.M., Phillips, R. & Milo, R. (2018). The biomass distribution on Earth. *Proc. Natl. Acad. Sci.*, 115, 6506–6511.

Barnosky, A.D., Matzke, N., Tomiya, S., Wogan, G.O.U., Swartz, B., Quental, T.B., *et al.* (2011). Has the Earth's sixth mass extinction already arrived? *Nature*, 471, 51–57.

Bastin, J.-F., Finegold, Y., Garcia, C., Mollicone, D., Rezende, M., Routh, D., *et al.* (2019). The global tree restoration potential. *Science*, 365, 76–79.

Bauman, A.G., Pratchett, M.S., Baird, A.H., Riegl, B., Heron, S.F. & Feary, D.A. (2013). Variation in the size structure of corals is related to environmental extremes in the Persian Gulf. *Mar. Environ. Res.*, 84, 43–50.

Beeden, R., Maynard, J., Puotinen, M., Marshall, P., Dryden, J., Goldberg, J., *et al.* (2015). Impacts and Recovery from Severe Tropical Cyclone Yasi on the Great Barrier Reef. *PLoS One*, 10, e0121272.

Beeden, R., Maynard, J., Puotinen, M., Marshall, P., Dryden, J., Goldberg, J., *et al.* (2016). Data from: Impacts and recovery from Severe Tropical Cyclone Yasi on the Great Barrier Reef.

Berkelmans, R., De'ath, G., Kininmonth, S. & Skirving, W.J. (2004). A comparison of the 1998 and 2002 coral bleaching events on the Great Barrier Reef: Spatial correlation, patterns, and predictions. *Coral Reefs*, 23, 74–83.

Berkelmans, R. & Oliver, J.K. (1999). Large-scale bleaching of corals on the Great Barrier Reef. *Coral Reefs*, 18, 55–60.

Bertrand, J. (1889). *Calcul de probabilités*. Gauthier-Villars, Paris.

Bjørnstad, O.N. & Falck, W. (2001). Nonparametric spatial covariance functions: Estimation and testing. *Environ. Ecol. Stat.*, 8, 53–70.

Bongaerts, P., Riginos, C., Brunner, R., Englebert, N., Smith, S.R. & Hoegh-Guldberg, O. (2017). Deep reefs are not universal refuges: Reseeding potential varies among coral

species. *Sci. Adv.*, 3, e1602373.

Brandl, S.J., Goatley, C.H.R., Bellwood, D.R. & Tornabene, L. (2018). The hidden half: ecology and evolution of cryptobenthic fishes on coral reefs. *Biol. Rev.*

Brandl, S.J., Tornabene, L., Goatley, C.H.R., Casey, J.M., Morais, R.A., Côté, I.M., *et al.* (2019). Demographic dynamics of the smallest marine vertebrates fuel coral reef ecosystem functioning. *Science*, 364, 1189–1192.

Bruckner, A.W. (2002). Proceedings of the Caribbean Acropora Workshop: Potential Application of the U.S. Endangered Species Act as a Conservation Strategy. *Proc. Caribb. Acropora Work.*, 199.

Bruno, J. (2016). Data from: Coral reef degradation is not correlated with local human population density. Dryad Digital Repository. https://doi.org/10.5061/dryad.48r68.

Bruno, J.F. & Selig, E.R. (2007). Regional Decline of Coral Cover in the Indo-Pacific: Timing, Extent, and Subregional Comparisons. *PLoS One*, 2, e711.

Bruno, J.F. & Valdivia, A. (2016). Coral reef degradation is not correlated with local human population density. *Sci. Rep.*, 6, 1–8.

Burgess, S.C., Baskett, M.L., Grosberg, R.K., Morgan, S.G. & Strathmann, R.R. (2016). When is dispersal for dispersal? Unifying marine and terrestrial perspectives. *Biol. Rev. Camb. Philos. Soc.*, 91, 867–882.

Bürkner, P.-C. (2017). brms: An R Package for Bayesian Multilevel Models Using Stan. *J. Stat. Softw.*, 80.

Butchart, S.H.M., Walpole, M., Collen, B., van Strien, A., Scharlemann, J.P.W., Almond, R.E.A., *et al.* (2010). Global Biodiversity: Indicators of Recent Declines. *Science*, 328, 1164–1168.

Caley, M.J., Carr, M.H., Hixon, M.A., Hughes, T.P., Jones, G.P. & Menge, B.A. (1996). Recruitment and the Local Dynamics of Open Marine Populations. *Annu. Rev. Ecol. Syst.*, 27, 477–500.

Callaghan, J. & Power, S.B. (2011). Variability and decline in the number of severe tropical cyclones making land-fall over eastern Australia since the late nineteenth century. *Clim. Dyn.*, 37, 647–662.

Canfield, R.H. (1941). Application of the Line Interception Method in Sampling Range

Vegetation. *J. For.*, 39, 388–394.

Capdevila, P., Stott, I., Beger, M. & Salguero-Gómez, R. (2020). Towards a comparative framework of demographic resilience. *Trends Ecol. Evol.*, 116544.

Cardoso, P., Borges, P.A. V, Triantis, K.A., Ferrández, M.A. & Martín, J.L. (2012). The underrepresentation and misrepresentation of invertebrates in the IUCN Red List. *Biol. Conserv.*, 149, 147–148.

Cardoso, P., Borges, P.A.V., Triantis, K.A., Ferrández, M.A. & Martín, J.L. (2011). Adapting the IUCN Red List criteria for invertebrates. *Biol. Conserv.*, 144, 2432–2440.

Carpenter, K.E., Abrar, M., Aeby, G., Aronson, R.B., Banks, S., Bruckner, A., *et al.* (2008). One-third of reef-building corals face elevated extinction risk from climate change and local impacts. *Science*, 321, 560–563.

Ceballos, G. & Ehrlich, P.R. (2002). Mammal population losses and the extinction crisis. *Science*, 296, 904–907.

Chesson, P. (2000). Mechanisms of maintenance of species diversity. *Annu. Rev. Ecol. Syst.*, 31, 343–66.

Chirayath, V. & Earle, S.A. (2016). Drones that see through waves – preliminary results from airborne fluid lensing for centimetre-scale aquatic conservation. *Aquat. Conserv. Mar. Freshw. Ecosyst.*, 26, 237–250.

Clements, C.F., Blanchard, J.L., Nash, K.L., Hindell, M.A. & Ozgul, A. (2017). Body size shifts and early warning signals precede the historic collapse of whale stocks. *Nat. Ecol. Evol.*, 1, 1–6.

Connell, J., Hughes, T. & Wallace, C. (1997). A 30-year study of coral abundance, recruitment, and disturbance at several scales in space and time. *Ecol. Monogr.*, 67, 461–488.

Connell, J.H. (1978). Diversity in Tropical Rain Forests and Coral Reefs. *Science*, 199, 1302–1310.

Connolly, S.R., Dornelas, M., Bellwood, D.R. & Hughes, T.P. (2009). Testing species abundance models: A new bootstrap approach applied to Indo-Pacific coral reefs. *Ecology*, 90, 3138–3149.

Connolly, S.R., Hughes, T.P. & Bellwood, D.R. (2017). A unified model explains

commonness and rarity on coral reefs. *Ecol. Lett.*, 20, 477–486.

Connolly, S.R., Hughes, T.P., Bellwood, D.R. & Karlson, R.H. (2005). Community structure of corals and reef fishes at multiple scales. *Science*, 309, 1363–1365.

Cornell, H. V., Karlson, R.H. & Hughes, T.P. (2007). Scale-dependent variation in coral community similarity across sites, islands, and island groups. *Ecology*, 88, 1707–1715.

Cornell, H. V., Karlson, R.H. & Hughes, T.P. (2008). Local-regional species richness relationships are linear at very small to large scales in west-central Pacific corals. *Coral Reefs*, 27, 145–151.

Costanza, R., D'Arge, R., de Groot, R., Farber, S., Grasso, M., Hannon, B., *et al.* (1998). The value of the world's ecosystem services and natural capital. *Nature*, 387, 253–260.

Costanza, R., de Groot, R., Sutton, P., van der Ploeg, S., Anderson, S.J., Kubiszewski, I., *et al.* (2014). Changes in the global value of ecosystem services. *Glob. Environ. Chang.*, 26, 152–158.

Crowther, T.W., Glick, H.B., Covey, K.R., Bettigole, C., Maynard, D.S., Thomas, S.M., *et al.* (2015). Mapping tree density at a global scale. *Nature*, 525, 201–205.

Crutzen, P.J. (2006). The "Anthropocene." In: *Earth System Science in the Anthropocene* (eds. Ehlers, E. & Krafft, T.). Springer Berlin Heidelberg, pp. 13–18.

Darling, E.S., Alvarez-Filip, L., Oliver, T. a., Mcclanahan, T.R. & Côté, I.M. (2012). Evaluating life-history strategies of reef corals from species traits. *Ecol. Lett.*, 15, 1378–1386.

Darling, E.S., McClanahan, T.R., Maina, J., Gurney, G.G., Graham, N.A.J., Januchowski-Hartley, F., *et al.* (2019). Social–environmental drivers inform strategic management of coral reefs in the Anthropocene. *Nat. Ecol. Evol.*, 3, 1341–1350.

De'ath, G., Fabricius, K.E., Sweatman, H. & Puotinen, M. (2012). The 27-year decline of coral cover on the Great Barrier Reef and its causes. *Proc. Natl. Acad. Sci.*, 109, 17995–17999.

DeAngelis, D.L. & Waterhouse, J.C. (1987). Equilibrium and Nonequilibrium Concepts in Ecological Models. *Ecol. Monogr.*, 57, 1–21.

Dirzo, R., Young, H.S., Galetti, M., Ceballos, G., Isaac, N.J.B. & Collen, B. (2014). Defaunation in the Anthropocene. *Science*, 345, 401–406.

Done, T.J. (1988). Simulation of recovery of pre-disturbance size structure in populations of Porites spp. damaged by the crown of thorns starfish Acanthaster planci. *Mar. Biol.*, 100, 51–61.

Done, T.J. (1992). Effects of tropical cyclone waves on ecological and geomorphological structures on the Great Barrier Reef. *Cont. Shelf Res.*, 12, 859–872.

Dornelas, M., Madin, J.S., Baird, A.H. & Connolly, S.R. (2017). Allometric growth in reef-building corals. *Proc. R. Soc. B Biol. Sci.*, 284, 20170053.

Eakin, C.M., Morgan, J.A., Heron, S.F., Smith, T.B., Liu, G., Alvarez-Filip, L., *et al.* (2010). Caribbean Corals in Crisis: Record Thermal Stress, Bleaching, and Mortality in 2005. *PLoS One*, 5, e13969.

Eakin, C.M., Sweatman, H.P.A. & Brainard, R.E. (2019). The 2014–2017 global-scale coral bleaching event: insights and impacts. *Coral Reefs*, 38, 539–545.

Edmunds, P. & Riegl, B. (2019). Urgent need for coral demography in a world where corals are disappearing. *Mar. Ecol. Prog. Ser.*, 635, 233–242.

Edmunds, P.J. (2015). A quarter-century demographic analysis of the Caribbean coral, Orbicella annularis, and projections of population size over the next century. *Limnol. Oceanogr.*, 60, 840–855.

Edwards, C.B., Eynaud, Y., Williams, G.J., Pedersen, N.E., Zgliczynski, B.J., Gleason, A.C.R., *et al.* (2017). Large-area imaging reveals biologically driven non-random spatial patterns of corals at a remote reef. *Coral Reefs*, 36, 1291–1305.

Fabricius, K.E. (2005). Effects of terrestrial runoff on the ecology of corals and coral reefs: review and synthesis. *Mar. Pollut. Bull.*, 50, 125–146.

Fabricius, K.E., De'ath, G., Puotinen, M.L., Done, T., Cooper, T.F. & Burgess, S.C. (2008). Disturbance gradients on inshore and offshore coral reefs caused by a severe tropical cyclone. *Limnol. Oceanogr.*, 53, 690–704.

Fabricius, K.E. & Metzner, J. (2004). Scleractinian walls of mouths: Predation on coral larvae by corals. *Coral Reefs*, 23, 245–248.

Fauset, S., Johnson, M.O., Gloor, M., Baker, T.R., Monteagudo M., A., Brienen, R.J.W., *et al.* (2015). Hyperdominance in Amazonian forest carbon cycling. *Nat. Commun.*, 6, 6857.

Ferrari, R., Figueira, W.F., Pratchett, M.S., Boube, T., Adam, A., Kobelkowsky-Vidrio, T., *et*

al. (2017). 3D photogrammetry quantifies growth and external erosion of individual coral colonies and skeletons. *Sci. Rep.*, 7, 1–9.

Figueiredo, J., Baird, A.H. & Connolly, S.R. (2013). Synthesizing larval competence dynamics and reef-scale retention reveals a high potential for self-recruitment in corals. *Ecology*, 94, 650–659.

Figueiredo, J., Baird, A.H., Harii, S. & Connolly, S.R. (2014). Increased local retention of reef coral larvae as a result of ocean warming. *Nat. Clim. Chang.*, 4, 498–502.

Fisher, R., O'Leary, R.A., Low-Choy, S., Mengersen, K., Knowlton, N., Brainard, R.E., *et al.* (2015). Species Richness on Coral Reefs and the Pursuit of Convergent Global Estimates. *Curr. Biol.*, 25, 500–505.

Frankham, R. (1995). Effective population size/adult population size ratios in wildlife: a review. *Genet. Res.*, 66, 95–107.

Franklin, B. (1751). Observations Concerning the Increase of Mankind. In: *The Papers of Benjamin Franklin* (ed. Leonard W. Labaree. New Haven: Yale University Press). pp. 225–234.

Gardner, T.A. (2003). Long-Term Region-Wide Declines in Caribbean Corals. *Science*, 301, 958–960.

Gaston, K.J. & Blackburn, T.M. (1997). How many birds are there? *Biodivers. Conserv.*, 6, 615–625.

Gaston, K.J. & Fuller, R.A. (2008). Commonness, population depletion and conservation biology. *Trends Ecol. Evol.*, 23, 14–19.

Gillespie, C.S. (2015). Fitting heavy tailed distributions: the poweRlaw package. *J. Stat. Softw.*, 64.

Gilmour, J.P., Smith, L.D., Heyward, A.J., Baird, A.H. & Pratchett, M.S. (2013). Recovery of an isolated coral reef system following severe disturbance. *Science*, 340, 69–71.

Goatley, C.H.R. & Bellwood, D.R. (2011). The roles of dimensionality, canopies and complexity in ecosystem monitoring. *PLoS One*, 6.

González-rivero, M., Bongaerts, P., Beijbom, O., Pizarro, O., Friedman, A., Rodriguez-Ramirez, A., *et al.* (2014). The Catlin Seaview Survey - kilometre-scale seascape assessment, and monitoring of coral reef ecosystems. *Aquat. Conserv. Mar. Freshw.*

Ecosyst., 24, 184–198.

Goodrich, J.M., Lynam, A., Miquelle, D.G., Wibisono, H.T., Kawanishi, K., Pattanavibool, A., *et al.* (2015). *Panthera tigris. The IUCN Red List of Threatened Species 2015: e.T15955A50659951*.

Graham, N.A.J. (2014). Habitat complexity: Coral structural loss leads to fisheries declines. *Curr. Biol.*, 24, R359–R361.

Graunt, J. (1662). *Natural and Political Observations Made Upon the Bills of Mortality*. The Johns Hopkins Press, Baltimore.

Green, E.P. & Bruckner, A.W. (2000). The significance of coral disease epizootiology for coral reef conservation. *Biol. Conserv.*, 96, 347–361.

Green, R.H., Lowe, R.J., Buckley, M.L., Foster, T. & Gilmour, J.P. (2019). Physical mechanisms influencing localized patterns of temperature variability and coral bleaching within a system of reef atolls. *Coral Reefs*, 38, 759–771.

Hall, V.R. & Hughes, T.P. (1996). Reproductive Strategies of Modular Organisms: Comparative Studies of Reef-Building Corals. *Ecology*, 77, 950–963.

Hansen, W.D., Braziunas, K.H., Rammer, W., Seidl, R. & Turner, M.G. (2018). It takes a few to tango: changing climate and fire regimes can cause regeneration failure of two subalpine conifers. *Ecology*, 99, 966–977.

Hawkins, S.J., Firth, L.B., McHugh, M., Poloczanska, E.S., Herbert, R.J.H., Burrows, M.T., *et al.* (2013). Data rescue and re-use: Recycling old information to address new policy concerns. *Mar. Policy*, 42, 91–98.

Healy, K., Ezard, T.H.G., Jones, O.R., Salguero-Gómez, R. & Buckley, Y.M. (2019). Animal life history is shaped by the pace of life and the distribution of age-specific mortality and reproduction. *Nat. Ecol. Evol.*, 3, 1217–1224.

Hedley, J., Roelfsema, C., Chollett, I., Harborne, A., Heron, S., Weeks, S., *et al.* (2016). Remote Sensing of Coral Reefs for Monitoring and Management: A Review. *Remote Sens.*, 8, 118.

Hoegh-Guldberg, O. (1999). Climate change, coral bleaching and the future of the world's coral reefs. *Mar. Freshw. Res.*

van den Hoogen, J., Geisen, S., Routh, D., Ferris, H., Traunspurger, W., Wardle, D.A., *et al.*

(2019). Soil nematode abundance and functional group composition at a global scale. *Nature*, 572, 194–198.

Hoogenboom, M.O., Frank, G.E., Chase, T.J., Jurriaans, S., Álvarez-Noriega, M., Peterson, K., *et al.* (2017). Environmental Drivers of Variation in Bleaching Severity of Acropora Species during an Extreme Thermal Anomaly. *Front. Mar. Sci.*, 4.

Van Hooidonk, R., Maynard, J., Tamelander, J., Gove, J., Ahmadia, G., Raymundo, L., *et al.* (2016). Local-scale projections of coral reef futures and implications of the Paris Agreement. *Sci. Rep.*, 6, 1–8.

van Hooidonk, R., Maynard, J.A. & Planes, S. (2013). Temporary refugia for coral reefs in a warming world. *Nat. Clim. Chang.*, 3, 508–511.

Huang, D., Licuanan, W.Y., Baird, A.H. & Fukami, H. (2011). Cleaning up the "Bigmessidae": molecular phylogeny of scleractinian corals from Faviidae, Merulinidae, Pectiniidae and Trachyphylliidae. *BMC Evol. Biol.*, 11, 37.

Hubbell, S.P. (2015). Estimating the global number of tropical tree species, and Fisher's paradox. *Proc. Natl. Acad. Sci.*, 112, 7343–7344.

Hubbell, S.P., He, F., Condit, R., Borda-de-Agua, L., Kellner, J. & ter Steege, H. (2008). How many tree species are there in the Amazon and how many of them will go extinct? *Proc. Natl. Acad. Sci.*, 105, 11498–11504.

Hughes, T.P. (1984). Population Dynamics Based on Individual Size Rather than Age: A General Model with a Reef Coral Example. *Am. Nat.*, 123, 778–795.

Hughes, T.P., Anderson, K.D., Connolly, S.R., Heron, S.F., Kerry, J.T., Lough, J.M., *et al.* (2018a). Spatial and temporal patterns of mass bleaching of corals in the Anthropocene. *Science*, 359, 80–83.

Hughes, T.P., Ayre, D. & Connell, J.H. (1992). The evolutionary ecology of corals. *Trends Ecol. Evol.*, 7, 292–295.

Hughes, T.P., Baird, a H., Bellwood, D.R., Card, M., Connolly, S.R., Folke, C., *et al.* (2003). Climate change, human impacts, and the resilience of coral reefs. *Science*, 301, 929–33.

Hughes, T.P., Baird, A.H., Dinsdale, E.A., Moltschaniwskyj, N.A., Pratchett, M.S., Tanner, J.E., *et al.* (2000). Supply-side ecology works both ways: The link between benthic adults, fecundity, and larval recruits. *Ecology*, 81, 2241–2249.

Hughes, T.P., Baird, A.H., Dinsdale, E.A., Moltschaniwskyj, N.A., Pratchett, M.S., Tanner, J.E., *et al.* (2012). Assembly rules of reef corals are flexible along a steep climatic gradient. *Curr. Biol.*, 22, 736–741.

Hughes, T.P., Barnes, M.L., Bellwood, D.R., Cinner, J.E., Cumming, G.S., Jackson, J.B.C., *et al.* (2017a). Coral reefs in the Anthropocene. *Nature*, 546, 82–90.

Hughes, T.P., Bellwood, D.R., Baird, a. H., Brodie, J., Bruno, J.F. & Pandolfi, J.M. (2011). Shifting base-lines, declining coral cover, and the erosion of reef resilience: Comment on Sweatman et al. (2011). *Coral Reefs*, 30, 653–660.

Hughes, T.P., Bellwood, D.R. & Connolly, S.R. (2002). Biodiversity hotspots, centres of endemicity, and the conservation of coral reefs. *Ecol. Lett.*, 5, 775–784.

Hughes, T.P., Bellwood, D.R., Connolly, S.R. & Cornell, H. V. (2014). Double Jeopardy and Global Extinction Risk in Corals and Reef Fishes. *Curr. Biol.*, 24, 2946–2951.

Hughes, T.P., Connolly, S.R. & Keith, S.A. (2013a). Geographic ranges of reef corals (Cnidaria: Anthozoa: Scleractinia) in the Indo-Pacific. *Ecology*, 94, 1659.

Hughes, T.P. & Jackson, J.B.C. (1980). Do corals lie about their age? Some demographic consequences of partial mortality, fission, and fusion. *Science*, 209, 713–715.

Hughes, T.P. & Jackson, J.B.C. (1985). Population dynamics and life histories of foliaceous corals. *Ecol. Monogr.*, 55, 141–166.

Hughes, T.P., Kerry, J.T., Álvarez-Noriega, M., Álvarez-Romero, J.G., Anderson, K.D., Baird, A.H., *et al.* (2017b). Global warming and recurrent mass bleaching of corals. *Nature*, 543, 373–377.

Hughes, T.P., Kerry, J.T., Baird, A.H., Connolly, S.R., Chase, T.J., Dietzel, A., *et al.* (2019a). Global warming impairs stock–recruitment dynamics of corals. *Nature*, 568, 387–390.

Hughes, T.P., Kerry, J.T., Baird, A.H., Connolly, S.R., Dietzel, A., Eakin, C.M., *et al.* (2018b). Global warming transforms coral reef assemblages. *Nature*, 556, 492–496.

Hughes, T.P., Kerry, J.T., Connolly, S.R., Baird, A.H., Eakin, C.M., Heron, S.F., *et al.* (2019b). Ecological memory modifies the cumulative impact of recurrent climate extremes. *Nat. Clim. Chang.*, 9, 40–43.

Hughes, T.P., Kerry, J.T. & Simpson, T. (2018c). Large-scale bleaching of corals on the Great Barrier Reef. *Ecology*, 99, 501.

Hughes, T.P., Linares, C., Dakos, V., van de Leemput, I.A. & van Nes, E.H. (2013b). Living dangerously on borrowed time during slow, unrecognized regime shifts. *Trends Ecol. Evol.*, 28, 149–55.

Hughes, T.P. & Tanner, J.E. (2000). Recruitment Failure, Life Histories, and Long-Term Decline of Caribbean Corals. *Ecology*, 81, 2250.

Hull, P.M., Darroch, S.A.F. & Erwin, D.H. (2015). Rarity in mass extinctions and the future of ecosystems. *Nature*, 528, 345–351.

IPCC. (2018). Summary for Policymakers. In: *Global Warming of 1.5°C. An IPCC Special Report on the impacts of global warming of 1.5°C above pre-industrial levels and related global greenhouse gas emission pathways, in the context of strengthening the global response to the threat of climate change,* (eds. Masson-Delmotte, V., Zhai, P., Pörtner, H.-O., Roberts, D., Skea, J., Shukla, P.R., et al.).

IUCN. (2020). *IUCN Red List of Threatened Species*. Available at: https://www.iucnredlist.org/resources/summary-statistics. Last accessed 17 May 2020.

Jackson, J.B., Kirby, M.X., Berger, W.H., Bjorndal, K.A., Botsford, L.W., Bourque, B.J., *et al.* (2001). Historical overfishing and the recent collapse of coastal ecosystems. *Science*, 293, 629–637.

Jackson, J.B.C., Donovan, M.K., Cramer, K.L. & Lam, V. V. (2014). *Status and Trends of Caribbean Coral Reefs: 1970-2012*. Global Coral Reef Monitoring Network, IUCN, Gland, Switzerland.

Johst, K. & Drechsler, M. (2003). Are Spatially Correlated or Uncorrelated Disturbance Regimes Better for the Survival of Species? *Oikos*, 103, 449–456.

Jones, G.P., Almany, G.R., Russ, G.R., Sale, P.F., Steneck, R.S., Oppen, M.J.H., *et al.* (2009). Larval retention and connectivity among populations of corals and reef fishes: history, advances and challenges. *Coral Reefs*, 28, 307–325.

Jones, O.R., Archer, C.R., Buckley, Y.M., Che-castaldo, J., Caswell, H., Hodgson, D., *et al.* (2015). The Compadre Plant Matrix Database: an open online repository for plant demography. *J. Ecol.*, 103, 202–218.

Kallimanis, A.S., Kunin, W.E., Halley, J.M. & Sgardelis, S.P. (2005). Metapopulation extinction risk under spatially autocorrelated disturbance. *Conserv. Biol.*, 19, 534–546.

Karlson, R.H., Cornell, H. V. & Hughes, T.P. (2004). Coral communities are regionally enriched along an oceanic biodiversity gradient. *Nature*, 429, 867–870.

Kayal, M., Lenihan, H.S., Brooks, A.J., Holbrook, S.J., Schmitt, R.J. & Kendall, B.E. (2018). Predicting coral community recovery using multi-species population dynamics models. *Ecol. Lett.*, 21, 1790–1799.

Keith, S.A., Woolsey, E.S., Madin, J.S., Byrne, M. & Baird, A.H. (2015). Differential establishment potential of species predicts a shift in coral assemblage structure across a biogeographic barrier. *Ecography*, 38, 1225–1234.

Kerry, J.T. & Bellwood, D.R. (2015). Do tabular corals constitute keystone structures for fishes on coral reefs? *Coral Reefs*, 34, 41–50.

Kindsvater, H.K., Dulvy, N.K., Horswill, C., Juan-Jordá, M.-J., Mangel, M. & Matthiopoulos, J. (2018). Overcoming the Data Crisis in Biodiversity Conservation. *Trends Ecol. Evol.*, 33, 676–688.

Kinlan, B.P. & Gaines, S.D. (2003). Propagule Dispersal in Marine and Terrestrial Environments: a Community Perspective. *Ecology*, 84, 2007–2020.

Knowlton, N. & Jackson, J.B.C. (1994). New taxonomy and niche partitioning on coral reefs: jack of all trades or master of some? *Trends Ecol. Evol.*, 9, 7–9.

Knowlton, N., Lang, J.C. & Keller, B.D. (1990). Case study of natural population collapse: post-hurricane predation on Jamaican staghorn corals. *Smithson. Contrib. Mar. Sci.*, 1–25.

Koons, D.N., Grand, J.B., Zinner, B. & Rockwell, R.F. (2005). Transient population dynamics: Relations to life history and initial population state. *Ecol. Modell.*, 185, 283–297.

Kullback, S. & Leibler, R.A. (1951). On Information and Sufficiency. *Ann. Math. Stat.*, 22, 79–86.

Lennon, J.J. (2000). Red-shifts and red herrings in geographical ecology. *Ecography*, 23, 101–113.

Lessios, H.A., Robertson, D.R. & Cubit, J.D. (1984). Spread of Diadema Mass Mortality Through the Caribbean. *Science*, 226, 335–337.

Levin, S.A. (1992). The Problem of Pattern and Scale in Ecology: The Robert H. MacArthur

Award Lecture. *Ecology*, 73, 1943–1967.

Lewis, S.L. & Maslin, M.A. (2015). Defining the Anthropocene. *Nature*, 519, 171–180.

Li, N. (2017). *Bayesian Method for Bertrand Probability Paradox Ning*. https://github.com/kgmacau/Bayesian-Method-for-Bertrand-Probability.

Liao, J., Ying, Z., Hiebeler, D.E., Wang, Y., Takada, T. & Nijs, I. (2015). Species extinction thresholds in the face of spatially correlated periodic disturbance. *Sci. Rep.*, 5, 1–9.

Liao, J., Ying, Z., Woolnough, D.A., Miller, A.D., Li, Z. & Nijs, I. (2016). Coexistence of species with different dispersal across landscapes: a critical role of spatial correlation in disturbance. *Proc. R. Soc. B*, 283, 20160537.

Lindenmayer, D.B. & Laurance, W.F. (2016). The Unique Challenges of Conserving Large Old Trees. *Trends Ecol. Evol.*, 31, 416–418.

Lindenmayer, D.B. & Laurance, W.F. (2017). The ecology, distribution, conservation and management of large old trees. *Biol. Rev.*, 92, 1434–1458.

Lindenmayer, D.B., Laurance, W.F. & Franklin, J.F. (2012a). Global decline in large old trees. *Science*, 338, 1305–1306.

Lindenmayer, D.B., Likens, G.E., Andersen, A., Bowman, D., Bull, C.M., Burns, E., *et al.* (2012b). Value of long-term ecological studies. *Austral Ecol.*, 37, 745–757.

Liu, G., Heron, S.F., Mark Eakin, C., Muller-Karger, F.E., Vega-Rodriguez, M., Guild, L.S., *et al.* (2014). Reef-scale thermal stress monitoring of coral ecosystems: New 5-km global products from NOAA coral reef watch. *Remote Sens.*, 6, 11579–11606.

Loya, Y. (1978). Plotless and transect methods. In: *Coral reefs: research methods, UNESCO, Paris* (eds. Stoddart, R.E. & Johannes, D.R.). pp. 197–217.

Loya, Y., Sakai, K., Yamazato, K., Nakano, Y., Sambali, H. & van Woesik, R. (2001). Coral bleaching: the winners and the losers. *Ecol. Lett.*, 4, 122–131.

MacArthur, R.H. & Wilson, E.O. (1967). *The Theory of Island Biogeography*. Princeton Unversity Press, Princeton, N.J.

Madin, E.M.P., Darling, E.S. & Hardt, M.J. (2019). Emerging Technologies and Coral Reef Conservation: Opportunities, Challenges, and Moving Forward. *Front. Mar. Sci.*, 6, 1–7.

Madin, J.S., Anderson, K.D., Andreasen, M.H., Bridge, T.C.L., Cairns, S.D., Connolly, S.R., *et al.* (2016). The Coral Trait Database, a curated database of trait information for coral

species from the global oceans. *Sci. Data*, 3, 160017.

Madin, J.S., Baird, A.H., Dornelas, M. & Connolly, S.R. (2014). Mechanical vulnerability explains size-dependent mortality of reef corals. *Ecol. Lett.*, 17, 1008–1015.

Marsh, L.M., Bradbury, R.H. & Reichelt, R.E. (1984). Determination of the physical parameters of coral distributions using line transect data. *Coral Reefs*, 2, 175–180.

Marshall, P.A. & Baird, A.H. (2000). Bleaching of corals on the Great Barrier Reef: differential susceptibilities among taxa. *Coral Reefs*, 19, 155–163.

Martin, T.G., Burgman, M.A., Fidler, F., Kuhnert, P.M., Low-Choy, S., Mcbride, M., *et al.* (2012). Eliciting Expert Knowledge in Conservation Science. *Conserv. Biol.*, 26, 29–38.

Matthews, S.A., Mellin, C., MacNeil, A., Heron, S.F., Skirving, W., Puotinen, M., *et al.* (2019). High-resolution characterization of the abiotic environment and disturbance regimes on the Great Barrier Reef, 1985–2017. *Ecology*, 100, 1–2.

McCarthy, M.A., Possingham, H.P., Day, J.R. & Tyre, A.J. (2001). Testing the accuracy of population viability analysis. *Conserv. Biol.*, 15, 1030–1038.

McClanahan, T.R., Ateweberhan, M. & Omukoto, J. (2008). Long-term changes in coral colony size distributions on Kenyan reefs under different management regimes and across the 1998 bleaching event. *Mar. Biol.*, 153, 755–768.

Meesters, E.H., Hilterman, M., Kardinaal, E., Keetman, M., de Vries, M. & Bak, R.P.M. (2001). Colony size-frequency distributions of scleractinian coral populations: spatial and interspecific variation. *Mar. Biol.*, 209, 43–54.

Middlebrook, R., Hoegh-Guldberg, O. & Leggat, W. (2008). The effect of thermal history on the susceptibility of reef-building corals to thermal stress. *J. Exp. Biol.*, 211, 1050–1056.

Miller, M., Williams, D.E., Huntington, B.E., Piniak, G.A. & Vermeij, M.J.A. (2016). Decadal comparison of a diminishing coral community: a study using demographics to advance inferences of community status. *PeerJ*, 4, e1643.

Moberg, F. & Folke, C. (1999). Ecological goods and services of coral reef ecosystems. *Ecol. Econ.*, 29, 215–233.

Moloney, K.A. & Levin, S.A. (1996). The effects of disturbance architecture on landscape-level population-dynamics. *Ecology*, 77, 375–394.

Morais, R.A., Depczynski, M., Fulton, C.J., Marnane, M.J., Narvaez, P., Huertas, V., *et al.*

(2020). Severe coral loss shifts energetic dynamics on a coral reef. *Funct. Ecol.*, 1–12.

Moritz, C., Vii, J., Lee Long, W., Tamelander, J., Thomassin, A. & Planes, S. (2018). *Status and trends of coral reefs of the Pacific*. Global Coral Reef Monitoring Network.

Muller-Landau, H.C., Condit, R.S., Harms, K.E., Marks, C.O., Thomas, S.C., Bunyavejchewin, S., *et al.* (2006). Comparing tropical forest tree size distributions with the predictions of metabolic ecology and equilibrium models. *Ecol. Lett.*, 9, 589–602.

Mumby, P.J. (1999). Bleaching and hurricane disturbances to populations of coral recruits in Belize. *Mar. Ecol. Prog. Ser.*, 190, 27–35.

O'Mahony, J., Simes, R., Redhill, D., Heaton, K., Atkinson, C., Hayward, E., *et al.* (2017). *At what price? The economic, social and icon value of the Great Barrier Reef*. Deloitte Access Economics, Brisbane.

Oliver, J. & Babcock, R. (1992). Aspects of the fertilization ecology of broadcast spawning corals: sperm dilution effects and in situ measurements of fertilization. *Biol. Bull.*, 183, 409–417.

Ovenden, J.R., Peel, D., Street, R., Courtney, A.J., Hoyle, S.D., Peel, S.L., *et al.* (2007). The genetic effective and adult census size of an Australian population of tiger prawns (Penaeus esculentus). *Mol. Ecol.*, 16, 127–138.

Pandi, A. V & Ranade, V. V. (2016). Chord length distribution to particle size distribution. *AIChE J.*, 62, 4215–4228.

Pauly, D. (1995). Anecdotes and the shifting baseline syndrome of fisheries. *Trends Ecol. Evol.*, 10, 430.

Pauly, D., Hilborn, R. & Branch, T.A. (2013). Does catch reflect abundance. *Nature*, 494, 3–6.

Pereira, H.M., Leadley, P.W., Proença, V., Alkemade, R., Scharlemann, J.P.W., Fernandez-Manjarrés, J.F., *et al.* (2010). Scenarios for global biodiversity in the 21st century. *Science*, 330, 1496–1501.

Pimm, S.L., Jenkins, C.N., Abell, R., Brooks, T.M., Gittleman, J.L., Joppa, L.N., *et al.* (2014). The biodiversity of species and their rates of extinction, distribution, and protection. *Science*, 344, 1246752.

Pratchett, M., Caballes, C., Wilmes, J., Matthews, S., Mellin, C., Sweatman, H., *et al.* (2017).

Thirty Years of Research on Crown-of-Thorns Starfish (1986–2016): Scientific Advances and Emerging Opportunities. *Diversity*, 9, 41.

Pratchett, M.S. (2005). Dietary overlap among coral-feeding butterflyfishes (Chaetodontidae) at Lizard Island, northern Great Barrier Reef. *Mar. Biol.*, 148, 373–382.

Pratchett, M.S. (2007). Feeding Preferences of Acanthaster planci (Echinodermata: Asteroidea) under Controlled Conditions of Food Availability. *Pacific Sci.*, 61, 113–120.

Pratchett, M.S., Gust, N., Goby, G. & Klanten, S.O. (2001). Consumption of coral propagules represents a significant trophic link between corals and reef fish. *Coral Reefs*, 20, 13–17.

Puotinen, M., Maynard, J.A., Beeden, R., Radford, B. & Williams, G.J. (2016). A robust operational model for predicting where tropical cyclone waves damage coral reefs. *Sci. Rep.*, 6, 1–12.

Régnier, C., Achaz, G., Lambert, A., Cowie, R.H., Bouchet, P. & Fontaine, B. (2015). Mass extinction in poorly known taxa. *Proc. Natl. Acad. Sci.*, 112, 7761–7766.

Riegl, B., Johnston, M., Purkis, S., Howells, E., Burt, J., Steiner, S.C.C., *et al.* (2018). Population collapse dynamics in Acropora downingi, an Arabian/Persian Gulf ecosystem-engineering coral, linked to rising temperature. *Glob. Chang. Biol.*, 24, 2447–2462.

Riegl, B.M., Bruckner, A.W., Rowlands, G.P., Purkis, S.J. & Renaud, P. (2012). Red Sea coral reef trajectories over 2 decades suggest increasing community homogenization and decline in coral size. *PLoS One*, 7, 5–11.

Robinson, R.A., Morrison, C.A. & Baillie, S.R. (2014). Integrating demographic data: Towards a framework for monitoring wildlife populations at large spatial scales. *Methods Ecol. Evol.*, 5, 1361–1372.

Roelfsema, C., Phinn, S., Jupiter, S., Comley, J. & Albert, S. (2013). Mapping coral reefs at reef to reef-system scales, 10s–1000s km2, using object-based image analysis. *Int. J. Remote Sens.*, 34, 6367–6388.

Salguero-Gómez, R., Jones, O.R., Archer, C.R., Bein, C., de Buhr, H., Farack, C., *et al.* (2016a). COMADRE: a global data base of animal demography. *J. Anim. Ecol.*, 85, 371–384.

Salguero-Gómez, R., Jones, O.R., Jongejans, E., Blomberg, S.P., Hodgson, D.J., Mbeau-

Ache, C., *et al.* (2016b). Fast–slow continuum and reproductive strategies structure plant life-history variation worldwide. *Proc. Natl. Acad. Sci.*, 113, 230–235.

Säterberg, T., Sellman, S. & Ebenman, B. (2013). High frequency of functional extinctions in ecological networks. *Nature*, 499, 468–70.

Schoepf, V., Stat, M., Falter, J.L. & McCulloch, M.T. (2015). Limits to the thermal tolerance of corals adapted to a highly fluctuating, naturally extreme temperature environment. *Sci. Rep.*, 5, 1–14.

Smith, S.R. (1992). Patterns of coral recruitment and post-settlement mortality on Bermuda's reefs: Comparisons to Caribbean and Pacific reefs. *Am. Zool.*, 32, 663–673.

Spalding, M.D., Fox, H.E., Allen, G.R., Davidson, N., Ferdaña, Z.A., Finlayson, M., *et al.* (2007). Marine Ecoregions of the World: A Bioregionalization of Coastal and Shelf Areas. *Bioscience*, 57, 573–583.

Stan Development Team. (2019). Stan Modeling Language Users Guide and Reference Manual Version.

ter Steege, H., Pitman, N.C. a, Sabatier, D., Baraloto, C., Salomao, R.P., Guevara, J.E., *et al.* (2013). Hyperdominance in the Amazonian Tree Flora. *Science*, 342, 1243092.

ter Steege, H., Pitman, N.C.A., Killeen, T.J., Laurance, W.F., Peres, C.A., Guevara, J.E., *et al.* (2015). Estimating the global conservation status of more than 15,000 Amazonian tree species. *Sci. Adv.*, 1, e1500936.

Steffen, W., Richardson, K., Rockstrom, J., Cornell, S.E., Fetzer, I., Bennett, E.M., *et al.* (2015). Planetary boundaries: Guiding human development on a changing planet. *Science*, 347, 1259855.

Stott, I., Franco, M., Carslake, D., Townley, S. & Hodgson, D. (2010). Boom or bust? A comparative analysis of transient population dynamics in plants. *J. Ecol.*, 98, 302–311.

Teo, A. & Todd, P.A. (2018). Simulating the effects of colony density and intercolonial distance on fertilisation success in broadcast spawning scleractinian corals. *Coral Reefs*, 37, 891–900.

Torda, G., Sambrook, K., Cross, P., Sato, Y., Bourne, D.G., Lukoschek, V., *et al.* (2018). Decadal erosion of coral assemblages by multiple disturbances in the Palm Islands, central Great Barrier Reef. *Sci. Rep.*, 8, 11885.

Turner, M.G. (2010). Disturbance and landscape dynamics in a changing world. *Ecology*, 91, 2833–2849.

Turner, M.G., Calder, W.J., Cumming, G.S., Hughes, T.P., Jentsch, A., LaDeau, S.L., *et al.* (2020). Climate change, ecosystems and abrupt change: science priorities. *Philos. Trans. R. Soc. B*, 375, 20190105.

UNEP-WCMC, WorldFish-Centre, WRI & TNC. (2010). *Global Distribution of Coral Reefs, compiled from multiple sources including the Millennium Coral Reef Mapping Project. Version 2.0, updated by UNEP-WCMC. Includes contributions from IMaRS- USF and IRD (2005), IMaRS-USF (2005) and Spalding et al. (2001).*

Urban, M.C. (2015). Accelerating extinction risk from climate change. *Science*, 348, 571–573.

US Fish and Wildlife Service. (2017). *California Condor Recovery Program: 2017 Annual Population Status*.

Vermeij, M. & Bak, R. (2000). Inferring demographic processes from population size structure in corals. *Proc 9th Int Coral Reef Symp*, 23–27.

Warner, R.R. (1997). Evolutionary ecology: how to reconcile pelagic dispersal with local adaptation. *Coral Reefs*, 16, S115–S120.

Warton, D.I. & Hui, F.K.C. (2011). The arcsine is asinine: the analysis of proportions in ecology. *Ecology*, 92, 3–10.

Webb, T.J. & Mindel, B.L. (2015). Global Patterns of Extinction Risk in Marine and Non-marine Systems. *Curr. Biol.*, 25, 1–6.

White, E.P., Enquist, B.J. & Green, J.L. (2008). On estimating the exponent of power-law frequency distributions. *Ecology*, 89, 905–912.

White, P.S. & Jentsch, A. (2001). The Search for Generality in Studies of Disturbance and Ecosystem Dynamics. In: *Progress in Botany* (eds. Esser, K., Lüttge, U., Kadereit, J.W. & Beyschlag, W.). Springer, Berlin, Heidelberg, pp. 399–450.

Wilkinson, C. (2008). *Status of Coral Reefs of the World: 2008*. Global Coral Reef Monitoring Network and Reef and Rainforest Research Centre, Townsville, Australia.

Wolff, N.H., Wong, A., Vitolo, R., Stolberg, K., Anthony, K.R.N. & Mumby, P.J. (2016). Temporal clustering of tropical cyclones on the Great Barrier Reef and its ecological

importance. *Coral Reefs*, 35, 613–623.

Woodley, J.D., Chornesky, E.A., Clifford, P.A., Jackson, J.B.C., Kaufman, L.S., Knowlton, N., *et al.* (1981). Hurricane Allen's Impact on Jamaican Coral Reefs. *Science*, 214, 749–755.

Worldometer. (2020). *Global human population size*. Available at: https://www.worldometers.info/world-population/. Last accessed 13 May 2020.

Yearsley, J. (2016). *Generate spatial data (version 1.0.0.0)*. Available at: https://nl.mathworks.com/matlabcentral/fileexchange/5091-generate-spatial-data?focused=6123568&tab=function. Last accessed 18 February 2018.

Zawada, K.J.A., Madin, J.S., Baird, A.H., Bridge, T.C.L. & Dornelas, M. (2019). Morphological traits can track coral reef responses to the Anthropocene. *Funct. Ecol.*, 33, 962–975.

Appendices

Appendix A

Publications arising from this thesis

Dietzel, Andreas, M. Bode, S. R. Connolly, T. P. Hughes. 2020. The population sizes of reef-building coral species at biogeographic scales. *Under review in Nature Ecology and Evolution*

Dietzel, Andreas, M. Bode, S. R. Connolly, T. P. Hughes. 2020. Long-term shifts in the colony size structure of coral populations along the Great Barrier Reef. *Under review in Proceedings of the Royal Society B*

Dietzel, Andreas, M. Bode, T. P. Hughes. 2020. Beyond cover: reconstructing population size structure from line-intercept data for demographic inference. *In preparation*

Dietzel, Andreas, M. Bode, S. R. Connolly, T. P. Hughes. 2020. The spatial clustering and patchiness of large-scale disturbances on coral reefs. *Under review in Global Change Biology*

Appendix B

Publications not arising from this thesis

Hughes, T.P., Kerry, J.T., Baird, A.H., Connolly, S.R., Chase, T.J., **Dietzel, A**., *et al.* (2019). Global warming impairs stock–recruitment dynamics of corals. *Nature*, 568, 387–390.

Hughes, T.P., Kerry, J.T., Baird, A.H., Connolly, S.R., **Dietzel, A**., Eakin, C.M., *et al.* (2018). Global warming transforms coral reef assemblages. *Nature*, 556, 492–496.

Appendix C

Supplementary Material for Chapter 2

Table C-1 Fitted parameters of unified model. Table showing for each metacommunity, the fitted parameters of the unified model, the size of the species pool, the number of observed and unobserved species, as well as the combined abundance of all unobserved species relative to the combined abundance of all species in the species pool.

Region	Habitat	mu	sig	a	b	Species pool	Observed	Unobserved	% combined abundance of unobserved species
Indonesia	crest	0.31	1.56	4.41	1.59	256	205	51	1.9
Indonesia	flat	0.49	1.59	6.22	1.63	148	122	26	1.6
Indonesia	slope	0.26	1.71	4.54	1.70	293	227	66	1.7
Papua New Guinea	crest	0.26	2.04	4.87	1.63	177	130	47	1.1
Papua New Guinea	flat	0.41	1.60	5.64	1.49	137	108	29	2.1
Papua New Guinea	slope	0.39	1.59	4.16	1.70	251	211	40	1.1
Solomon Islands	crest	0.15	2.04	4.20	1.28	158	96	62	2.4
Solomon Islands	flat	0.32	1.43	5.11	1.47	101	79	22	3.5
Solomon Islands	slope	0.39	1.53	2.97	1.39	210	177	33	1.3
American Samoa	crest	0.43	1.45	5.45	1.37	64	51	13	2.8
American Samoa	flat	0.23	1.97	7.43	1.48	49	32	17	3.2
American Samoa	slope	0.56	1.81	4.38	1.73	102	88	14	0.5
French Polynesia	crest	0.12	2.94	4.43	1.43	69	40	29	0.5
French Polynesia	flat	0.57	1.67	4.26	1.43	46	39	7	1.0
French Polynesia	slope	0.58	2.46	3.56	1.51	69	56	13	0.2

Table C-2 Geographic location of the fifteen islands across five regions at which species abundances were measured. Coordinates are given in degrees latitude and longitude.

Region	Island/Location	Latitude	Longitude
Indonesia	Manado, North Sulawesi	1.62 N	124.76 E
Indonesia	Wakatobi, South Sulawesi	5.45 S	123.76 E
Indonesia	Bird's Head, Irian Jaya	0.34 S	130.4 E
Papua New Guinea	Madang	5.21 S	145.82 E
Papua New Guinea	Kimbe Bay, New Britain	5.43 S	150.1 E
Papua New Guinea	Kavieng, New Ireland	2.62 S	150.7 E
Solomon Islands	Uepi Island	8.42 S	157.94 E
Solomon Islands	Munda, New Georgia	8.36 S	157.24 E
Solomon Islands	Gizo Island	8.11 S	156.86 E
American Samoa	Tutuila Island	14.32 S	170.7 W
American Samoa	Ofu Island	14.17 S	169.68 W
American Samoa	Tau Island	14.24 S	169.47 W
French Polynesia	Raiatea Island	16.79 S	151.49 W
French Polynesia	Moorea Island	17.54 S	149.83 W
French Polynesia	Tahiti Island	17.64 S	149.44 W

Table C-3 Coral reef habitat maps compiled from different sources

Location	Region	Source	Lat	Lon
Manua	American Samoa	NOAA_NCCOS	-14.2	-169.7
Rose Atoll	American Samoa	NOAA_NCCOS	-14.5	-168.2
Swains Island	American Samoa	NOAA_NCCOS	-11.1	-171.1
Tutuila	American Samoa	NOAA_NCCOS	-14.3	-170.7
Sarigan	CNMI	NOAA_NCCOS	16.7	145.8
Tinian	CNMI	NOAA_NCCOS	15	145.6
Saipan	CNMI	NOAA_NCCOS	15.2	145.7
Rota	CNMI	NOAA_NCCOS	14.1	145.2
Agrihan	CNMI	NOAA_NCCOS	18.8	139.7
Alamagan	CNMI	NOAA_NCCOS	17.6	145.8
Anatahan	CNMI	NOAA_NCCOS	16.4	145.7
Asuncion	CNMI	NOAA_NCCOS	19.7	145.4
Medinilla	CNMI	NOAA_NCCOS	16	146.1
Guguan	CNMI	NOAA_NCCOS	17.3	145.8
Pajaros	CNMI	NOAA_NCCOS	20.5	144.9
Maug	CNMI	NOAA_NCCOS	20	145.2
Pagan	CNMI	NOAA_NCCOS	18.1	145.8
Aguijan	CNMI	NOAA_NCCOS	16.4	145.7
Palmerston	Cook Islands	Living Oceans Foundation	-18	-163.2
Rarotonga	Cook Islands	Living Oceans Foundation	-21.2	-159.8
Danajon	Fiji	Roelfsema *et al.* 2013	10.2	124.1
Kadavu	Fiji	Roelfsema *et al.* 2013	-19	178.2
Cicia	Fiji	Living Oceans Foundation	-17.7	-179.3
Fulaga	Fiji	Living Oceans Foundation	-19.1	-178.6
Kobara	Fiji	Living Oceans Foundation	-19	-179
Mago	Fiji	Living Oceans Foundation	-17.4	-179.2
Moala	Fiji	Living Oceans Foundation	-18.6	179.9
Nayau	Fiji	Living Oceans Foundation	-18	-179
Totoya	Fiji	Living Oceans Foundation	-18.9	-179.8

Tuvuca	Fiji	Living Oceans Foundation	17.7	-178.8
VanuaBalavu	Fiji	Living Oceans Foundation	-17.2	-178.9
VanuaVatu	Fiji	Living Oceans Foundation	-18.4	-179.3
Aratika	French Polynesia	Living Oceans Foundation	-15.5	-145.5
Bellingshausen	French Polynesia	Living Oceans Foundation	-15.8	-154.5
Hao	French Polynesia	Living Oceans Foundation	-18.2	-140.9
Huahine	French Polynesia	Living Oceans Foundation	-16.8	-151
Maiao	French Polynesia	Living Oceans Foundation	-17.7	-150.6
Maria Oeste	French Polynesia	Living Oceans Foundation	-21.8	-154.7
Mopelia	French Polynesia	Living Oceans Foundation	-16.8	-154
Raivavae	French Polynesia	Living Oceans Foundation	-23.9	-147.7
Rimatara	French Polynesia	Living Oceans Foundation	-22.6	-152.8
Rurutu	French Polynesia	Living Oceans Foundation	-22.5	-151.3
Scilly	French Polynesia	Living Oceans Foundation	-16.5	-154.7
Tahaa and Raiatea	French Polynesia	Living Oceans Foundation	-16.7	-151.5
Tetiaroa	French Polynesia	Living Oceans Foundation	-17	-149.6
Tubuai	French Polynesia	Living Oceans Foundation	-23.4	-149.5
Tupai	French Polynesia	Living Oceans Foundation	-16.3	-151.8
Guam	Guam	NOAA_NCCOS	13.4	144.6
Isle of Pines	New Caledonia	Living Oceans Foundation	-22.6	167.8
Palau	Palau	NOAA_NCCOS	7.3	134.5
Kubulau	Philippines	Roelfsema *et al.* 2013	-16.9	179
Roviana	Solomon Islands	Roelfsema *et al.* 2013	-8.4	157.3
Gizo	Solomon Islands	Living Oceans Foundation	-8	157
Sikopo and Kerehikapa	Solomon Islands	Living Oceans Foundation	-7.5	158.2
Reef Islands	Solomon Islands	Living Oceans Foundation	-10.2	166.4
Marovo	Solomon Islands	Living Oceans Foundation	-8.6	158.4
Malakobi	Solomon Islands	Living Oceans Foundation	-7.4	158.1
Vanikoro	Solomon Islands	Living Oceans Foundation	-11.7	167.1
Utupua	Solomon Islands	Living Oceans Foundation	-11.2	166.7
Vavau	Tonga	Living Oceans Foundation	-18.6	-174

Haapai	Tonga	Living Oceans Foundation	-19.9	-173.9

NOAA NCCOS: National Oceanic and Atmospheric Administration's (NOAA) National Centers for Coastal Ocean Science (NCCOS).
Link: https://products.coastalscience.noaa.gov/collections/benthic/default.aspx

Living Oceans Foundation: Reef habitat data from the Khaled bin Sultan Living Oceans Foundation were obtained manually using the "habitat analysis tool" of the KSLOF's online, interactive World Reef Map.
Link: https://www.livingoceansfoundation.org/maps/

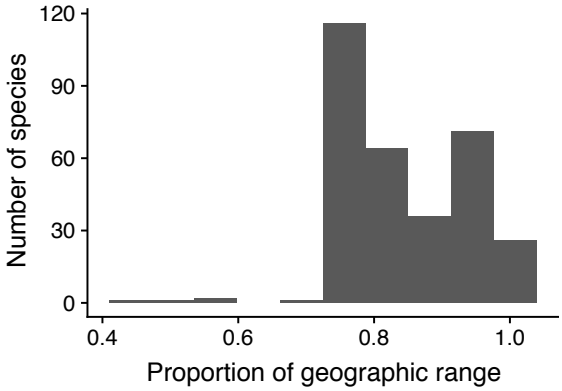

Figure C-1 The proportion of a species' geographic range contained by the boundary of the study. For almost all examined species at least 70% of their geographic range (defined as total reef area or area of occupancy rather than extent of occurrence) lies within the domain of the study. Hence, the presented estimates of population size are conservative compared to global totals.

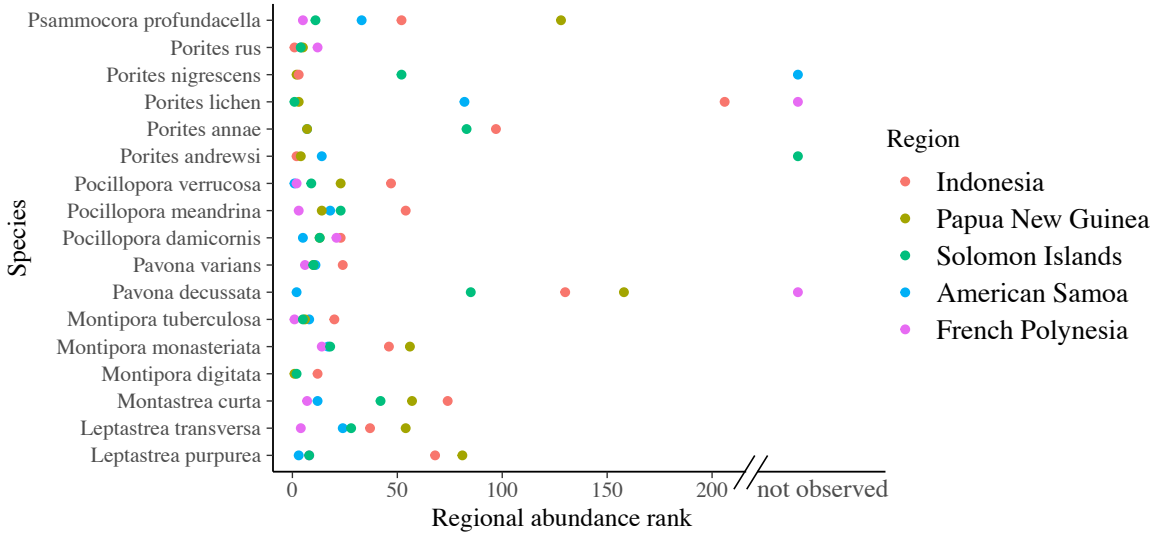

Figure C-2 The regional abundance ranks of hyperdominant coral species. For each of the 17 hyperdominant species, their abundance ranks in each of the regions across their geographic range are shown. While most globally hyperdominant species rank among the most common species in regions throughout their range, some are rare or were not observed at all in parts of their geographic range.

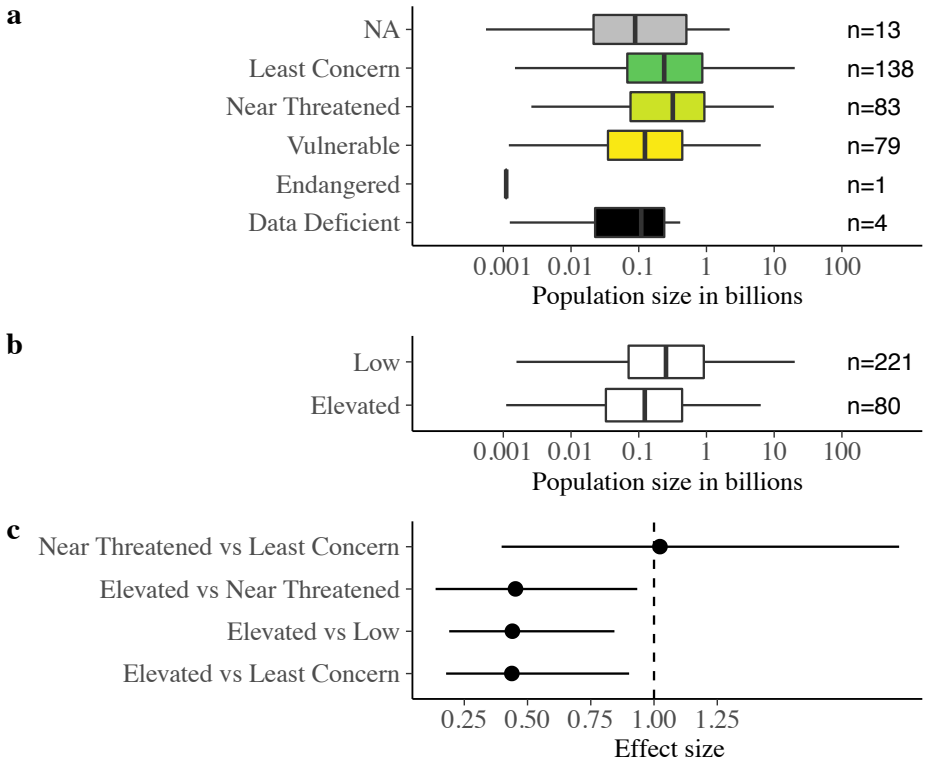

Figure C-3 Coral population sizes and IUCN Red List status. **a**, The distribution of population sizes by IUCN Red List conservation status. **b**, The distribution of population sizes by regrouped conservation status (low risk: least concern or near threatened, elevated risk: vulnerable or endangered). Boxplots show centre line (median), box limits (upper and lower quartiles) and whiskers (×1.5 interquartile range). **c**, Effect size plot showing the estimates and 95% credible intervals of pairwise contrasts. An intersection of the 95% credible interval with the dashed vertical line (effect size = 1) indicates non-significant differences.

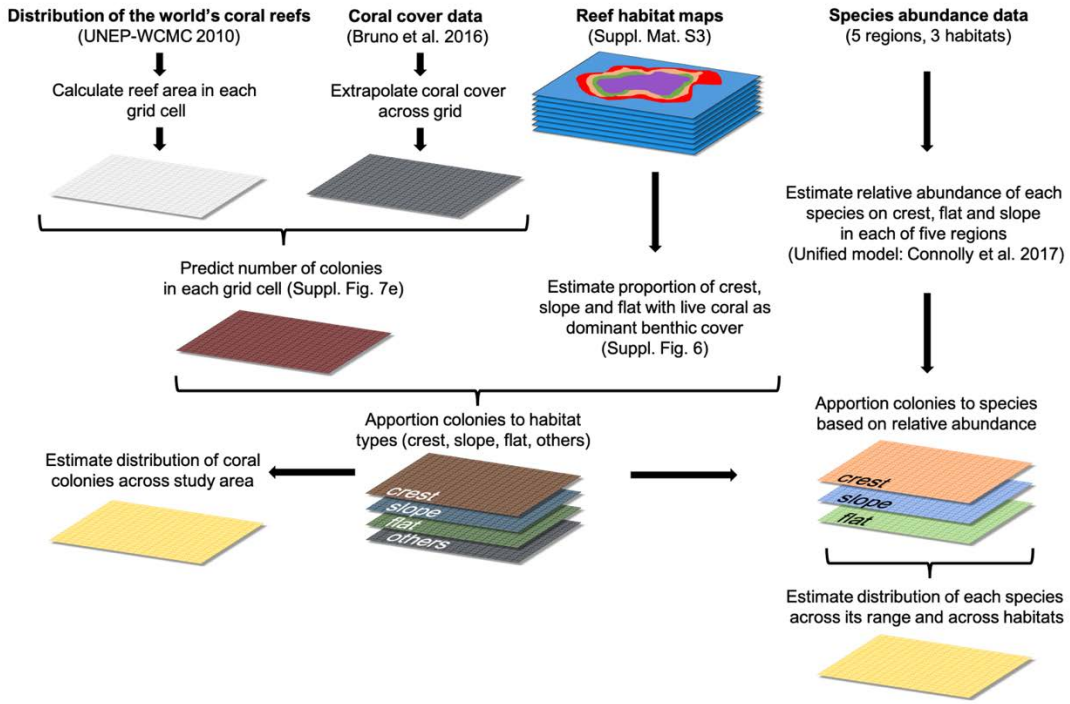

Figure C-4 Schematic overview of analysis. Flow diagram showing how physical and ecological data were used to estimate the total number of colonies in the study area and of the population sizes of 318 Indo-Pacific coral species.

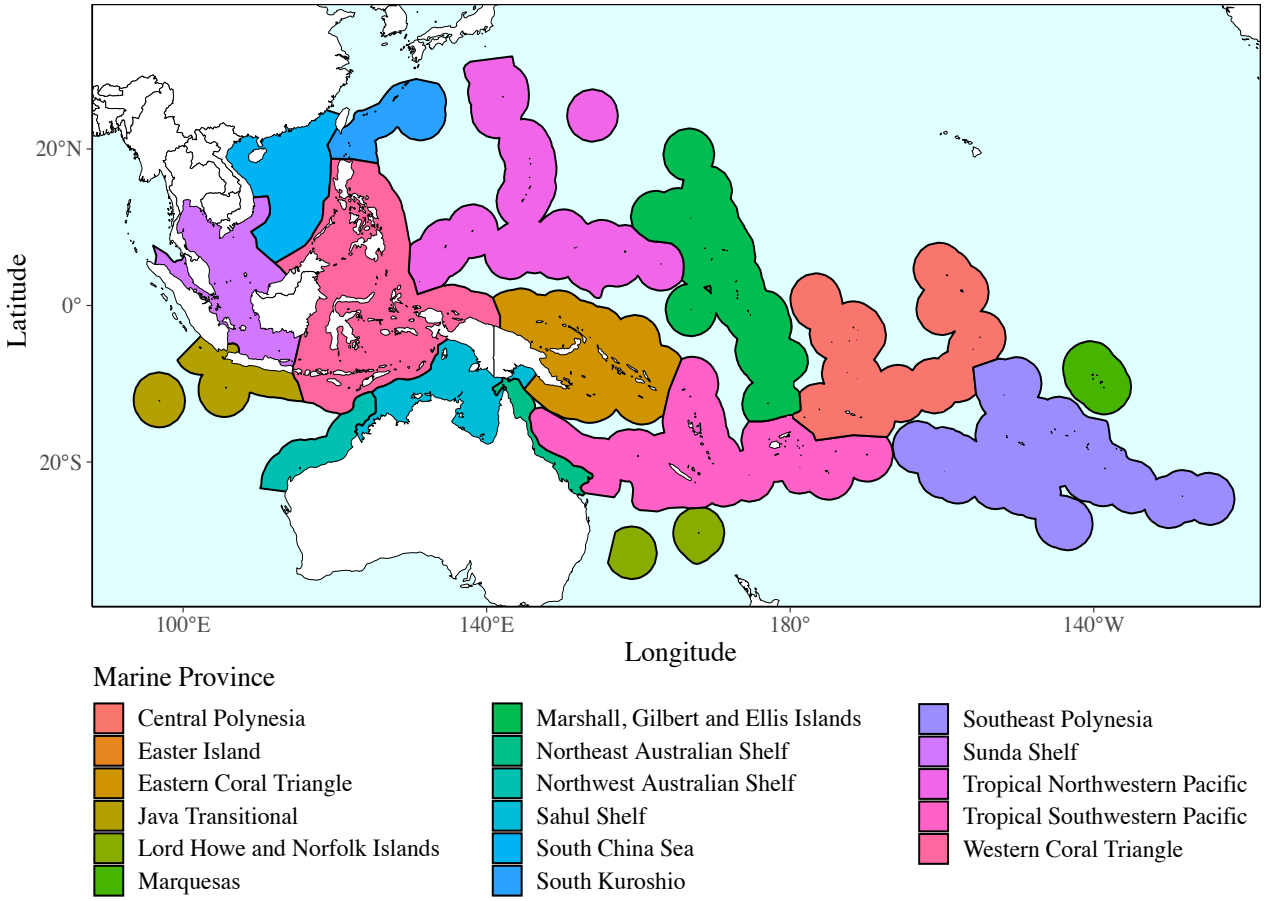

Figure C-5 Map showing the spatial extent of the study. I used the marine provinces defined in Spalding *et al.* (2007) to delineate the spatial extent or domain of the analysis, stretching from Indonesia in the west to French Polynesia in the east.

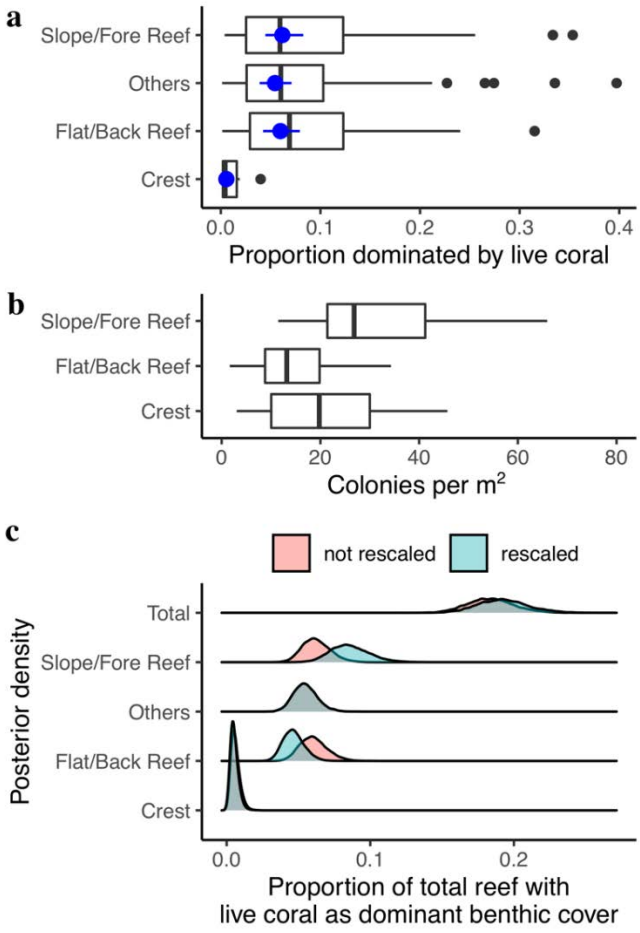

Figure C-6 Proportion of total reef classified as live-coral dominated slope, crest, flat and "other" habitat. **a**, The proportions of live-coral dominated reef slope, crest, flat and other habitat types relative to the total mapped reef area. Boxplots show centre line (median), box limits (upper and lower quartiles) and whiskers (×1.5 interquartile range). Blue dots (●) and lines (—) indicate the fitted parameter estimates and the corresponding 95% credible interval. **b**, Boxplot showing distribution of colony density estimates for the reef flat, reef crest and reef at each of the 60 sites where species abundances were surveyed. **c**, Density plots showing the posterior distributions of the estimated proportions of the total reef classified as live-coral dominated crest, flat, slope and "other" habitat before (red) and after (blue) rescaling by relative colony densities.

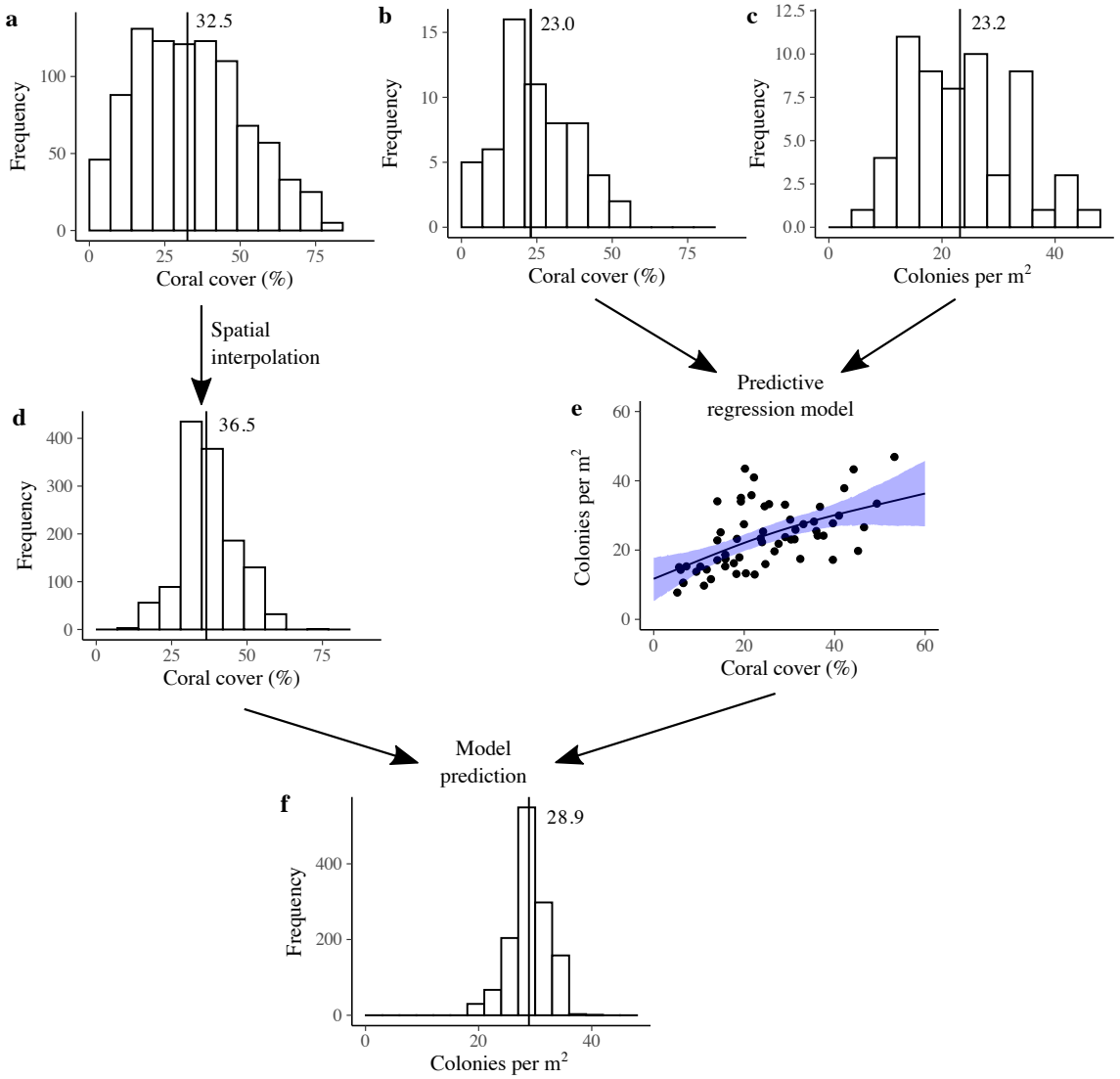

Figure C-7 Model inputs and outputs for predicting coral abundances. **a**, Frequency distribution of coral cover from 931 locations throughout the study domain (Bruno 2016; Bruno & Valdivia 2016). **b**, Frequency distribution of coral cover for 60 sites where species abundances were surveyed. Medians (vertical black line) of coral cover estimates are comparable. **c**, Frequency distribution of colony density estimates at species abundance survey sites (reef slope, crest and flat at four sites on three islands in each of five regions). **d**, Frequency distribution of interpolated grid cell-level coral cover data. **e**, Model fit of Bayesian generalised additive model used to predict the colony density in each grid cell given its interpolated coral cover. Each point corresponds to one of 60 species abundance survey sites and the blue ribbon indicates the 95% credible interval of the fitted Bayesian generalised additive model. **f**, Frequency distribution of predicted colony density estimates at the grid cell level (only grid cells with reef area > 0 are included).

Appendix D

Supplementary Material for Chapter 5

Table D-1 Comparison of disturbance severity scores for coral mass bleaching (Hughes *et al.* 2017b) and Cyclone Yasi (Beeden *et al.* 2015).

Score		**Coral bleaching**	**Cyclone Yasi**	
Ordinal	Binary	% bleached	Cyclone damage index	Damage level description
0		< 1 %	0	No damage
1	0 (not severe)	1 – 10 %	10 – 30	Minor coral damage
2		10 – 30 %	40 – 75	Moderate coral damage
3		30 – 60 %	100 – 120	High coral damage/ Minor reef damage
4	1 (severe)	> 60 %	150 – 200	Severe coral damage/ Moderate reef damage
5			300 - 400	Extreme coral damage/ High reef damage

Table D-2 Overview of model parameters.

Parameter	Value
Number of cells	100 x 100
Annual percentage of cells experiencing background mortality	50%
Background mortality rate (% decline in coral cover)	15% (of cover)
Catastrophic mortality (% decline in coral cover)	60% (of cover)
Deterministic annual growth	5% (of cover)
Years till large-scale disturbance	30 years
Total time horizon	150 years
Degrees of spatial autocorrelation	Random/none, low, medium, high
Magnitude: percentage of cells affected by disturbance	0 – 100%
"Larval" production of source cell spread across sink cells as contribution to coral growth	10% (of cover)

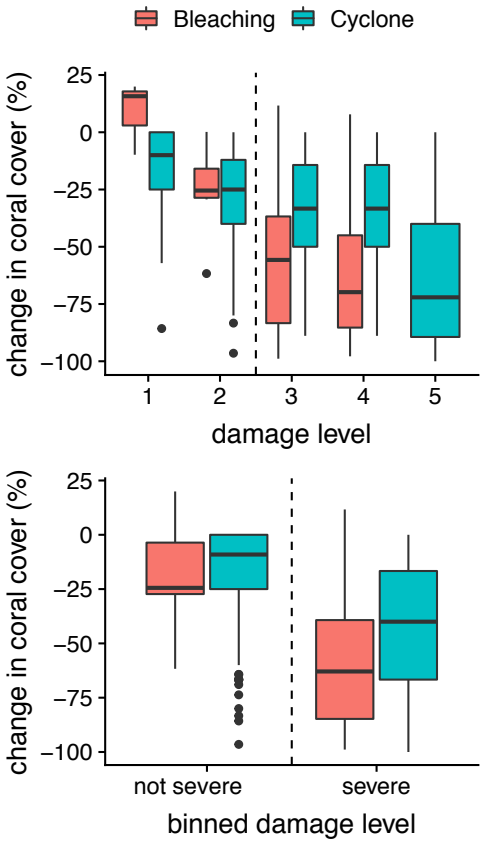

Figure D-1 Loss of coral cover due to 2016 bleaching event and Cyclone Yasi. Four levels of damage from bleaching were recorded (Hughes *et al.* 2018b), and five levels from Cyclone Yasi (Beeden *et al.* 2015). The dashed vertical line indicates the threshold chosen to delineate threshold between not severe and severe.

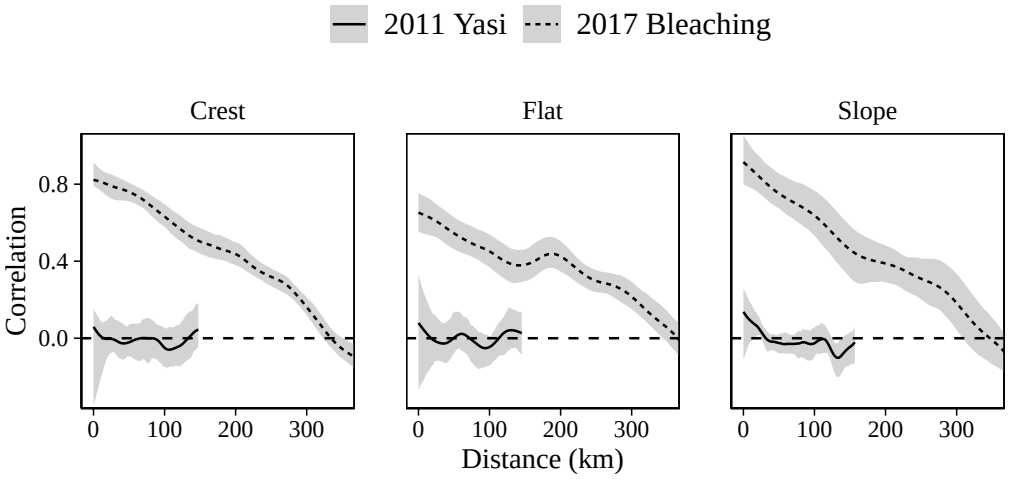

Figure D-2 The spatial clustering of disturbances by habitat type. Spline cross-correlograms showing the distance decay of spatial autocorrelation in disturbance severity in three habitats – reef crest, flat and slope, for the bleaching event in 2017 and Cyclone Yasi in 2011. Ribbons show 95% uncertainty interval.

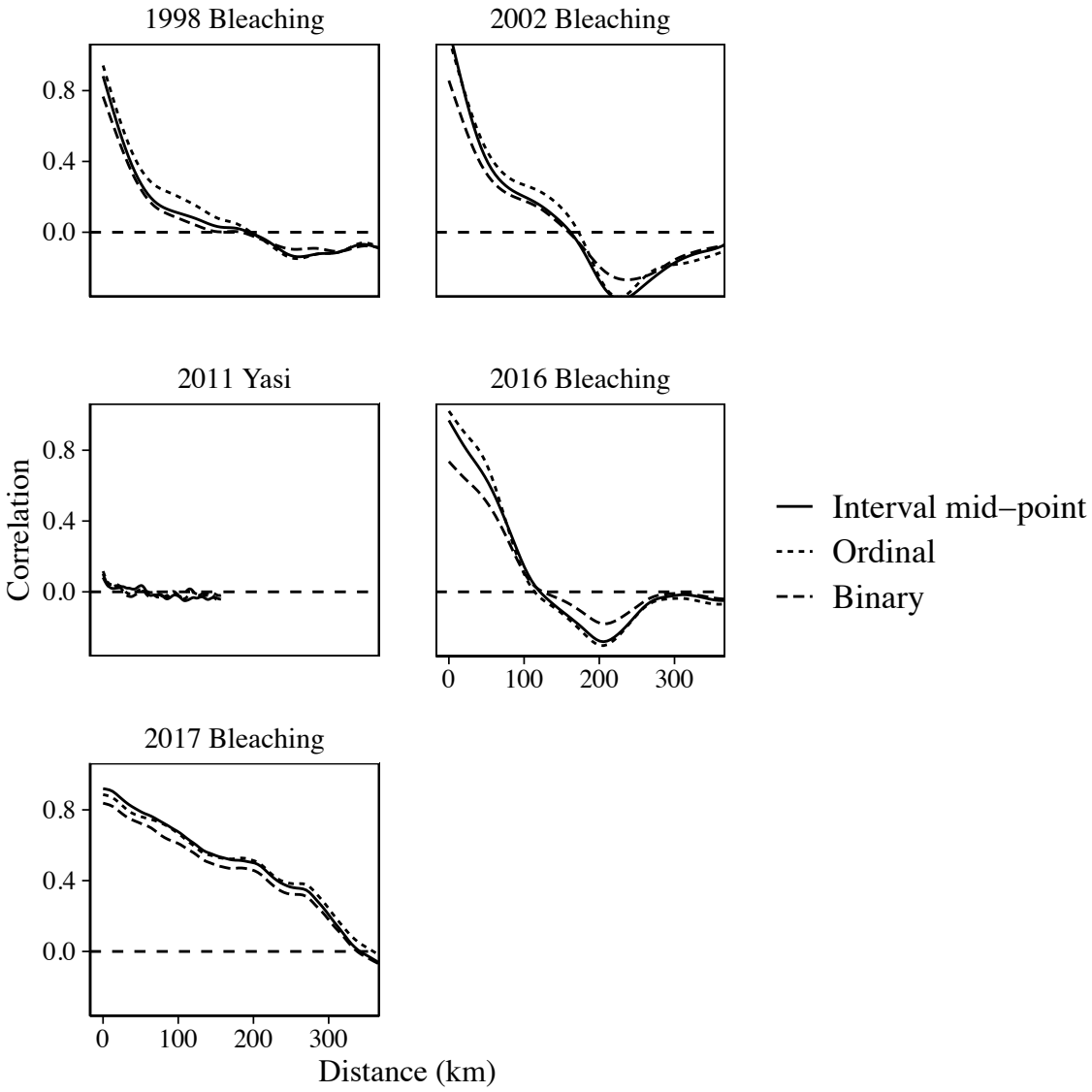

Figure D-3 Correlograms of disturbance events using different data transformations. Figure D-Three transformations – binary, interval mid-point and ordinal – were applied to Cyclone Yasi and the four bleaching episodes.

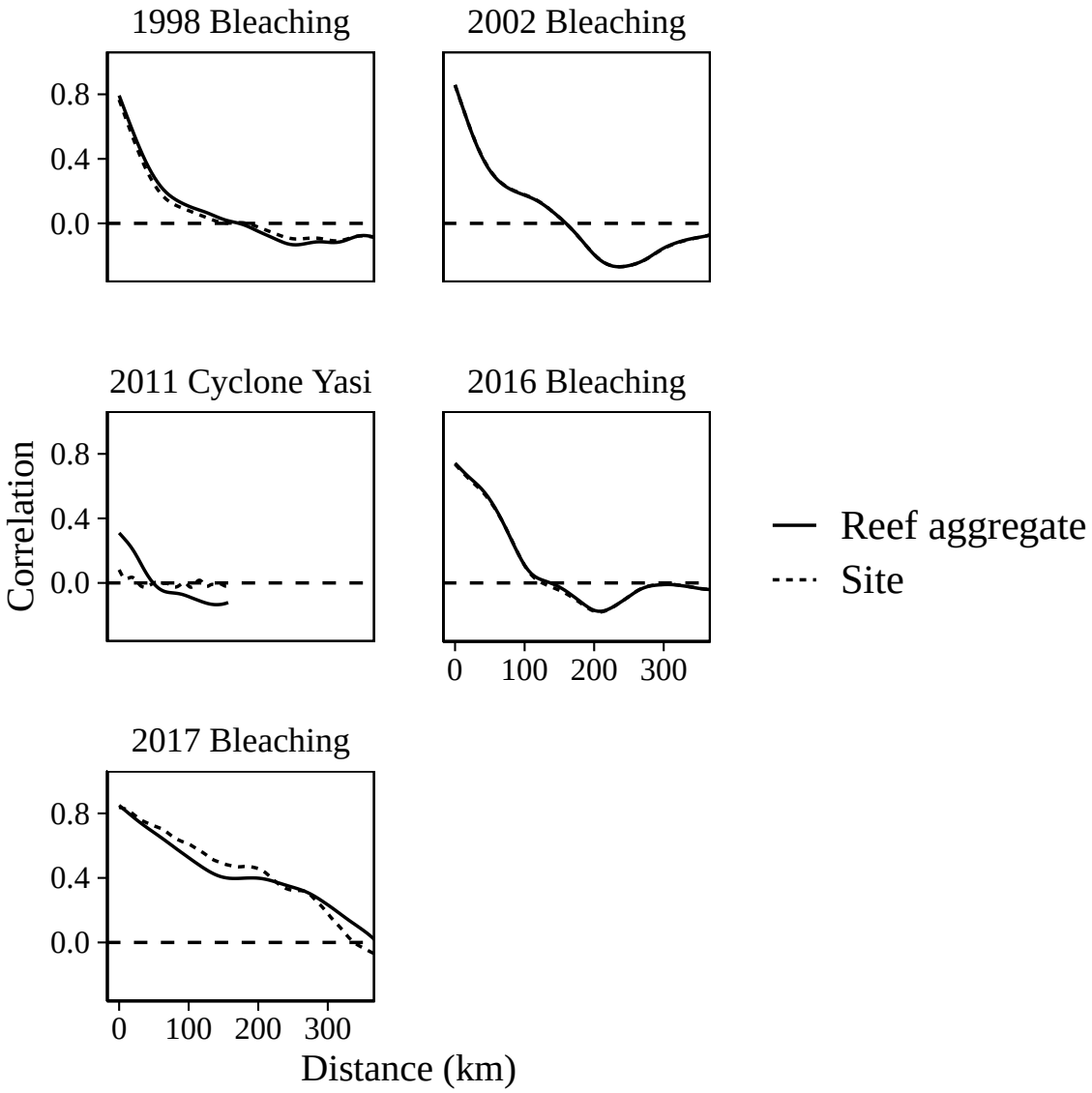

Figure D-4 Spline cross-correlograms of disturbance events using original, site-level data and reef aggregates.

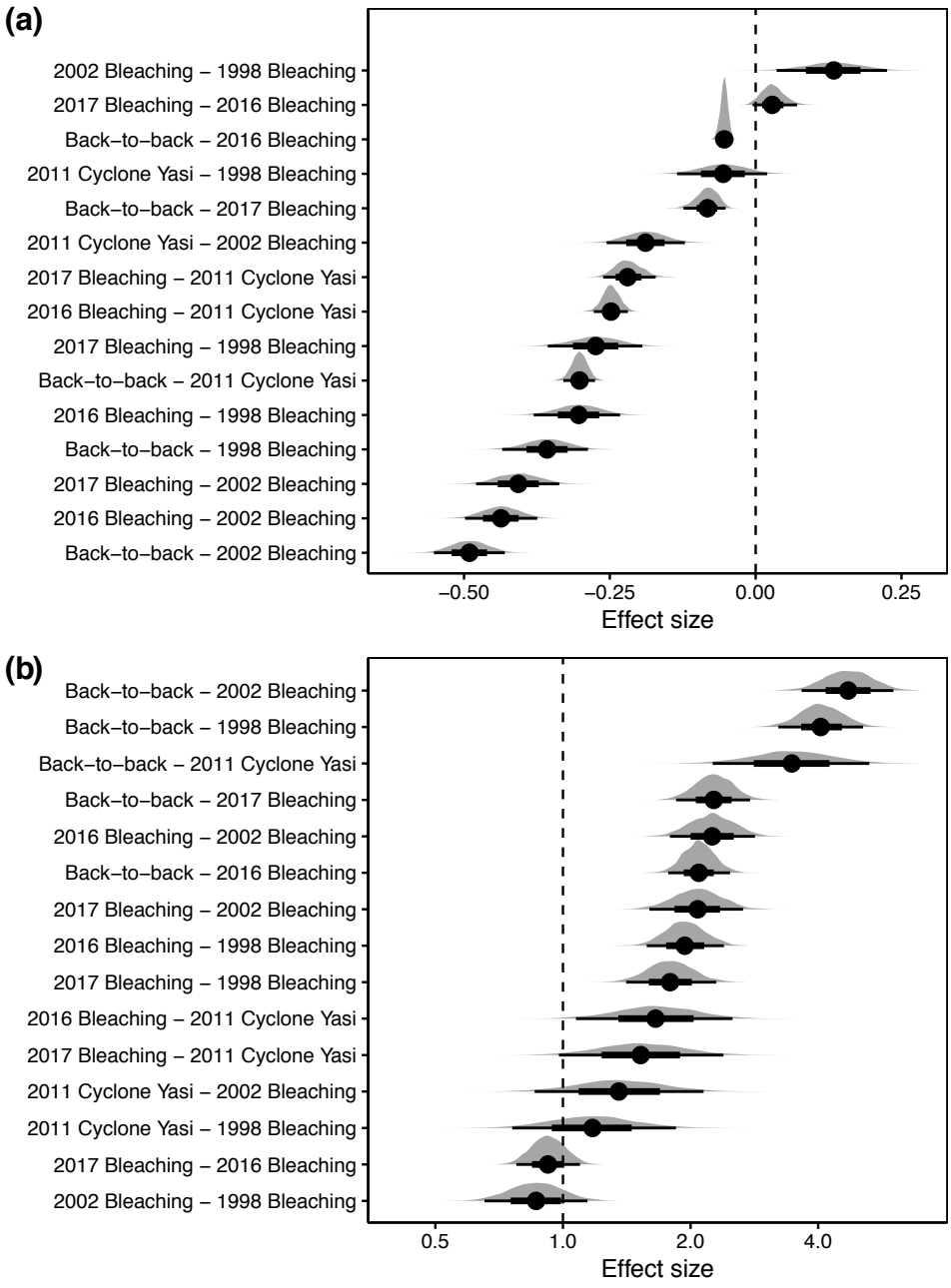

Figure D-5 Pairwise comparisons of posterior effect sizes for spatial isolation metrics and each combination of disturbance events. **(a)** Pairwise comparison for proportion of not severely disturbed reefs within 100km of a severely disturbed reef. **(b)** Pairwise comparison for minimum distance to not severely disturbed reef for each severely disturbed reef. Shaded curves indicate the distribution of the posterior contrasts, circles the posterior medians, thick lines the 50% uncertainty intervals and thin lines the 95% uncertainty intervals. Effect sizes indicate differences in proportions (a) and fractional difference in distances (b) between the posterior distributions of two events and the dashed lines indicate the reference for no difference between two disturbance events.

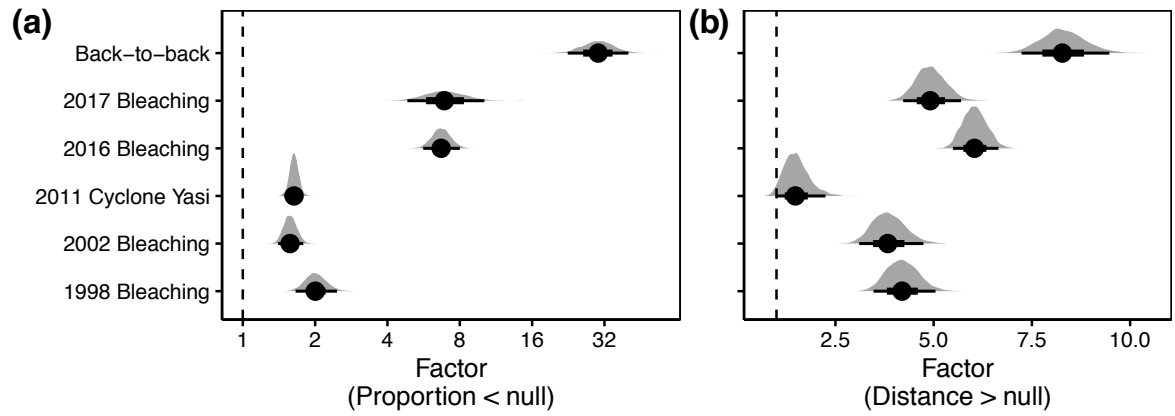

Figure D-6 Comparison of distance metrics to null expectation under random spatial distribution of impact. **(a)** For each disturbance event the posterior distribution of the proportion of not severely disturbed reefs within 100 km of a severely disturbed reef relative to the corresponding null expectation is shown. **(b)** For each disturbance event the posterior distribution of the distance to the nearest not severely disturbed reef relative to the corresponding null expectation is shown. Shaded area indicates posterior distribution, black circles the posterior medians, thick lines the 50% uncertainty interval and thin lines the 95% uncertainty intervals. Dashed lines indicate the reference for no difference from null expectation.

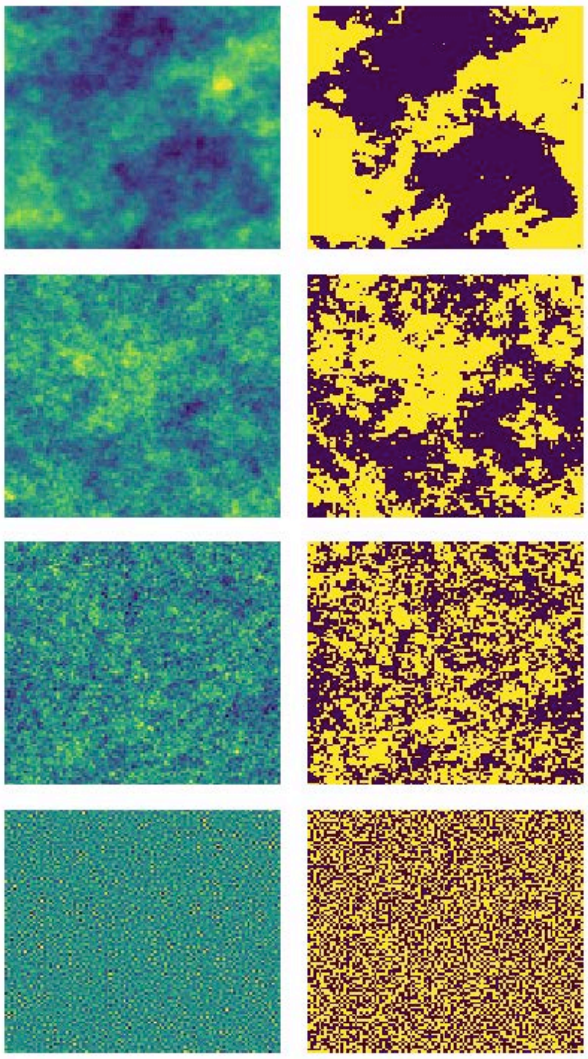

Figure D-7 Spatial patterns of disturbances with different degrees of spatial autocorrelation from highly spatially autocorrelated (top) to randomly distributed in space (bottom). Panels in the right column show discretisation of disturbance pattern for disturbances with magnitude equal to 0.5, i.e. half the cells are affected.

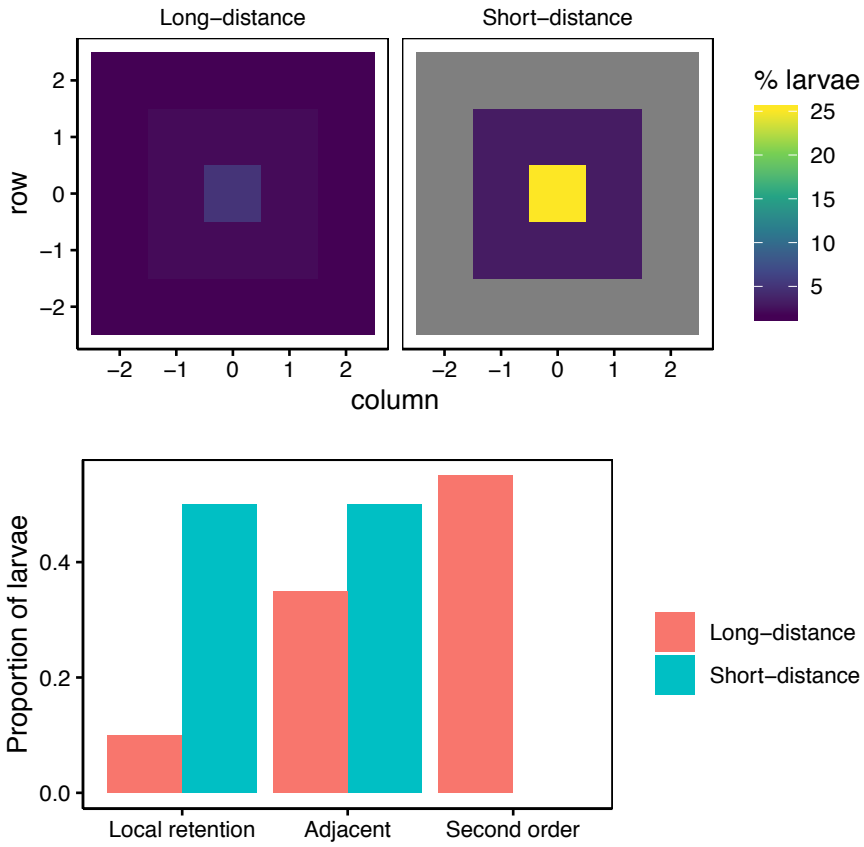

Figure D-8 Dispersal kernels of short-distance and long-distance dispersers. Top: Proportion of larvae dispersing from source (centre) to sink populations/cells. Long-distance dispersers have low levels of local retention and ability to disperse to second-order neighbours. Short-distance dispersers retain half of their larvae locally and disperse only to adjacent cells. Bottom: total proportion of larvae locally retained, dispersing to adjacent cells and to second-order neighbouring cells.